SILICON BASED PRECERAMIC POLYMERS AS A MATRIX MATERIAL IN COMPOSITE TECHNOLOGY

Master of Science Thesis

Tuğçe Aybüke ARICA

Eskişehir, 2017

SILICON BASED PRECERAMIC POLYMERS AS A MATRIX MATERIAL IN COMPOSITE TECHNOLOGY

Tuğçe Aybüke ARICA

MASTER OF SCIENCE THESIS

Graduate School of Sciences

Material Science and Engineering Program

Supervisor: Assist. Prof. Dr. Erhan AYAS

Co-advisor: Prof. Dr. Paolo COLOMBO

Eskişehir

Anadolu University

Graduate School of Science

January, 2017

This thesis work is supported by the Scientific Research Projects Commission of Anadolu University under the Master Thesis grant 1605F515.

FINAL APPROVAL FOR THESIS

This thesis titled "Silicon Based Preceramic Polymers as a Matrix Material in Composite Technology" has been prepared and submitted by Tuğçe Aybüke ARICA in partial fulfillment of the requirements in "Anadolu University Directive on Graduate Education and Examination" for the Degree of Master of Science in Material Science and Engineering Department has been examined and approved on 24/01/2017.

Committee Members		Signature
Member (Supervisor)	: Assist. Prof. Dr. Erhan AYAS	…….
Member	: Assoc. Prof. Dr Abdullah Tuğrul SEYHAN	…….
Member	: Assoc. Prof. Dr. Hakan GAŞAN	..……..

…… ….....…….

Date Director

Graduate School of Science

ABSTRACT

SILICON BASED PRECERAMIC POLYMERS AS
A MATRIX MATERIAL IN COMPOSITE TECHNOLOGY

Tuğçe Aybüke ARICA

Department of Material Science and Engineering
Anadolu University, Graduate School of Science, January, 2017

Supervisor: Assist. Prof. Dr. Erhan AYAS

Co-supervisor: Prof. Dr. Paolo COLOMBO

In this thesis, two preceramic polymers with different side groups, polymethylsilsesquioxane (PMSQ) and polyphenylsilsesquioxane (PPSQ), used as matrix material for preparation of ceramic matrix composite by addition of four different ingredients (i.e., steel fiber, silicon carbide, tin sulfide and vermiculite). PMSQ and PPSQ matrix composite materials were produced by mixing powder components, and pressed with uniaxial warm pressing under 100 MPa pressure for 2 min at 60^0C and 150^0C, then, cross-linked at 250^0C and 300^0C for 4.0 h, respectively. The cross-linked samples were heat treated at five different pyrolysis temperatures (i.e., 400, 500, 600, 700, and 800°C) for 2 h. The effect of different side groups and pyrolysis temperature on the thermal, physical, mechanical property of the materials, and phase and micro-structural development in the produced composite samples were investigated by thermal (TG-DTA), phase (XRD), microstructural (SEM-EDX) analysis and density and compressive strength measurements.

As a result of this study, it was observed that the PPSQ polymer have positive effect on the thermal degradation of composite material and the compressive strength values of the PPSQ matrix composite samples have considerably stable at between 150 and 600^0C by comparison with PMSQ matrix samples. The formation of the pore quantity and pore size distribution was depended on the used preceramic polymer side group and applied heat treatment temperatures.

Keywords: Polysilsesquioxanes, Uniaxial warm pressing, Ceramic matrix composite.

ÖZET

Sİ ESASLI ÖNCÜ SERAMİK POLİMERLERİN KOMPOZİT MALZEME TEKNOLOJİSİNDE MATRİS FAZ OLARAK KULLANIMI

Tuğçe Aybüke ARICA

Malzeme Bilimi ve Mühendisliği Anabilim Dalı
Anadolu Üniversitesi, Fen Bilimleri Enstitüsü, Ocak, 2017

Danışman: Yard. Doç. Dr. Erhan AYAS

İkinci Danışman: Prof. Dr. Paolo COLOMBO

Bu tez çalışmasında, farklı yan gruplara sahip iki öncül seramik polimer, polimetilsilseskioksan (PPSQ) ve polimetilsilseskioksan (PPSQ), matris malzeme olarak seçilmiş ve dört farklı bileşenin (çelik lif, silikon karbür, kalay sülfit ve vermikülit) ilavesi ile seramik matris kompozit malzeme üretimi yapılmıştır. PMSQ ve PPSQ matrisli kompozit malzemeler, toz bileşenlerin karıştırılması, hazırlanan karışımın tek eksenli ılık presleme yöntemiyle 100 MPa basınç altında sırasıyla 60°C ve 150°C'de 2 dk süreyle sıkıştırılması ve 250°C ve 300°C'de 4.0 sa çapraz bağlanmasıyla üretilmiştir. Çapraz bağlanan numuneler, 2 sa boyunca beş farklı piroliz sıcaklığında (400, 500, 600, 700 ve 800°C) ısıl işleme tabi tutulmuştur. Farklı yan grupların ve piroliz sıcaklığının kompozit malzemenin termal, fiziksel, mekanik özelliklerine ve, faz ve mikroyapısal gelişimi üzerine olan etkisi, termal (TG-DTA), faz (XRD), mikroyapı (SEM-EDX) analizleri ile yoğunluk ve basma mukavemet ölçümleri yapılarak incelenmiştir.

Yapılan çalışmalar sonucunda, PPSQ polimerinin, PMSQ polimeri ile karşılaştırıldığında kompozit malzemenin termal bozunumu üzerinde olumlu etkisi olduğu ve PPSQ matrisli kompozit numunelerin basma mukavemet değerlerinin 150 ile 600°C arasında oldukça tutarlı olduğu görülmüştür. Oluşan gözenek miktar ve gözenek boyut dağılımının kullanılan preceramik polimer yan grubuna ve uygulanan ısıl işlem sıcaklıklarına bağlı olduğu gözlenmiştir.

Anahtar Kelimeler: Polilsilseskioksan, Tek yönlü ılık presleme, Seramik matris kompozit.

ACKNOWLEDGMENTS

First, I would like to thank my supervisor, Assist. Prof. Dr. Erhan AYAS for his continuous support and advice throughout my thesis work.

I am also grateful to Prof. Paolo COLOMBO for his guidance, understanding as well as for introducing me to his valuable research groups, who are helpful and open to sharing ideas. Besides, I would like to thank him for his advice in the preparations and formulations of the materials in his laboratory, valuable discussions concerning the pre-ceramic polymer precursors, as well as many useful support.

I am thankful to PhD candidate Alberto CONTE for his valuable help, contributions and friendship support in University of Padova.

I am also thankful to Dr. Kılıçaslan Noyan BAYRAKTAR for his valuable suggestions.

I also thank to Seyfi YAMAK for his help in technical problem in the laboratory and Mustafa ÇOBANLI for STA analyses.

I would like to thank, Oğuzhan SAKARYA, Meriç GÜVENÇ, Berkay YAZIRLI, Levent KARACASULU, Merve TANER, Kübra GÜRCAN and Levent KÖROĞLU for their supportive friendship. I would also like to thank, Ezgi PİLİÇER and Ayhan Ece ŞİRİN who always give me their friendship support.

Finally, I am eternally grateful to my family for their endless encouragement and support.

Tuğçe Aybüke ARICA

07/02/2017

STATEMENT OF COMPLIANCE WITH ETHICAL PRINCIPLES AND RULES

I hereby truthfully declare that this thesis is an original work prepared by me; that I have behaved in accordance with the scientific ethical principles and rules throughout the stages of preparation, data collection, analysis and presentation of my work; that I have cited the sources of all the data and information that could be obtained within the scope of this study, and included these sources in the references section; and that this study has been scanned for plagiarism with "scientific plagiarism detection program" used by Anadolu University, and that "it does not have any plagiarism" whatsoever. I also declare that, if a case contrary to my declaration is detected in my work at any time, I hereby express my consent to all the ethical and legal consequences that are involved.

……

Tuğçe Aybüke ARICA

TABLE OF CONTENTS

Page

LIST OF TABLES

LIST OF FIGURES

1. GENERAL LITERATURE

1.1. Introduction

A ceramic is inorganic non-metallic solid material comprising metal, non-metal or metalloid atoms primarily held in ionic and covalent bonds. The crystallinity of ceramic materials ranges from highly oriented to semi-crystalline, and often completely amorphous for example glasses. Varying crystallinity and electron consumption in the ionic and covalent bonds cause most ceramic materials to be good thermal and electrical insulators. In the ceramic structure or composition a large range of possible options can be observed such as nearly all of the elements, all types of physical and chemical bonding, and all levels of crystallinity. In general, the ceramic materials have high melting temperature, high hardness, and low conductivity, high moduli of elasticity, chemical resistance and low ductility. The earliest ceramics made by humans were pottery objects (i.e. *pots* or *vessels*) or figurines made from clay, either by itself or mixed with other materials like silica, then hardened and sintered under fire. The special character of ceramic materials gives rise to many applications in materials engineering, electrical engineering, chemical engineering and mechanical engineering. The ceramic materials are heat resistant, they can be used for many tasks for which materials like metal and polymers are unsuitable. It should be remembered that ceramic engineering is the science and technology of creating objects from inorganic, non-metallic materials. This is done either by the action of heat, or at lower temperatures using precipitation reactions from high-purity chemical solutions.

Ceramic materials are preferred in many areas such as aerospace, automotive, defense, biomedical device, electronic device, magnetic device and nuclear industry due to their extreme heat resistance, mechanical strength at high temperatures, hardness, abrasion resistance, chemical inertness and lightness. Ceramic materials are usually produced by shaping of fine ceramic powders by conventional methods and then sintering of shaped product at high temperatures. However, since the melting temperatures and hardness of ceramic materials are high and their workability is difficult, the production cost of materials in near net shape and complex shapes is high, and processing operations are time consuming and difficult.

The preceramic polymers, studied for more than 50 years, are an alternative to the materials produced from ceramic powders by traditional methods due to their easy to

shape features in the desired geometric form, low processing temperatures and low production cost. The preceramic polymers are inorganic polymeric precursors which can be transferred to the ceramic form by crosslinking and then proper pyrolyzing process. These polymers can be prepared in desired geometric form by using a lot of different method used for plastic shaping technology such as pressing, extrusion, injection molding, resin transfer molding and fiber drawing. It is possible to obtain desired physical, mechanical, electrical, optical and thermal properties by tailoring the molecular structure of the polymers. And also, addition of various fillers (Ti, Mo, B, Al, SiC, Si_3N_4, Al_2O_3, B_4C, BN, etc.) to the preceramic polymers enables to adjustment of these properties. Differences in the structure of the chain and side groups of the polymeric precursor cause very high difference in the obtained material by means of composition and, macro and micro properties of material.

Due to the properties given above, many research and development studies on the precursor ceramic polymers have been made. Preceramic polymer are used in transportation, microelectromechanical systems (MEMS), energy and defense systems industry in various forms such as ceramic matrix composites, fibers, micro-components, coatings and high-porosity structures.

In this work, the preceramic polymers were utilized as matrix for preparation of composite ceramic materials. Two different type of preceramic polymer (i.e., polymethylsilsesquioxane and polyphenylsilsesquioxane) with different side groups in the polymer chain were selected, and used as matrix in the preparation of composite ceramic materials with different properties. The compositions and ratios of the ingredients were kept constant while changing the preceramic polymer type. Produced composite materials were crosslinked and then pyrolyzed at different temperatures. In this way, the effect of preceramic polymer type having different side groups and pyrolysis temperature on the microstructure, thermal, physical and mechanical properties of the composite materials have been investigated. The surface morphology and the properties of the composite materials were comparatively characterized by Scanning Electron Microscope (SEM), Helium pycnometer, Thermogravimetric Analysis (TGA) and Differential Thermal analysis (DTA), and X-ray diffraction (XRD) techniques.

1.2. Polymer Derived Ceramics

Most of the ceramic products are manufactured by conventional ceramic processing techniques which are required shaping and then high temperature sintering of fine ceramic powders [1-2]. Sintered ceramic parts are commonly machined to obtain final shape. Hard and brittle nature of the ceramics increases the machining processing costs. In some instances, machining cost of the sintered ceramic can amount to more than 50% of the production costs depending on the component size, shape and surface quality [3]. Because of the high temperature (1000°C-2500°C) requirement of sintering process and difficulty in obtaining complex and near net shape conventional ceramic processes are became expensive and time consuming. Additionally, high temperature requirements of processes is incompatible with many materials when considering the composite design [1, 4]. Therefore, Sol-Gel and polymer pyrolysis techniques are develop which operates at lower temperature with the possibility of obtaining complex and near net shape ceramic products [4].

The preceramic polymers have inorganic/organometallic structure that derive amorphous as well as nano-crystalline ceramic material by releasing of organic constituents with proper curing and pyrolysis process. Ceramic materials produced in this way named as polymer derived ceramics (PDCs) [1, 5, 6]. A wide range of ceramic materials such as SiOC, SiCN, SiC, B_4C, Si_3N_4, and BN can be produced by this technique and it is possible to produce net shape product at lower temperatures (500°C-1500°C) compared to ceramic powder sintering process [1, 3, 5].

The “polydiphenylsilanes” preceramic polymer were firstly prepared and reported by Kipping and Sands (1921) and later polydimethylsilanes were synthesized by Burkhard (1949). At this years, the fully characterization of synthesized orgonosilicon polymer was not possible due to the technical limitations of the characterization methods [6-8]. In the early 1960s, Ainger and Herbert (1960) and Chantrell and Popper (1965) reported the production of nonoxide ceramics starting from molecular precursors [9,10]. In the 1970’s, Verbeek et al. (1974, 1975) studied from polymer to ceramic transformation of polysilazanes, polysiloxanes and polycarbosilanes for the production of Si3N4/SiC ceramic fibers for high-temperature applications [11, 12]. Following these significant researches Yajima et al. (1975, 1978) reported their achievement in the production of SiC ceramic materials from pyrolysis of polycarbosilanes. [5, 13, 14].

Recently, a large variety of new organosilicon and organoelement polymers have been developed as precursors for preparation of Si-based and A1-, B- or Ti- based non-oxide ceramics [6]. Some of the prepared preceramic polymers and their pyrolytic products with percent ceramic yields are given in Table 1.1 [15].

Table 1.1. *Preceramic polymers and their pyrolytic ceramic products with percent ceramic yield values.*

Ceramic Product	**Organoelement Polymer**
A1N	$[RAlNH]_n$, $[Cl_2Al\text{-}N(H)Si(CH_3)_3]_n$
BN	$[HNBC1]_3 + ((CH_3)_3Si)_2NH$
BC_4N	$C_5H_5N.BH_3$
BC_2N	$HNC_4H_8NH.BH_3$
B_4C/BN	$[B_{10}H_{12}.H_2N\text{-}CH_2\text{-}CH_2\text{-}NH_2]_2$
SiC	$H\text{-}[CH_3SiH]_n\text{-}H$
SiC/C composite	$[(CH_3)Si(H)\text{-}CH_2]_n$, $[((CH_3)_2Si)_x(CH_3SiC_6H_5)_y]_n$
$Si_xC_yN_z$	$[CH_3SiHNH]_m.[CH_3SiN]_n$
$Si_xC_yO_z$	$[(CH_3)_2SiO]_m.[CH_3SiO_{1.5}]_n$
TiN	$[(C_4H_9N)_2Ti]_n$
ZrB_2	$Zr[BH_4]_4$

Reference: *[15]*

Chemistry of main polymer chain and side groups, molecular weight and phase (solid or liquid) of polymer, and structure of polymer (linear, branched, cage) greatly affect the properties and processing condition of preceramic polymer and the properties of the final ceramic product produced from them [4]. It is possible to obtain desired ceramic composition by modifying the chemistry of main chain or its side groups. And also, proper pyrolysis atmosphere (reactive or inert) provide further tailoring capability of the final ceramic composition.

In polymer derived ceramic production silicon (Si) based polymers has drawn considerable interest due to their easy and low cost processing, tailoring possibility of chemical composition, low manufacturing temperature and versatile plastic shaping technologies [2]. Simplified structural formula of Si based preceramic polymer is given in Figure 1.1. Parameters X and R^1 and R^2 make possible modification of preceramic precursor on the molecular level. Class of Si based polymers determined by the X group

such as polysiloxanes and polysilsesquioxanes with X=O, polysilazanes with X=NH, polycarbosilanes with X=CH_2 and polysilanes with X=Si. Functional side groups, R^1 and R^2, in the polymer chain designate the characteristic of polymers such as chemical and thermal stability, solubility of the polymer, and their electronic, optical, and rheological properties. Additionally, type and the quantity of the side groups determine the carbon content in final ceramic. Side groups, R, could be hydrogen or alkyl or aryl organic groups (commonly methyl or phenyl) [5, 16].

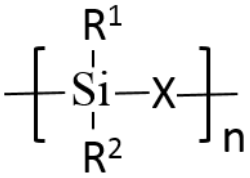

Figure 1.1. *Simplified chemical formula of Si based preceramic polymer.*
Reference: *[5].*

The general classes of silicon-based preceramic polymers as shown in Figure 1.2 Preceramic polymer can include more than one X group in the polymer backbone. For example, polyborosilazane polymers are hybrid polymers which is X=B and X=N at the same time [16].

1.2.1. Types of Si-based preceramic polymers

Polysiloxane and polysilsesquioxanes

Polysiloxanes are usually expressed as silicones. They have the lowest cost among all the Si-based polymers. They are generally odorless, colorless, water resistant, chemical resistant, electrically insulating. They exhibit stability at high temperatures and in oxidative environments. Their thermal stability as well as relatively high melting and boiling points makes them alternative materials for applications which organic polymers cannot be used [5,17,18]. Polysiloxanes are widely used in high-technology fields such as aerospace industry, as protecting materials in the semiconductor industry, or during the processing of products like optical glass fibers, silicon wafers and chips [16]. Additionally**,** they can be also used in the personal care products industry due to their

non-toxic property such as in biomedical applications like breast implants, oral anti-foaming agent (e.g. simethicone) and food additives [16].

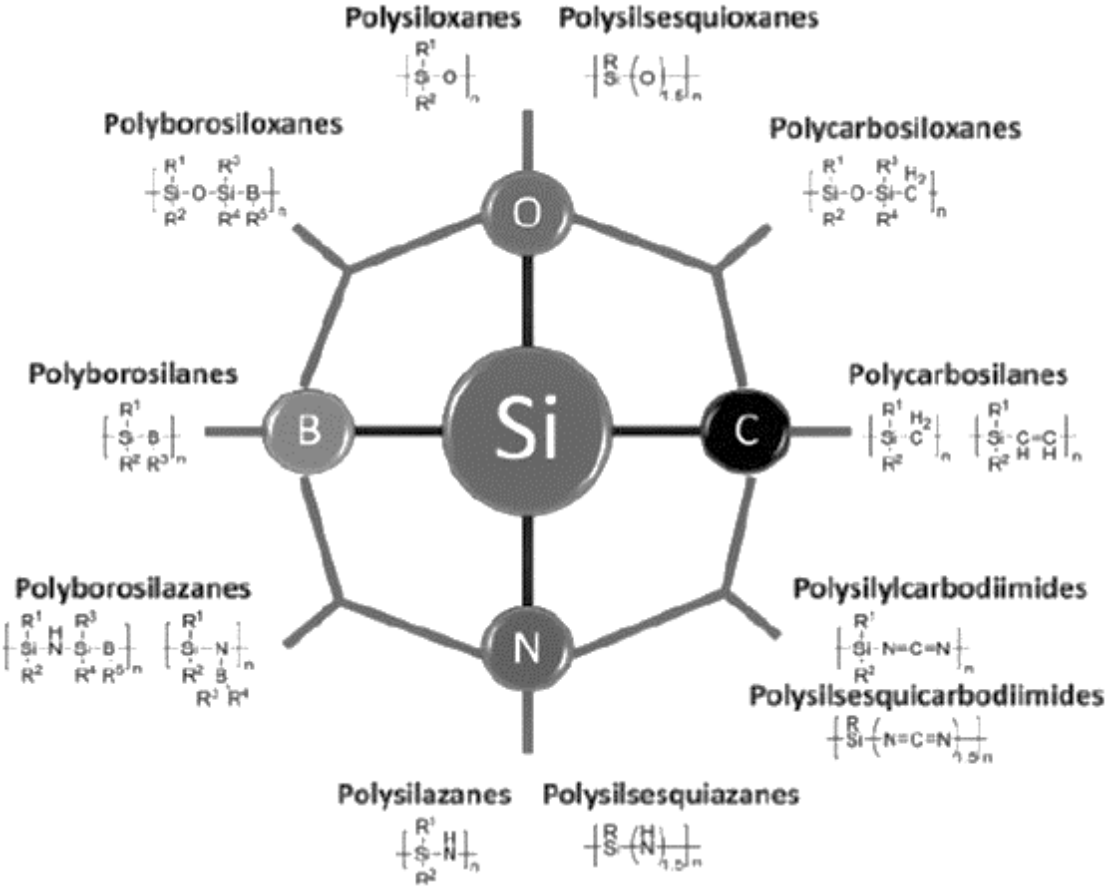

Figure 1.2. *The general classes of Si- based preceramic polymers.*
Reference: *[5].*

Polysilsesquioxanes are subset of polysiloxanes. They are also referred as silicone resins and they are generally in solid form at room temperature. Chemistry of main chain and, type and number of organic group of polysilsesquioxanes can be easily varied which makes them useful preceramic polymers [16, 19]. Number of organic groups attached to per silicon atom on the structural unit is called as "degree of substitution". There are four structural unit as shown in Figure 1.3. The D unit is capable of expanding the polymer in two directions while significant number of T and Q units in the polymer structure make possible to obtainment of branched polymers or resins which will allow an expansion of the material in three or four directions [20]. Branched polysiloxanes shows higher thermal

stability then its linear counterpart due to its contribution to formation of crosslink in the solid residue [21]. Commercial silicone resin in general means the DT-type resins [22].

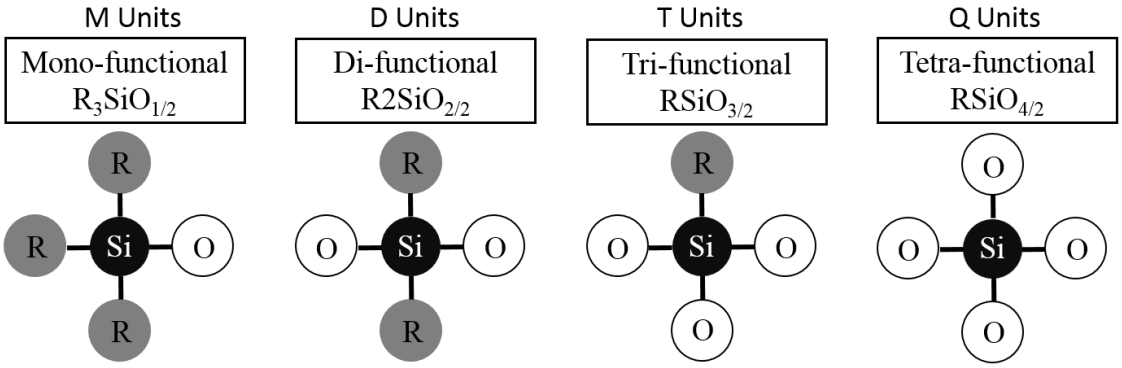

Figure 1.3. *Types of structural unit compose the polysiloxane.*

Both polysiloxanes and polysilsesquioxanes have Si-O in their main chain but the difference is that siloxanes ($[R_2SiO]_n$) are linear or cyclic polymers while silsesquioxanes ($[RSiO_{1.5}]_n$) are highly crosslinked three-dimensional structures which are random, cages and ladders as shown in Figure 1.4. This already highly crosslinked structure provide higher ceramic yield upon pyrolysis [16, 22]. Both of the polysiloxane and polysilsesquioxanes are used to synthesis of oxide ceramics, such as SiO_2, Si-C-O, and Si-C-N-O ceramics, depending on the processing atmosphere [6].

Polysilazanes

Polysilazanes polymers contain alternating Si-N in their main chain. They are preferred in applications where high-temperature stability, corrosion resistance and durability are desired as ceramic coating or components. They are generally find application in protective coating fields due to their oxidation and corrosion resistance, UV stability and high hardness [5, 16]. They are used as precursors for production of amorphous Si_3N_4 and Si-C-N ceramics [23]. "They can be chemically modified by reactions with transition metal alkoxides, as it has been shown for Al or group IV metal alkoxides (M = Ti, Zr, Hf) [18]. Additionally, there are several studies showed that polysilazanes can be modified with non-oxidic organometallics [24-27]. The obtained metal containing precursors provide to synthesis of different ultrahigh temperature resistance ceramic nanocomposites (such as MN/Si3N4, MN/SiCN, MCN/SiCN, *etc.*, with M = Ti, Zr, Hf), depending on the conditions used for the ceramization [18].

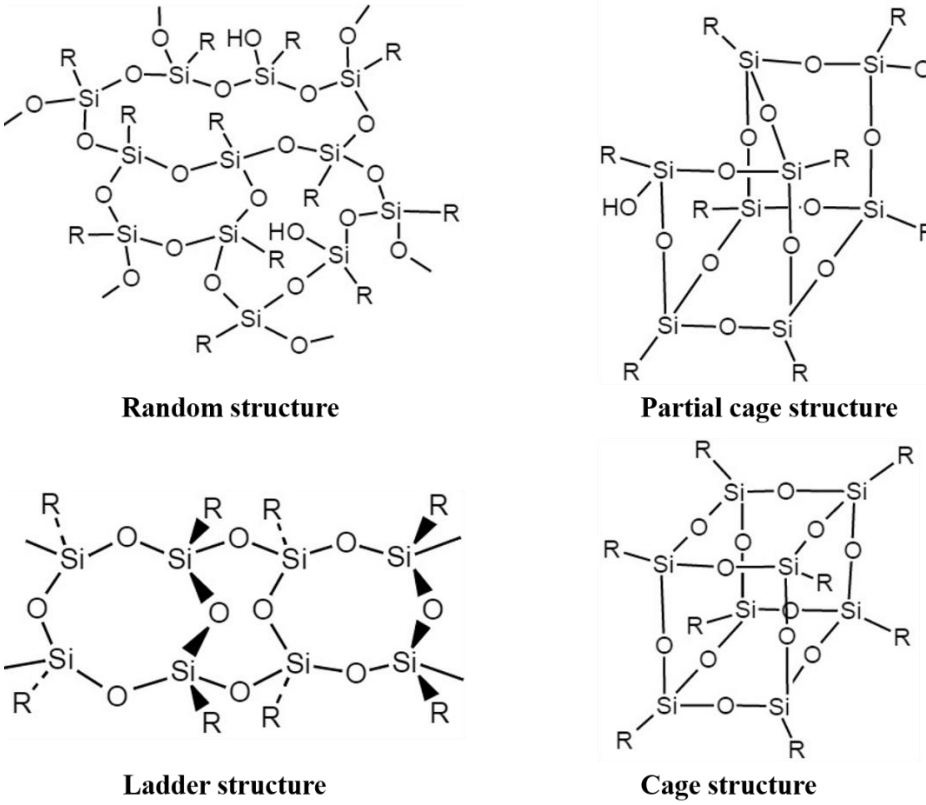

Figure 1.4. *Structures of polysilsesquioxane.*
Reference: *[22].*

Polysilazanes

Polysilazanes polymers contain alternating Si-N in their main chain. They are preferred in applications where high-temperature stability, corrosion resistance and durability are desired as ceramic coating or components. They are generally find application in protective coating fields due to their oxidation and corrosion resistance, UV stability and high hardness [5, 16]. They are used as precursors for production of amorphous Si_3N_4 and Si-C-N ceramics [23]. "They can be chemically modified by reactions with transition metal alkoxides, as it has been shown for Al or group IV metal alkoxides (M = Ti, Zr, Hf) [18]. Additionally, there are several studies showed that polysilazanes can be modified with non-oxidic organometallics [24-27]. The obtained metal containing precursors provide to synthesis of different ultrahigh temperature resistance ceramic nanocomposites (such as MN/Si3N4, MN/SiCN, MCN/SiCN, *etc.*, with M = Ti, Zr, Hf), depending on the conditions used for the ceramization [18].

Polycarbosilanes

Polycarbosilanes have Si-C backbone and Si-Si bonds could be present. Final ceramic yield and Si:O ratio can be modified by this way [5]. First pioneering study on polymer derived ceramic is achieved with polycarbosilane precursor group by Yajima et al to make SiC fibers. [13, 14] This technology was commercially used to production of NICALON™ (Nippon Carbon Co., Ltd. of Japan) ceramic fibers. This precursors can be used in production of photoresist and semiconductors. They are also find an application in electronic applications such as compact capacitors, piezoelectric sensors, smart windows (with tunable color and transparency) and solar cells due to the unsaturated polycarbosilanes [16].

Polysilanes

Polysilanes consist of Si-Si backbone structure and organic side groups attached to the silicon atoms. They have unique optoelectronic and photochemical properties due to the σ conjugation and also high thermal stability [5]. This type precursors are used for semiconductors, photoresists in microlithography, photoreceptors in copiers and printers, UV electroluminescent devices and synthesis of the silicon carbide ceramics. [5, 18, 28].

1.2.2. Shaping, crosslinking and pyrolysis of preceramic polymers

Transformation of preceramic polymers to ceramics consist of three following steps [1]:

(i) Synthesis of the preceramic polymer.

(ii) Shaping of the product followed by crosslinking for obtainment of the thermoset green body which could retain its shape during pyrolysis step.

(iii) Pyrolysis of the crosslinked product in inert or reactive atmosphere at between 500 and 1500^0C temperatures and organic to inorganic transition is occurred at between 400 and 800^0C.

Moreover, further heat treatment of amorphous ceramic material at higher temperatures (>1000^0C - 2000^0C) result in crystalline structure. All these steps shown in Figure 1.5 and will be defined in detail below except the first step. Synthesis of the preceramic polymer will not be covered in this study due to the lots of ceramic precursors are commercially available. Besides that chemical structure of polymeric precursors have great effect on the final ceramic composition and morphology, and ceramic yield. For

instance, different side groups such as methyl and phenyl with similar polymer backbone can alter the ceramic yield and carbon content in the final ceramic product [5]. Effect of side groups will be covered in detail in Section 1.2.3.

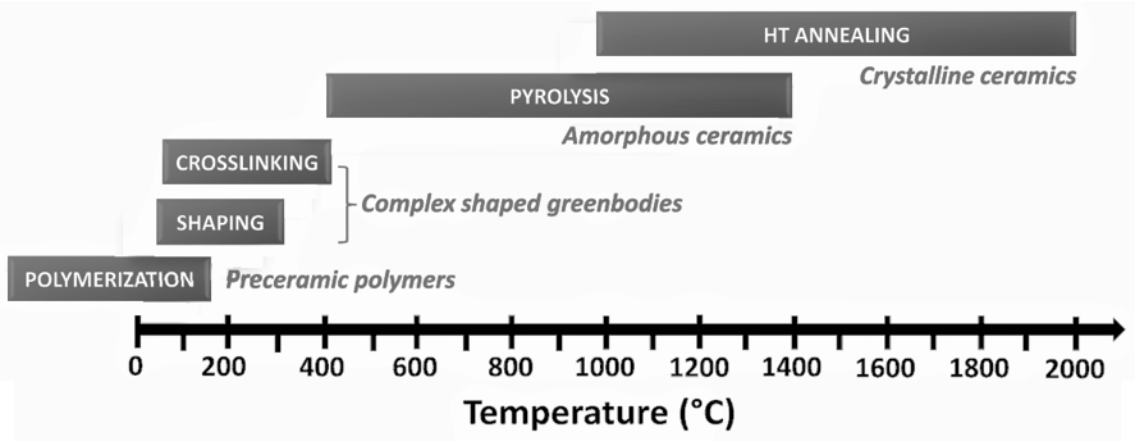

Figure 1.5. *Transformation of preceramic polymers to ceramics.*
Reference: *[5,18].*

Shaping process of preceramic polymer is one of the significant advantages of the PDC route over the conventional powder processing of ceramic materials due to all plastic forming technologies can be used in this route. Complex green body product can be obtained by these methods and also make possible further handling with its sufficient mechanical consistency. Most of the preceramic polymers are thermosets and can be liquid or solid at room temperature. Solid precursor can be dissolved in solvent or can be melted at low temperatures (usually $<150^0$C) [5]. Some of the preceramic polymer shaping techniques are that warm pressing [29-32], fiber drawing [33, 34], extrusion [35], injection molding [36], coating of substrates [37-39], rapid prototyping, lithographic techniques [40, 41] polymer infiltration pyrolysis (PIP) technique [42], and resin transfer molding (RTM). Some of the shaping technologies are shown in Figure 1.6.

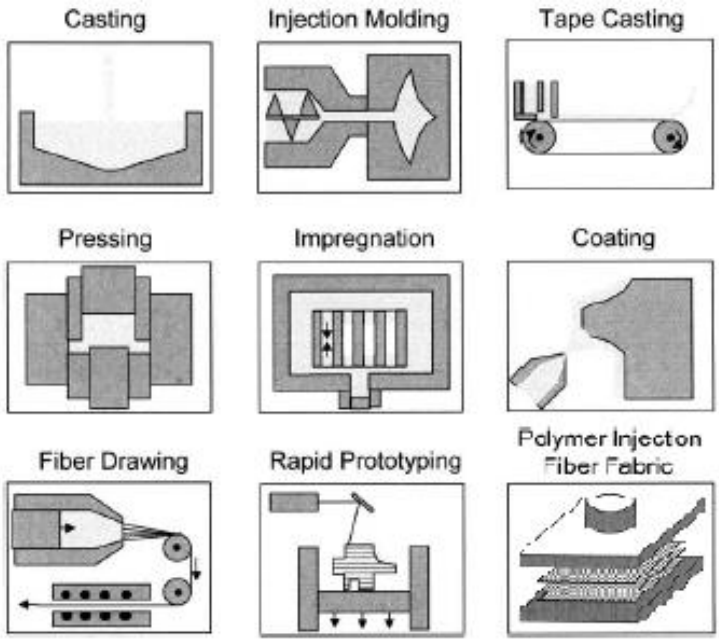

Figure 1.6. *Shaping techniques for polymer derived ceramic manufacturing.*
Reference: *[1].*

After shaping process preceramic polymers are cured to obtain non-melteble thermoset materials which could retain its shape during pyrolysis by this way. In the crosslinking step**,** polymer chains rearrange themselves by condensation reactions under favor of functional groups such as Si–H, Si–OH, or Si-vinyl functionalities to obtain highly bonded network structure [1, 5]. Crosslinking is achieved, typically, between 100^0C -250^0C temperature (thermal crosslinking) with or without catalyst. Using of catalyst have some benefits such as lowering the crosslinking temperature, avoiding the evaporation of oligomers with formation of bubbles increasing the ceramic yield [5]. Besides the oxidative curing, other curing methods such as selective laser curing, UV curing and γ-ray radiation curing is applicable for preceramic polymers [1, 5, 43]. Crosslinking step increase the ceramic yield by preventing the loss of low molecular weight components from preceramic polymer [18]. Moreover, it is possible to obtain machinable parts by crosslinking which permits a more precise shape control [16].

Pyrolysis is the last step which shaped and cured preceramic polymer is converted into the ceramic. Thermal or non-thermal processes can be applied such as oven pyrolysis, hot isostatic pressing, spark plasma sintering, laser pyrolysis and ion radiation [5]. As shown in Figure 1.5 thermal pyrolysis of preceramic polymer happen approximately

between 400°C- 1400°C. In this stage, cured preceramic polymer is decomposed by rearrangements and radical reactions which causes cleavage of chemical bonds (e.g. Si–H, Si–C and C–H), and releasing of organic functional groups (CH_4, C_6H_6, CH_3NH_2 etc.) in gases form [1,5]. Pyrolysis process consist of different decomposition reaction at specific temperature range. For instance, Sorarù et al. report that $Si(CH_3)_4$ and CH_4 are main volatile species of polymethylsilsesquixane at between 550-700°C and 700-800°C, respectively [16,44]. The organic-inorganic conversion is terminated at 800-1000°C, further heat treatment at higher temperatures (1000- 2000°C), annealing, can be used to develop crystallization and nanostructure such as SiC, Si_3N_4, SiO_2 and carbon (turbo-stratic or graphitic) [1,6, 16]**.** Greil**,** shows the temperature dependent microstructural transitions of various preceramic polymer composition in Figure 1.7 [1]. Depending on the application preceramic polymers can be produced as amorphous or polycrystalline ceramics. Amorphous ceramic structure consist of mixture of covalent bonds, the most important ones are Si–C, Si–O, Si–N and C–C. Depending on the precursor type other bonds with other atoms like B, Ti, Al or Zr could also be present [16].

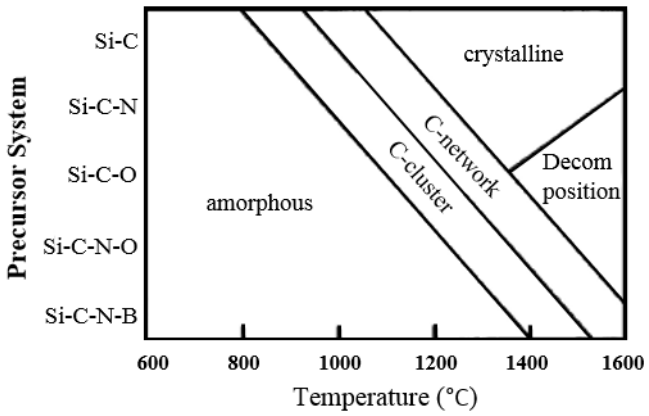

Figure 1.7. *Tentative phase transition diagram of ceramic derived from various preceramic polymer systems.*

Reference: *[1].*

The ceramic yield is defined by the Equation 1.1 and high ceramic yield is desired for low weight loss and minimal shrinkage. High ceramic yields are generally obtained with high molecular weight polymers, proper crosslinking process and highly branched polymer [5].

$$\alpha^P = \frac{mass_{pyrolyzed\ ceramic}}{mass_{starting\ polymer}} \quad (1.1)$$

In general ceramic yields are in the 70-90% (w/w) range. Ceramic yield of various preceramic polymers are shown in Table 1.2.

Table 1.2. *Ceramic yield of typical preceramic polymer.*

Preceramic polymers	**Polymeric unit**	**Ceramic**	**Ceramic yield (%)**
Polycarbosilane	$(-R_2SiCH_2-)_n$	SiC	65
Polysiloxane	$(-R_2SiO-)_n$	Si-O-C	30 - 60
Polysilazane	$(-R_2SiNR-)_n$	Si_3N_4	20 - 90
Aluminum amide	$(=AlNR-)_n$	AlN	20 - 50
Polyborazine	$(-B_3N_3H_x-)_n$	BN	85
Polytitanium imide	$(=Ti(NR)_2-)_n$	TiN	50 - 70

Reference: ***[45]***

During pyrolysis step releasing of gaseous, porosity and shrinkage development and density increase limits the bulk components production from polymeric precursors. Density typically increases by a factor of 2 to 3 from the precursor (1 g/cm^3) to the ceramic residue (SiO_2, 2.2-2.6 g/cm^3, Si_3N_4 and SiC, 3.0-3.2 g/cm^3); and volume shrinkage may exceed 50 % [1]. Addition of secondary fillers to preceramic polymers can decrease the shrinkage and pore formation during conversion of polymer. "Fillers could be of various nature (ceramic, metallic, polymeric), shape (equiaxed particles, elongate grains, whiskers, platelets, nanotubes, fibers) and dimensions (from nanoparticles to fibers of several centimeters)" [5]. Fillers are classified into two groups; passive and active. Passive fillers such as SiC, B_4C, Si_3N_4, BN and Al_2O_3 stay inert during polymer to ceramic conversion and reduce shrinkage by filler volume effect. In the case of active filler, fillers are expand as a result of reaction with decomposition product which derived from pyrolysis process or reaction with furnace atmosphere. Expansion of filler compensate the polymer shrinkage and make possible to obtain near net shape polymer to ceramic conversion. Reactive metals, intermetallic or ceramic phases such as Ti, Cr, V, Si, B, $CrSi_2$, $MoSi_2$, AlN, etc. can be used as active fillers [1, 5, 16] Schematic representation of passive and active filler effects are shown in Figure 1.8. In some cases, when the amount of fillers is predominant over the amount of polymer, the preceramic polymer acts as a low-loss binder that could increase the density of the final part with the lowest packing densities (ultrafine powders) [5].

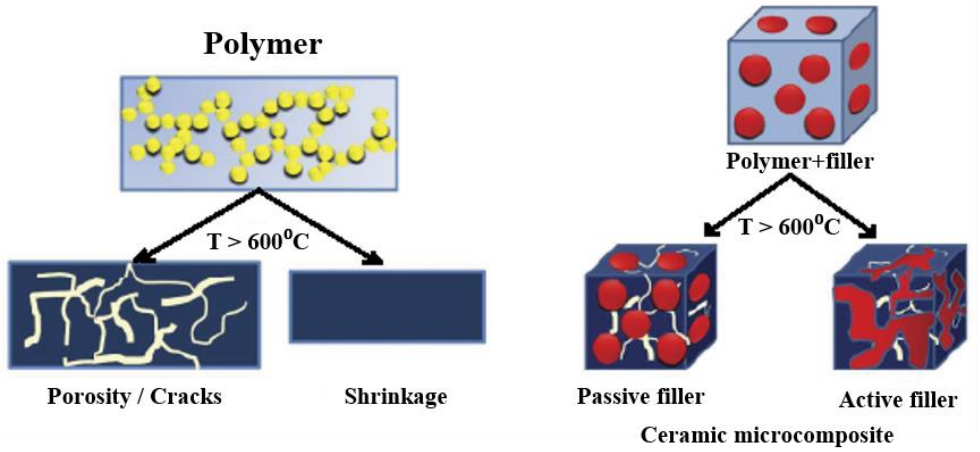

Figure 1.8. *Schematic representation of passive and active filler effects.*
Reference: *[5].*

1.2.3. Effect of side groups on the polymer derived ceramics

As mentioned in previous section, type of different side groups (i.e., methyl, ethyl, phenyl and vinyl etc.) on the same precursor main chain have great influence on the processing conditions, ceramic yield and final ceramic properties. In the presented work, methyl and phenyl groups containing polysilsesquioxane polymers were used as matrix in the preparation of composite materials. The effect of these side groups on the properties of composite material were also well examined. Thus, the effect of methyl and phenyl side groups on polysilsesquioxanes polymers [i.e., polymethylsilsesquioxanes (PMSQ) and polyphenylsilsequioxanes (PPSQ)] will be compiled from literature in this section.

Polysilsesquioxanes are highly crosslinked organosilicon compounds, silicone resins, with a general chemical formula $[RSiO_{3/2}]_n$ (R = H, alkyl, aryl or alkoxy groups), and they have attracted attention as precursors to ceramic materials and nanocomposites. It should be note that polysilsesquioxanes are preferred over other silicon based compounds due to its main polymer backbone structure, and the amount of organic functional side groups and their types can be easily varied [19].The molecules have unusual properties because of the presence of exterior organic functionality on the inorganic silicate core. The polymer backbone structures are already oxidized (i.e., Si-O-Si) and, therefore, these materials are resistance for oxidation to many chemical agents [22]. In addition, the silica core confers rigidity and thermal stability.

Many studies have been performed to determine the properties of PMSQs and PPSQs [4, 19, 21, 22, 46-51]. The observed characteristics of methyl and phenyl

functionalized polysilsesquioxanes are presented in Table 1.3 [22]. In general, PMSQ precursors are characterized for its low weight loss on pyrolysis while PPSQs precursors are characterized by their high thermal stability [22, 46, 47]. Zhou, Yang, Guo, and Lu have analyzed thermal degradation behaviors of some polysiloxanes with thermogravimetric (TG) analysis method from room temperature to 800^0C with 10^0C/min under nitrogen and air flow. TG analysis results show that introduction of phenyl group increase the initial decomposition temperature of silicon polymer while decrease ceramic yield at 800^0C both in N2 and air flow. And also carbon content in ceramic residue is increased with increase in phenyl content [21]. Phenyl groups in silicon polymers show higher thermal stability at low temperature due to the steric hindrance effect of bulky aryl group [21, 22, 48]. The high ceramic yield of methyl containing silicon polymers can be explained by their high Si:C ratio. While the methyl side groups are evolved more readily than the larger phenyl group, which can remain in the matrix as amorphous carbon, the total mass percentage of carbon lost compared to the remaining silicon is still relatively small [4]. It should also note that pyrolysis temperature of phenyl functionalized silicon polymer is higher than methyl ones under air atmosphere while it is lower under N2 atmosphere [21]. In the pyrolysis process carbon atoms are removed as volatiles and left of them is bonded in part to silicon (SiC), and in part to itself, forming free carbon [44]. Amount of free carbon is increased with the increase in phenyl content in silicon polymer [19].

1.3. Applications of Polymer Derived Ceramics

Preceramic polymers are used in various applications due to its physical-chemical, mechanical, thermal and electrical properties with the possibility of obtainment of desired property product with various shaping technology. Thus, they have found application in several fields such as information technology, transport, defense, energy as well as environmental systems, biomedical components and micro- or nanoelectromechanical systems (MEMS/NEMS) [5]. Mainly applications of preceramic polymers can be sorted as ceramic fibers, ceramic coatings and porous ceramics, micro components, and ceramic matrix composites (CMC).

Table 1.3. *Characteristics of PMSQ and PPSQ.*

PMSQ	**PPSQ**
Hydrophobic	Thermally stable
Small weight loss on pyrolysis	Oxidative stable
Flexible at low temperature	Softens at high temperature
Chemically resistant	Becomes tack free at room temperature
Arc resistant	Compatible with organic polymers

Reference: *[22]*

Ceramic fibers from preceramic polymers is the oldest and most successful applications. SiC fibers are produced from polycarbosilane and commercialized as NicalonTM-SiC fiber which has a microstructure containing β-SiC crystals and C-precipitations in an amorphous SiOC matrix [1, 14, 52, 53]. Introduction of B and N into fiber structure provides amorphous structure up to ~1700^0C in inert atmospheres, with strengths equaling those of SiC-based fibers, with superior oxidation and creep resistance [5, 54]. Additionally, BN fibers and SiCN fibers containing multi-walled carbon nano-tubes (CNTs) have been produced. Addition of multi-walled CNTs greatly improve the tensile strength of fiber [5, 55, 56].

Polymer derived ceramics are utilized as coatings to protect surface of carbon, porous non-oxidic ceramics, and refractory metals against corrosion, oxidation, and wear via dipping, spinning, painting, or spraying methods [1, 4, 5]. For optoelectronic applications, coatings which include Si or C clusters have been developed [5, 57]. Protective coating on C/C composites and carbon fibers have realized to increase oxidation resistance [5, 58, 59]. Porous polymer derived ceramic materials can be used as ceramic filters, thermal insulation, and light-weight structural reinforcements [60, 61]. Colombo and colleagues have been done lots of study on macro- and microporous foams from preceramic polymers [62-65].

Preceramic polymers make possible to produce ceramic part below 1.0 mm in size by various lithographic methods. Moreover, the excellent thermomechanical, oxidation, and corrosion resistance properties of PDCs allow the application of MEMS/NEMS in harsh environments at high temperatures under oxidizing conditions [5, 66]. Additionally, low viscosity polysiloxane polymers have been used in 3D printed components which is one of the interesting subject of polymer derived ceramics applications [67-69].

Preceramic polymers have been used in manufacturing of ceramic composites as matrix (CMC) or low loss binder materials to improve thermal, chemical and mechanical property of materials. They are suitable for melt infiltration technique (i.e., resin transfer molding (RTM), polymer infiltration pyrolysis (PIP), and chemical vapor infiltration (CVI)) to form prepreg or infiltration of pre-sintered porous ceramics [70, 71]. Use of preceramic polymers as binders provide advantage over the conventional organic binders in that they are converted into ceramics with higher green density while conventional organic binders are burned out and caused porous structure. Furthermore, fibers are coated with preceramic polymers to assist adhesion between fibers and/or fiber-matrix by act as a binder [72]. In several studies, bulk ceramic composites are produced from liquid or solid form of ceramic precursors with or without addition of fillers by diverse plastic forming methods (i.e., warm pressing, isostatic pressing, and uniaxial pressing). In this way, preceramic polymers make possible to obtainment of complex shaped, improved green strength and higher densification material with lowered porosity and crack formation via binding the ingredients of composite material by viscous flow [30-32, 73-78].

Processing of ceramic matrix composites, one of the most common applications of polymer derived ceramics, by warm pressing technique is covered under this thesis. In this technique, polysilsesquioxane polymers (i.e., PMSQ and PPSQ) and other ingredients were mixed in solid form and then shaped into a die, which is heated over the glass transition (T_g) temperature of the polymers, by applying certain pressure. Here, the heated polymers are deformed and resultant low viscous precursor fill the pores and hold the space between the ingredients by act as a low loss binder matrix material. In this way, machinable green body was obtained, and then passed through to crosslinking and pyrolysis processes to form amorphous ceramic matrix in the composite material.

2. SCOPE AND OBJECTIVE OF THE STUDY

The aim of this thesis is to develop ceramic matrix composite materials by using preceramic polymers as a binder matrix phase. Preceramic polymers are suitable materials to process with plastic forming techniques due to that they could be prepared in low viscous precursor form at low temperature (~45-150^{0}C) or in solution form. They can be produced at low temperature with plastic forming techniques (i.e., warm pressing, PIP, RTM, fiber drawing and injection molding) to desired near net shape and be converted to a ceramic material at relatively low temperatures (~ 400-1400^{0}C). Therefore, processing of polymer derived ceramic materials have several advantages over conventional powder processing methods in that control of shape and purity of material is possible, and it requires lower cost. Variation on the preceramic polymer main chain and side groups greatly affect the final composition and micro- and macro- properties of the final ceramic. In the pyrolysis process, side groups (i.e., methyl and phenyl) of ceramic precursor are burned off and cause the shrinkage of the final product. Polysilsesquieoxanes are combined with various inorganic filler materials to reduce the shrinkage [1, 79]. In order to reduce the shrinkage of the final materials, two different active or passive filler material (i.e., Ti, Cr, Mo, B, Al, $MoSi_2$) or (i.e., SiC, Si_3N_4, Al_2O_3, B_4C, BN vb.), respectively, are added to the preparation of the preceramic polymer mixture. It should be noted the additives have a significant effect on the physical, thermal and mechanical properties of the final ceramics. In literature, there are many reports about properties and various applications of the polysilsesquioxanes polymers, one of the primary class of preceramic polymers. In addition, many studies have reported that the polysilsesquioxanes precursors are homogeneously dispersed within the selected composite formulation and provides low porosity, especially when warm pressing method was selected [32, 76, 80].

In this study, two different types of ceramic matrix composite materials were produced from two different polysilsesquioxane preceramic polymer, namely, polymethylsilsesquioxane (PMSQ) or polyphenylsilsesquioxane (PPSQ). They were mixed with other four inorganic ingredient [(i) steel fiber, (ii) tin sulfide powder mixtures (i.e., SnS_2, Sn_2S_3, and SnS), (iii) silicon carbide (SiC) and (iv) vermiculite] and then warm pressed. Compositions and ratios of four different inorganic ingredient were kept constant for both type of preceramic polymers mixtures. The PMSQ and PPSQ polymers were used as matrix materials to create binding between the used inorganic ingredient.

Expectations from the added steel fiber, tin sulfide powder mixture (i.e., SnS_2, Sn_2S_3, and SnS), silicon carbide (SiC) and vermiculite inorganic materials are; enhancement of their mechanical properties, increase in chemical and environmental inertness, provide hardness and resistance of high temperature, and heat insulation. Produced CMC materials were pyrolyzed at five different temperatures (i.e., 400, 500, 600, 700, and 800 ^{0}C) to obtain Si-O-C amorphous ceramic matrix phase which provide high temperature resistance up to 1200^{0}C [81].

The objective of this study is to investigate the effect of different side groups (i.e., methyl and phenyl) in polysilsesquioxane polymer and pyrolysis temperature on the thermal properties, densification and amount of porosity, compressive strength, phase development and microstructure of the final products of the composite materials. Characterizations of the composite materials were made by Thermogravimetric Analysis (TGA) and Differential Thermal Analysis (DTA), Helium pycnometer, X-ray diffraction (XRD) and Scanning Electron Microscope (SEM) techniques. Additionally, the secondary objective of the study is determining the preceramic polymer type with low porosity, and high compressive strength and determination of pyrolysis temperature which provide it.

3. MATERIALS AND EXPERIMENTAL TECHNIQUES

3.1. Materials

The polymethylsilsesquioxane (PMSQ; Silres MK) was obtained from Wacker-Chemie GmbH, München, Germany. The polyphenylsiloxane (PPSQ; RSN-0217 Flake Resin) was provided from Dow Corning Co., Midland, Michigan, ABD. The steel fibers, tin sulfide powder mixture (i.e., SnS_2, Sn_2S_3, and SnS), silicon carbide (SiC) and vermiculite were supplied from [SO1, Green Steel Group Oggiono, Italy], [Stannolube®, Tribotecc, Vienna, Austria], [Tangshan Xinye Silicon Carbide Co., Ltd. Tangshan City, China] and [Minerals I Derivats S.A. Tarragona, Spain], respectively. The former two preceramic polymers were used as binding phase while the other four ingredients were used as inorganic additives. After complete of oxidation, the silica (SiO_2) content of PMSQ and PPSQ are ~82 % and ~47%, respectively. Melting range of the PMSQ is between 35 and 55^0C while PPSQ glass transition temperature (Tg) is 64^0C, and it was stable up to 150^0C in the molten state without any observable degradation.

The pyrolyzed preceramic polymers formed Si-O-C amorphous ceramic phase. The obtained amorphous phase provide high temperature resistance up to 1200^0C [81]. Expectations from the added steel fiber is the enhancement of the mechanical properties. Tin (II) sulfide (SnS) is a layer-structured compound. The layers in SnS compound are coupled with weak van der Waals forces, and the presence of week forces in SnS provides intrinsically a chemical inert surface without dangling bonds. Thus, the presence of weak force makes SnS to be chemically and environmentally inert. Additionally, SnS exhibits chemical stability in acidic solutions, high melting and boiling points of 880^0C and 1230^0C [82]. SiC mineral has high thermal and chemical stability, high strength, high thermal conductivity, controllable electrical conductivity, and low temperature coefficient of linear expansion. And also, SiC is a non-oxide and it has the tendency to get oxidized in presence of oxygen or oxidizing agents [83].

Vermiculite is the geological name given to a group of hydrated laminar minerals which are aluminium-iron-magnesium silicates, resembling mica in appearance. It is an inert material and when heated it expands (exfoliates) up to 30 times its original volume. The exfoliation process converts the dense flakes of ore into lightweight porous granules containing innumerable minute air layers. Exfoliated (expanded) vermiculite is light and clean to handle, has a high insulation value, acoustic-insulating properties and will absorb

and hold a wide range of liquids. These granules are non-combustible, and are insoluble in water *and* all organic solvents. Expanded vermiculite is easily poured, is light, clean absorbent and provides baffle against impact shock when used for packaging. Exfoliated vermiculite is used in the friction brake linings market, high temperature insulation, loft insulation, various construction products, animal feeds, horticulture and many other industrial applications. Vermiculite with its layered structure and surface characteristics, is utilised in products such as intumescent coatings and gaskets, the treatment of toxic waste and air-freight packaging of hazardous goods [84].

3.2. Experimental Techniques

Microstructural, physical, thermal and phase analysis of raw materials and produced specimens were investigated by using variety of characterization techniques. Additionally, compressive strength of the produced composite specimens were analyzed.

3.2.1. Microstructural analysis (SEM)

The scanning electron microscopy (SEM) image of the ingredients were obtained with ProX, FENOM after coating with a thin layer palladium/gold under reduced pressure to obtain size and microstructure of particles. On the other hand, the synthesized PMSQ and PPSQ matrix composite samples were studied using a Zeiss Supra 50VP SEM, with backscatter electron (BSE) mode to observe distribution of ingredients, morphology and the amount of pore on the studied sample surface. All the samples were analyzed through the pressed and polished surface, and also distribution of the ingredients, inside the cracked samples were studied. Additionally, the composition of the composite specimens were analyzed using by energy dispersive x-ray spectroscopy (EDX) method.

3.2.2. Physical characterization (particle size and density measurement)

The apparent (ρ_a) and true density (ρ_t) measurements of the PMSQ and PPSQ matrix composite samples were carried out by using (AccuPyc 1330, Micromeritics, Norcross, GA) and (Multi pycnometer, Quanta Chrome) a gas (helium) pycnometers, respectively.

Particle size measurements of tin sulfide powder mixture (i.e., SnS_2, Sn_2S_3, and SnS), SiC powders and vermiculite were obtained using a laser diffraction method (Mastersizer 2000, Malvern Instruments).

3.2.3. Thermal analysis (TGA-DTA)

Thermogravimetric analysis (TGA) and differential thermal analysis (DTA) of the raw materials and, the PMSQ and PPSQ matrix powder composite mixtures were studied to obtain mass changes and phase developments of each component. The thermal analysis of raw materials were performed for better understanding of thermal behavior of the composite specimens. The PMSQ and PPSQ silicone resins, steel fiber, tin sulfide powder mixture (i.e., SnS_2, Sn_2S_3, and SnS), silicon carbide powders, vermiculite and PMSQ and PPSQ powder matrix composite mixtures were analyzed in air atmosphere with 10K/min (STA 449 F3 Jupiter, NETZSCH, Gerätebau GmbH, Selb, Germany).

3.2.4. Phase analysis (XRD) and chemical analysis (XRF)

The phase analysis of the raw materials and their heat treated counterpart, and produced all the other specimens (i.e., binary mixtures and composite samples) were analyzed by x-ray diffraction (XRD) technique by using Cu-Kα radiation, between 2θ of 5-70° and 1°/min scan speed using an X-ray diffraction (XRD) instrument (MiniFlex 600, Rigaku). Heat treatment of the raw materials were carried out at 800°C for 2 h, with 2°C/min heating rate. Before the XRD analysis, all the samples, except as received steel fiber, were ground in an agate mortar and sieved under 63μm and then used in the analysis. Chemical analysis of vermiculite was performed by x-ray fluorescence technique (ZSX Primus, Rigaku).

3.2.5. Mechanical characterization (compressive strength)

Compressive strength measurements of the PMSQ and PPSQ matrix composite specimens were realized with a cross-head speed of 1mm/min (Instron 1121 UTM, Danvers, MA). Test samples were cut into the size of 7x7mm using a cut-off machine (Struers Labotom-3) and their shape correction were made by SiC sand-paper with 180 grit size.

3.3. Characterization of Materials

3.3.1. Microstructural analysis and particle size measurement

Morphology of the inorganic ingredients were observed by SEM with backscattered electron (BSE) imaging mode. Particle size of tin sulfide powder mixture and SiC powders were measured by software of the SEM instruments (ProX, FENOM). The particles size and size distributions curves were presented as surface area of the particles

due to their non-spherical particles shape via laser diffraction method (Mastersizer 2000, Malvern Instruments).

The SEM images of the tin sulfide powder mixture (i.e., SnS_2, Sn_2S_3, and SnS), were obtained at three different magnifications (i.e., 750x, 1500x, 5000x), and presented in Figure. 3.1.a, 3.1.b and 3.1.c, respectively. As shown in these figures, the tin sulfide micro-particles mixture have two different type of particle shapes (i.e., elongated lamellar and irregular aggregated particles) (Figure.3.1.b and c).

Tin sulfide powder size was also analyzed by using two different dispersion medium (i.e., water and ethanol). The results are presented in Figure.3.2a and 2b, respectively. As observed in these figures, the particles size and size distribution of tin sulfide powder mixtures are around between 0.1 and 100 μm. It should be noted that the particles were better dispersed in water than that of the ethanol, and an expanded particle distribution curve was observed compared with ethanol dispersed counterpart.

The SEM images of the silicon carbide powders were obtained at three different magnifications (i.e., 2500x, 5000x, 7500x), and presented in Figure.3.3a, 3b and 3c, respectively. As can be seen from these figures, the silicon carbide powder has an angular shape particles.

Silicon carbide powder size and size distribution were determined via dispersion in water, the results are presented in Figure.3.4. As can be observed from this figure, the particles size and size distribution of the silicon carbide powder are around between 1.0 and 10.0 μm. As observed in this figure, silicon carbide powder has a narrow size distribution.

The SEM image of vermiculite was studied to observe its morphology and particle size distribution. An exemplified SEM micrograph of the vermiculite is presented in Figure. 3.5, as observed in this figure, vermiculite has a multi-lamellar structure.

The particles size and size distribution of the vermiculite were obtained with a particle size analyzer by using ethanol as dispersion medium (Figure. 3.6). The vermiculite particles were dispersed in ethanol and then analyzed. As observed in Figure 3.6, the particles size and size distribution of the vermiculite are around between 10 and 1100 μm.

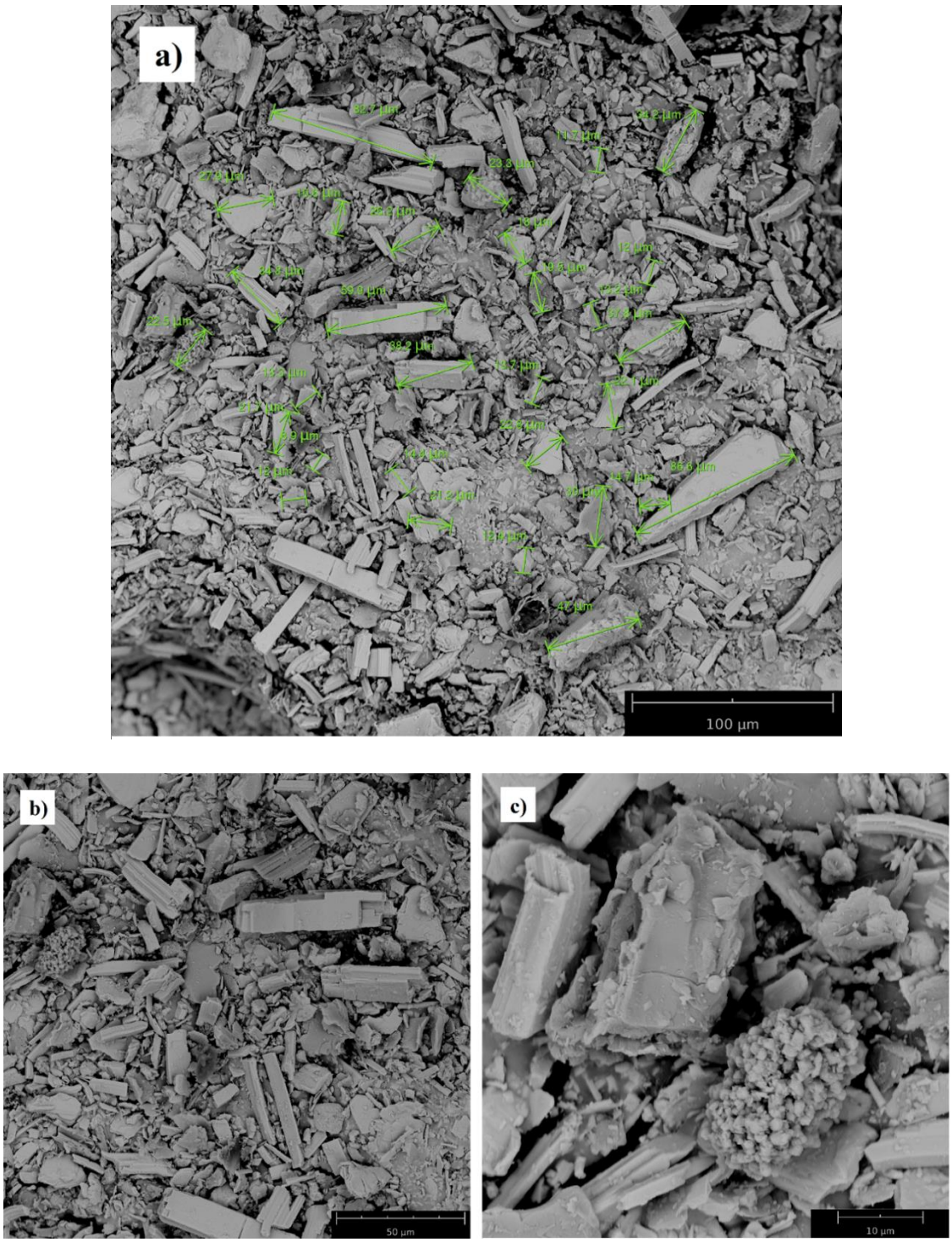

Figure 3.1. *BSE images of tin sulfide powder mixture at three different magnifications of (a) 750x, (b) 1500x, and (c) 5000x.*

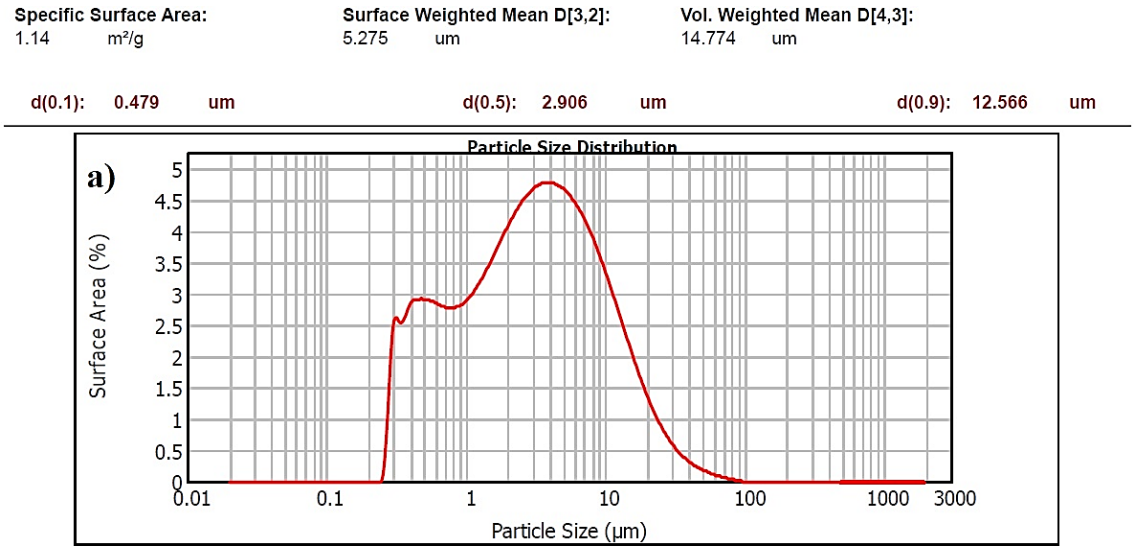

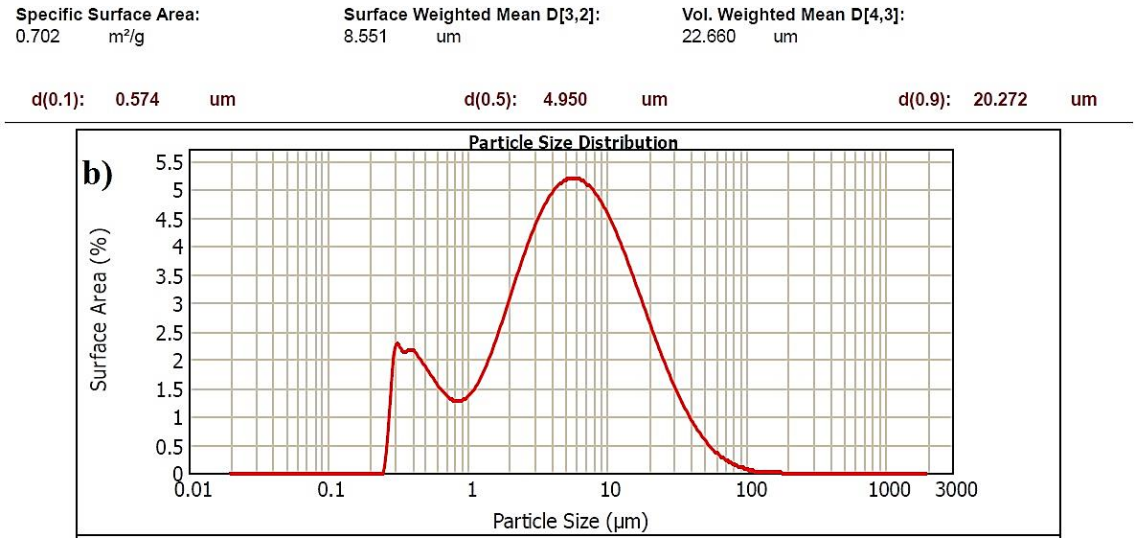

Figure 3.2. *Particle size measurement of tin sulfide powder mixture in (a) water and (b) ethanol as dispersion medium.*

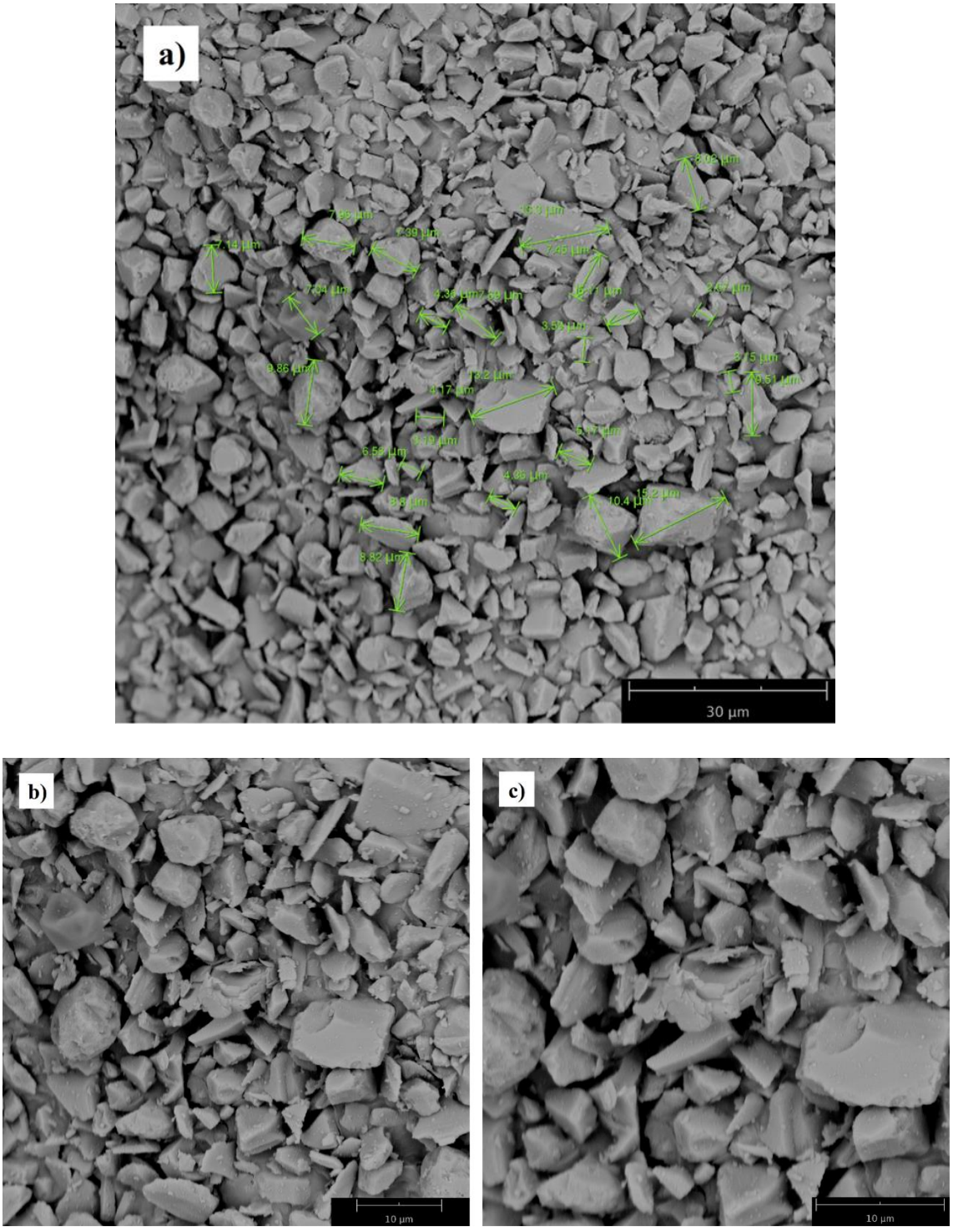

Figure 3.3. *BSE images of silicon carbide powder at different magnifications of (a) 2500x, (b) 5000x, and (c) 7500x.*

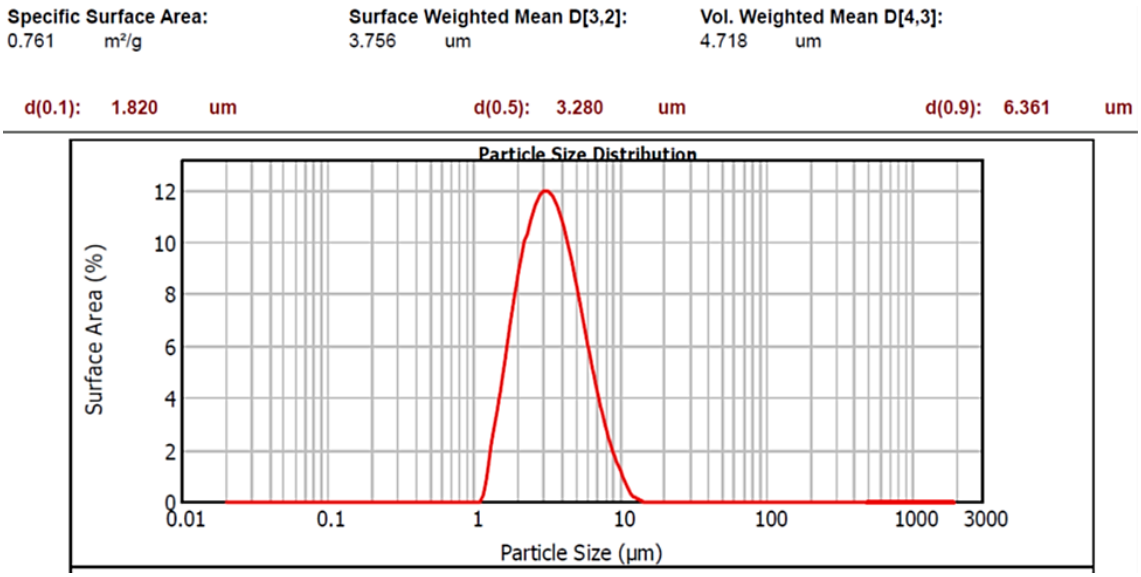

Figure 3.4. *Particle size measurement of silicon carbide powder (in water).*

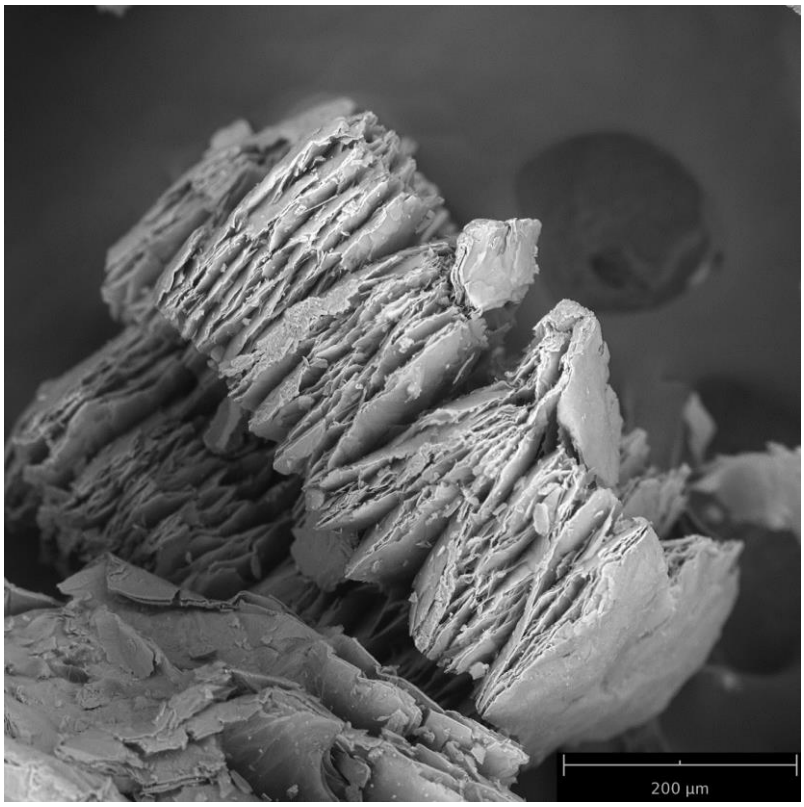

Figure 3.5. *BSE images of vermiculite particle at magnification of 400x.*

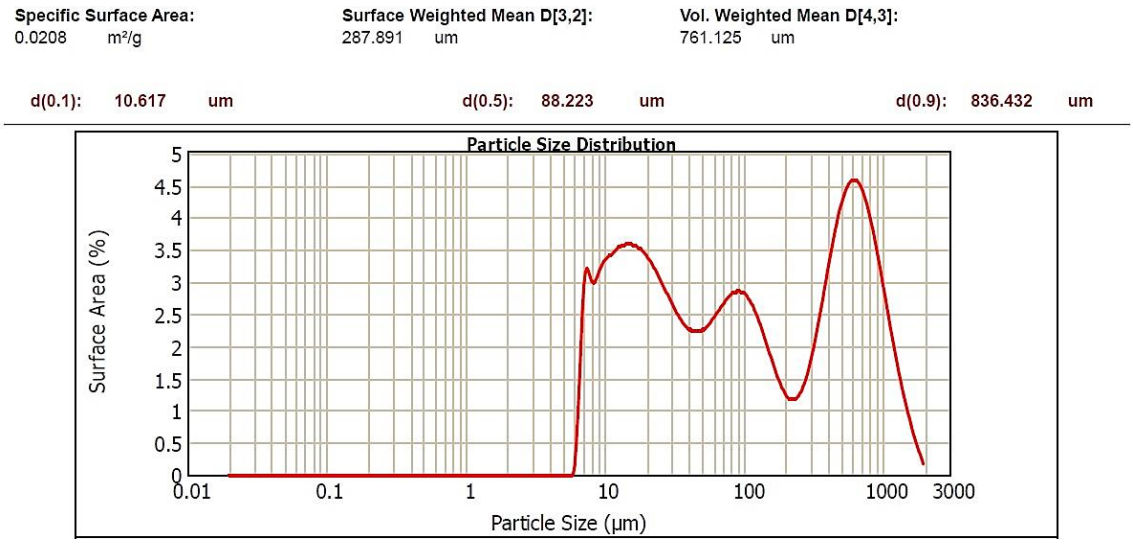

Figure 3.6. *Particle size distribution of vermiculite (in ethanol).*

3.3.2. Thermal analysis

The thermal behaviors of the PMSQ and PPSQ were studied in nitrogen atmosphere with 5 K/min whereas thermal behavior of steel fiber, tin sulfide powder mixture, silicon carbide powder, and vermiculite were analyzed in air atmosphere with 10K/min heating rate.

Figure 3.7 shows the TG-DTA graph of PMSQ polymer. Two significant weight loss were observed for PMSQ polymer; one of them was seen at between 150 and 400^{0}C, the latter was obtained at between 400 and 800^{0}C. It is known that first significant weight loss related with crosslinking reaction of the polymer, and loss of low molecular weight compound from the PMSQ structure [46]. In this crosslinking process, water and/or alcohols from polymer backbone can be released upon elevation of temperature, and under this condition, polymer could be sublimated consequently materials lost its weight [76]. Second significant weight loss could be resulted from the organic to ceramic conversion. At this stage, dehydrocarbonation condensation reactions can be realized in polymer. It is thought that the weight loss at between 520 and 650°C was attributed to evolution of CO, while at between 700 and 750°C was related to evolution of CH_4 [51]. The weight loss was significantly decreased after 800°C, and it could be probably attributed to the evolution of hydrogen [51].

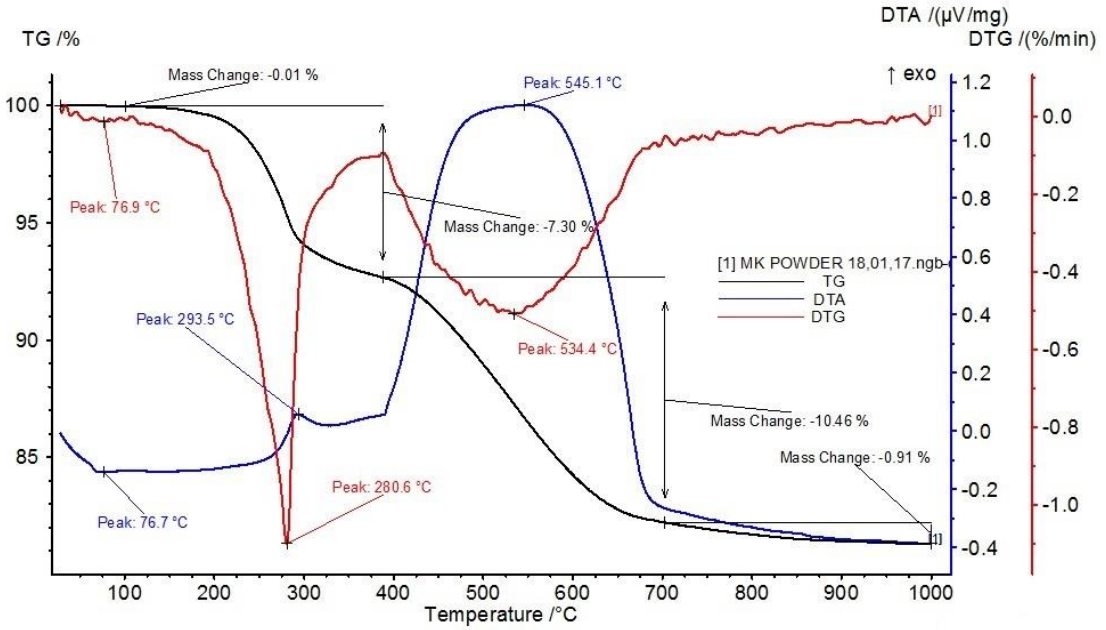

Figure 3.7. *TG-DTA curve of polymethylsilsesquioxane (PMSQ) in air.*

The TG-DTA curves of PPSQ is shown in Figure 3.8. Two main weight loss steps were observed. The first step was appeared at between 150 and 400^{0}C, and it could be mainly related to the evolution of free water, and polycondensation reaction of the residual silanol [51, 85]. The second weight loss step was observed at between 425 and 800^{0}C, this weight loss was caused by the evolution of benzene and dehydrogenation reactions via cleavage of the silicon-phenyl and C-H bonds [21, 85]. Stagnation of mass loss is observed after 800^{0}C for both PMSQ and PPSQ from their TG-DTA curves which means that pyrolysis of polymers are completed. As it seen from Figure 3.7 and 3.8, at the end of the thermal analysis the mass loss of PMSQ polymer is lower than that of PPSQ polymer which are 18.68 and 41.4% when analysis were carried out from room temperature to 1000^{0}C. Phenyl side group in the polymer structure provide higher thermal stability at low temperature (up to 500) in comparison with the polymer having methyl side group in its structure. This could be caused by phenyl (Ph) group being of higher steric hindrance to hamper Si-O bond scission. But at higher temperature the rate of Si-Ph bond scission is higher than the rate of Si-CH_3 bond cleavage by the effect of Si-OH bond. With the cleaving of the Si-Ph bond, the rate of Si-O bond scission of the phenyl content polymer is faster than methyl containing polymer. It is consistent with the amount

of degradation residues at 800^{0}C, which is higher in methyl side group content polymer [21].

As seen in Figure 3.9, there was no mass change for steel fibers until 300^{0}C, after this temperature, the steel fibers started a weight gain up to 800^{0}C about 7.19% due to the oxidation of the steel fibers (Figure 3.9). As observed in this figure, exothermic DTA curve confirms the oxidation process.

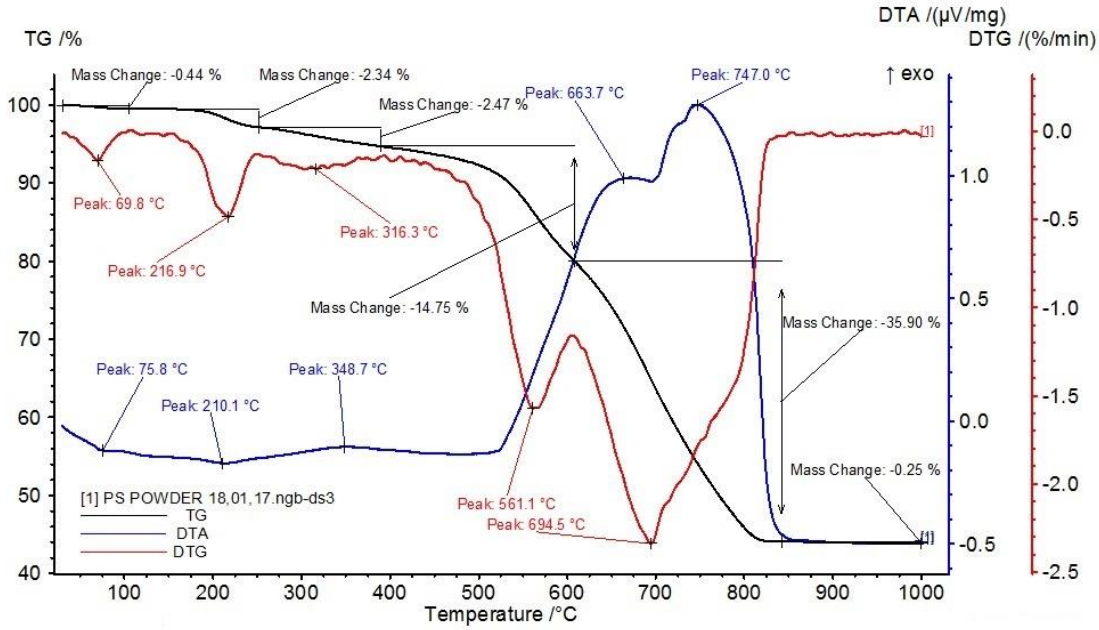

Figure 3.8. *TG-DTA curve of polyphenylsilsesquioxane (PPSQ) in air.*

The TG-DTA curves for tin sulfide powder mixture (i.e. SnS_2, Sn_2S_3, and SnS) is depicted in Figure 3.10. It should be noted that at 200-300 ^{0}C some weight loss were observed about 3.85%, it may be resulted from the loss of the bound water molecules. Then, a two steps oxidation process was observed for tin sulfide powder mixture; the first significant weight loss step was observed at between 450 and 600 ^{0}C about 7.39%, the second oxidation step was started from 700 and ended at 900 ^{0}C. The weight loss was found to be at these temperature ranges about 6.04%. This observed mass loss at above 500 and 800°C corresponds to the passage of sulfur in the vapor state and oxidation of tin sulfide [86].

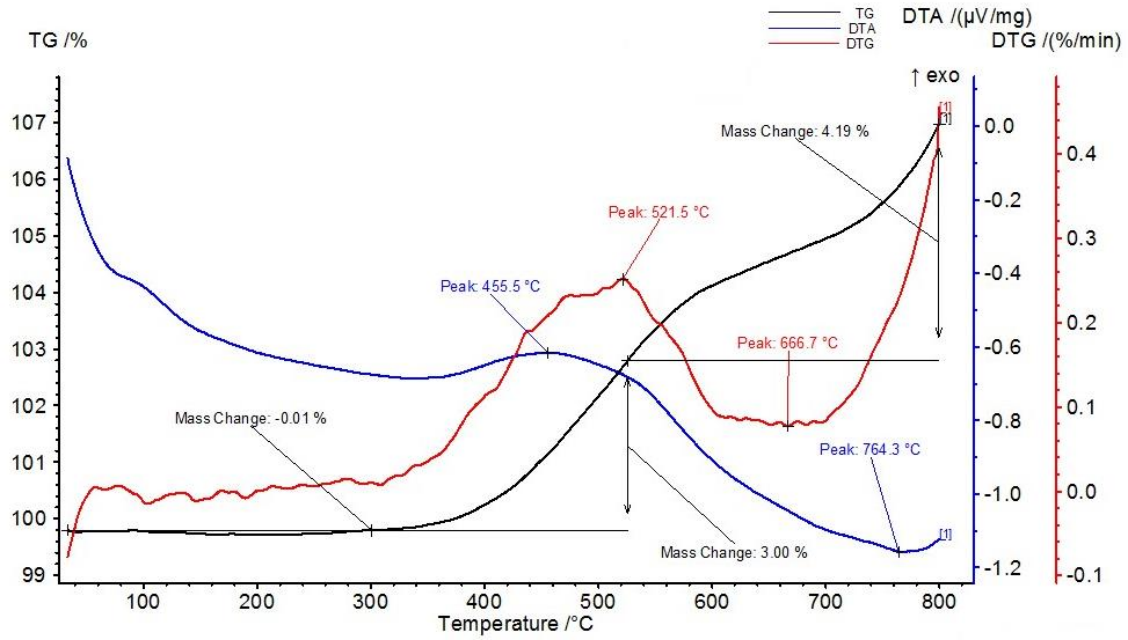

Figure 3.9. *TG-DTA curve of steel fibers in air.*

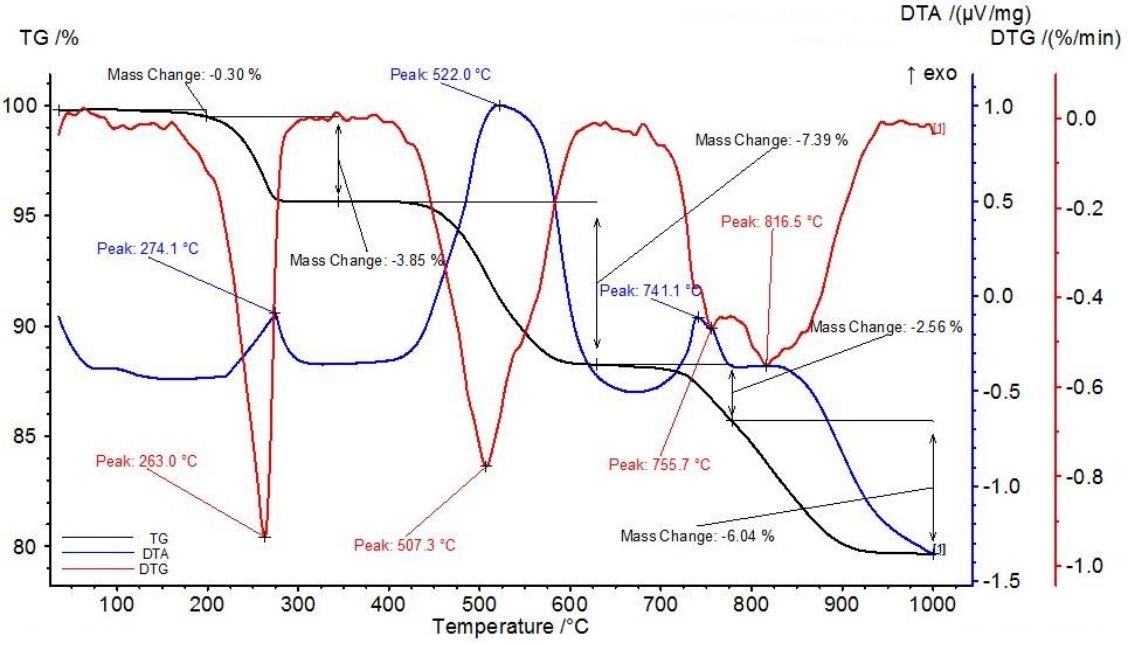

Figure 3.10. *TG-DTA curve of tin sulfide powder in air.*

The DTA curve of SiC powder exhibited a slight decomposition at between 350 and 800 ^{0}C with a mass loss about 0.47% (Figure 3.11). As observed in this figure, SiC was stable in the studied temperature range.

The TG-DTA curve of vermiculite is presented in Figure 3.12. A two dehydration step was observed at between until 50 and 275^{0}C. Then, also a two steps dihydroxylation was obtained at between 600 and 1000^{0}C [87].

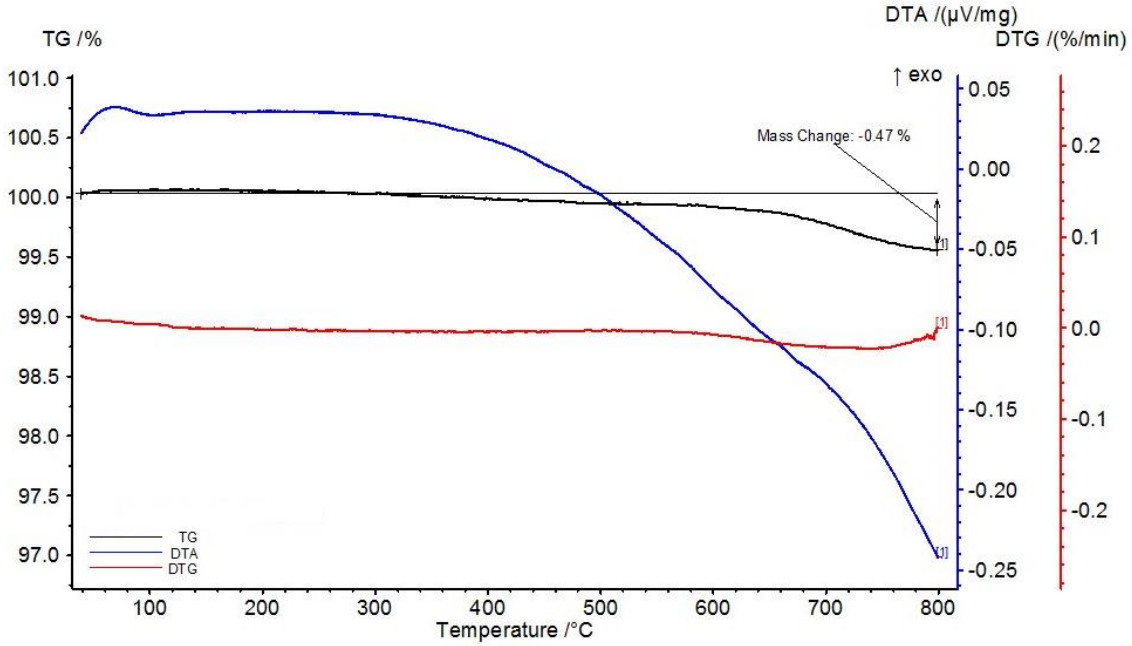

Figure 3.11. *TG-DTA curve of SiC powder in air.*

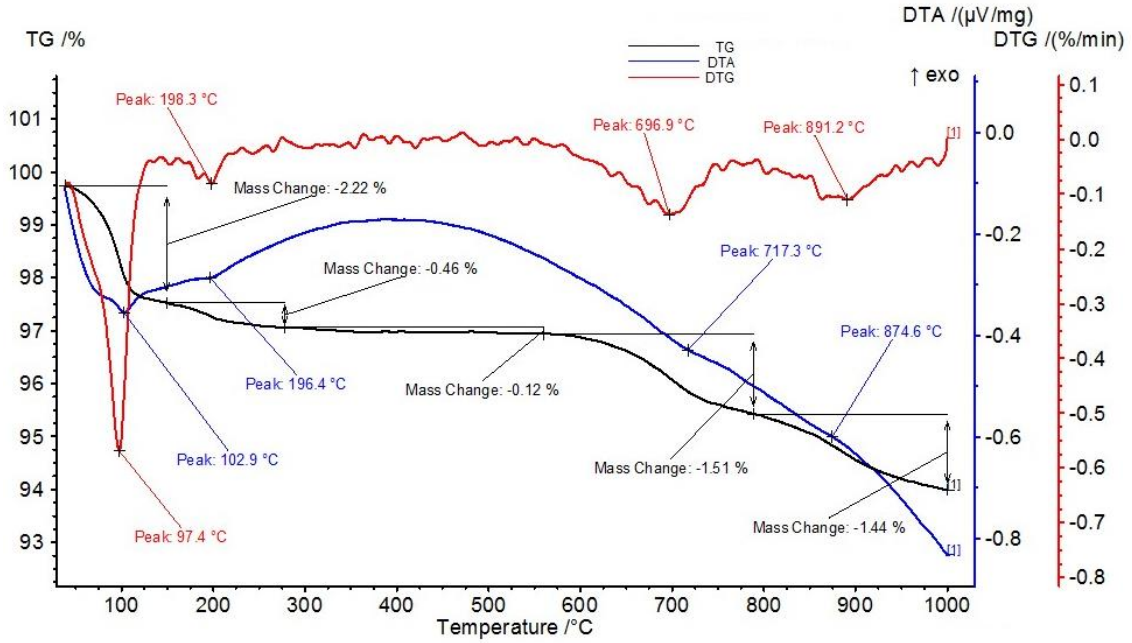

Figure 3.12. *TG-DTA curve of vermiculite in air.*

3.3.3. Phase analysis

Phase analysis of heat treated preceramic polymers (i.e., PMSQ and PPSQ), inorganic raw materials and their heat treated counterpart were realized by XRD technique. The polymethylsilsesquioxane and polymethylsilsesquioxane polymers were crosslinked before heat treatment at 250 and 300°C, respectively, for 4 h with a heating rate of 10°/min from the room temperature by using furnace (Carbolite, CWF 1200). Heat treatment of crosslinked preceramic polymers and inorganic raw materials were occurred in furnace at 800°C for 2.0 h with a heating rate of 2°/min from the room temperature (NABER Industrieofenbau D-2804 Lilienthal/Bremen). Inorganic raw materials and heat treated materials and were prepared for XRD analysis by grinding in agate mortar and then sieving under <63µm, except that steel fiber was used as received. Steel fiber, tin sulfide powder mixture (SnS_2, Sn_2S_3, and SnS), and silicon carbide and their heat treated counterparts were analyzed between 2θ of 5-70°, while vermiculite and its heat treated counterpart, and pyrolized preceramic polymers were analyzed between 2θ of 2-70° with a 1°/min scan speed. The XRD pattern of analyzed materials are shown in Figure 3.13, 3.14, 3.15 and 3.16.

3.3.4. Chemical analysis of vermiculite

In order to resolve to the most probable reaction that occur in the composite materials during heat treatment at different temperatures, therefore, the chemical analysis of vermiculite was performed by using x-ray fluorescence (XRF) technique. The chemical composition of the vermiculite is presented in Table 2.

3.4. Investigation of Interaction between Preceramic Polymers and Ingredients

3.4.1. Processing of each ingradient with two different preceramic polymer in the binary mixture composition

New phase formation between the ingredients (i.e., steel fiber, tin sulfide powder mixture, SiC, vermiculite) with each preceramic polymer (i.e., polymethylsilsesquioxane or polyphenylsilsesquioxane) were studied with preparation of their binary mixtures of each preceramic polymer with each ingredient. One of the preceramic polymer and one of the ingredient were mixed and heated up to 800°C. Firstly, a five gram from one inorganic ingredient (i.e., steel fiber, tin sulfide powder mixture, SiC, or vermiculite) was mixed separately with PMSQ or PPSQ preceramic polymer (5.0 g). The PMSQ preceramic polymer and each inorganic ingredient were separately mixed by using a

mixer mills (Retsch Mixer Mills MM 301) for 15 min with 20 (1/s) frequency. On the other hand, an axial mill (76 rpm) was used for the mixing of PPSQ preceramic polymer and each inorganic ingredient. After mixing process, each binary mixture of preceramic polymer (i.e., PMSQ or PPSQ) with each inorganic ingredient were transferred in a die and shaped by warm pressing technique. The mold (diameter 40 mm) of mounting heating press (Model Prontopress-2, Struers A/S, Copenhagen, Denmark) was filled with binary mixture of the PMSQ, and one of the ingredient, and then the sample was pressed at 105°C with 30 kN force for 10 min (5.0 min heating and 5.0 min cooling rate). On the other hand, the binary mixture of the PPSQ preceramic polymer with each ingredient was transferred in a mold (30 mm inner diameter) of mounting heating press (Model LaboPress-3, Struers A/S, Copenhagen, Denmark). The mold was then pressed at 150°C under 17kN pressing force for 10 min (5.0 min heating and 5.0 min cooling rate).

Table 3.1. *Vermiculite chemical analysis with XRF.*

Equivalent compound	**Content (%)**
Na_2O	0.197
MgO	22.716
Al_2O_3	7.476
SiO_2	38.701
P_2O_5	2.091
K_2O	3.820
CaO	10.108
TiO_2	0.883
CrO_3	0.097
MnO	0.074
Fe_2O_3	7.531
Loss of ignition	6.307

After initial warm pressing process, the pressed PMSQ containing samples with each ingredient were crosslinked at 250°C in chamber furnace (Model, CWF 1200, Carbolite Gero GmbH & Co. KG., Germany) while the crosslinking of heat treated the PPSQ samples with each ingredient were realized in ash furnace at 300°C for 4.0 h with a heating rate of 10°C/min from the room temperature. After the crosslinking process, all

the samples were further treated with heat at 800°C for 2.0 h with a heating rate of 2°/min from the room temperature. The final heat treatment process of the PMSQ containing binary samples were carried out by placing the samples in a furnace (NABER-Industrieofenbau 2804 Lilienthal, Bremen, Germany), on the other hand, heat treatment of PPSQ containing binary samples were studied in an ash furnace. This final heat treatment process removed mainly the organic part of the samples by combustion with heat.

3.4.2. Phase analysis

The XRD analysis of the binary mixture samples of PMSQ or PPSQ preceramic polymer with one of the following ingredient [i.e., steel fiber, tin sulfide powder mixture (SnS_2, Sn_2S_3, and SnS) or silicon carbide] were studied between 2θ of 5-70° while PMSQ or PPSQ preceramic polymer binary samples with vermiculite were analyzed between 2θ of 2-70° with a 1°/min scan speed. XRD analysis of PMSQ or PPSQ containing binary samples were studied with (MiniFlex 600, Rigaku) and (D8 Advance, Bruker), respectively.

3.4.3. Result and discussion

The resultant XRD patterns of heat treated binary mixtures of the PMSQ or PPSQ preceramic polymer at 800^0C, were compared with raw materials and their heat treated counter parts XRD patterns. Comparative XRD patterns are given in Figure 3.13, 3.14, 3.15 and 3.16.

The XRD pattern of inorganic raw materials and their heat treated counterpart, pyrolyzed preceramic polymers and heat treated binary mixtures (PMSQ and/or PPSQ + one of the inorganic material) are given in Figure 3.13, 14, 15 and 16, respectively. In the XRD pattern of pyrolyzed PMSQ, large hump was appeared in 15-30° range which could be attributed to amorphous SiOC ceramic structure [88]. On the other hand, pyrolyzed PPSQ preceramic polymer exhibited three hump, which were observed at between 2 and 7.5°, 10 and 15° and 15 and 30° range which indicates the amorphous ceramic structure. As seen from the Figures 3.13, 3.14, 3.15 and 3.16, after heat treatment at 800^0C, any delectable change or new phases formation between preceramic polymer and inorganic ingredients were not observed. However, in the XRD graphs of the binary mixtures, amorphous structure of pyrolyzed polymers may mask the recognition of the formation

of the small quantity new phases. This might be caused by the decrease in the resolution of the peaks. The XRD analysis of vermiculite was performed between 2θ of 2 and 70^0 (Figure 3.16). XRD patterns of the pristine vermiculite showed different phases (i.e., vermiculite, hydrobiotite, biotite and phologopite). After heat treatment at 800^0C, the heat treated vermiculite and heat treated binary mixtures (with PMSQ or PPSQ polymer) had different phases compared with the pristine vermiculite. As seen in Figure 3.16, these are phologopite, SiC and augite phases. These identified phases are the most probable ones according to the semi–automatic phase identification software Match! program. The thermal decomposition of vermiculite leads to the removal of the interlayer water molecules and to formation of series of less hydrated phases [89]. The observed peaks for vermiculite at between 2.5 and 10 º shifted into in a single peak (7.5 º) after at 800^0C heat treatment for 2.0 h. However, the hydroxyl groups remained in the structure of the vermiculite as can be seen from TG-DTA curve of vermiculite (Figure 3.12) [87]. Whereas XRD graph of heat treated binary mixture had some difference compared with the heat treated vermiculite (at 800^0C for 2.0 h). This observed difference can be resulted from the amorphous structure of the polymer at that temperature which may hinder the low intensity vermiculite peaks, or it can be occurred by difference in the vermiculite layer orientation and distribution. Additionally, the observable hump arising from the amorphous pyrolyzed polymers which were more pronounced in Figure 3.16 in comparison with the other binary mixtures patterns. Increase in disorder due to the diffusion of polymer between vermiculite layers which increase the layer spacing may be responsible from pronounced hump appearance [90]. All phase identification was performed using Match! software package (Crystal Impact GbR, Bonn, Germany) supported by ICDD PDF-2 Powder Diffraction File (International Center for Diffraction Data, Newtown Square, PA, USA) as the reference database.

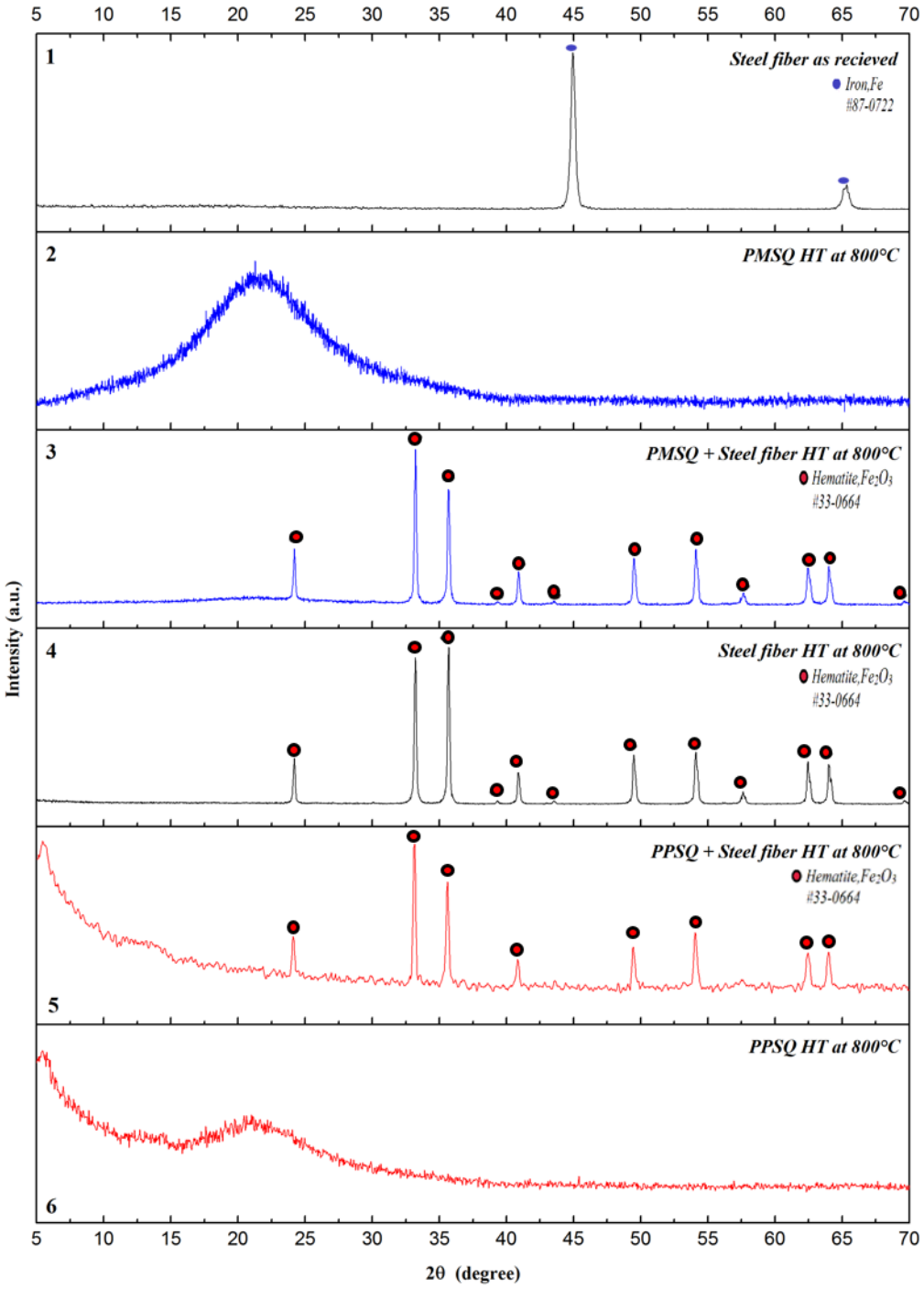

Figure 3.13. *XRD pattern comparison of PMSQ-steel fiber. (1) As received steel fiber, (2) heat treated (HT) PMSQ at 800 ℃, (3) PMSQ polymer + steel fiber binary mixtures heat treated at 800 ℃, (4) heat treated steel fiber at 800 ℃, (5) PPSQ polymer + steel fiber binary mixtures heat treated at 800 ℃, and (6) heat treated PPSQ at 800 ℃.*

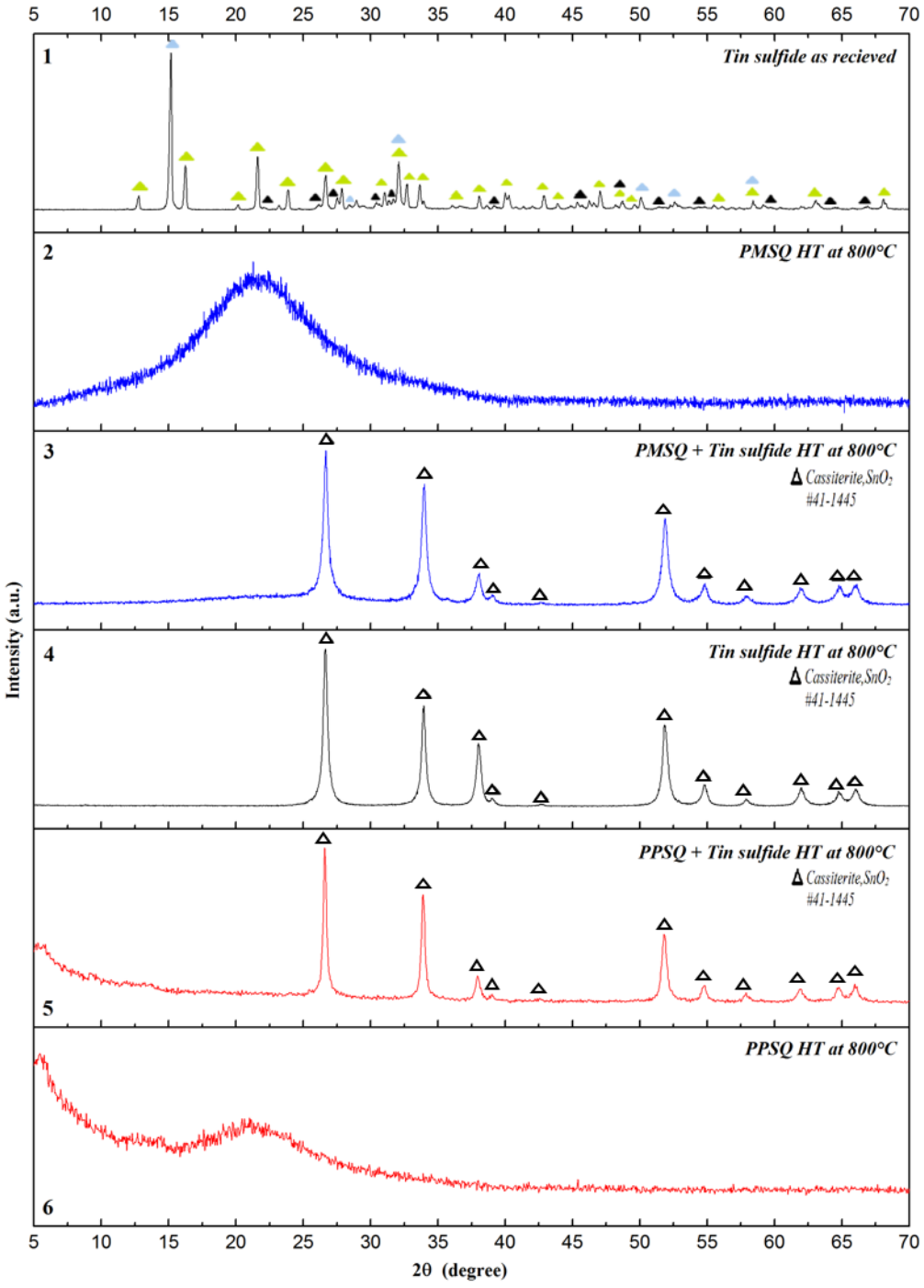

Figure 3.14. *XRD pattern comparison of PMSQ-tin sulfide. (1) As received tin sulfide, (2) heat treated (HT) PMSQ at 800 ℃, (3) PMSQ polymer + tin sulfide binary mixtures heat treated at 800 ℃, (4) heat treated tin sulfide at 800 ℃, (5) PPSQ polymer + tin sulfide binary mixtures heat treated at 800 ℃, and (6) heat treated PPSQ at 800 ℃.*

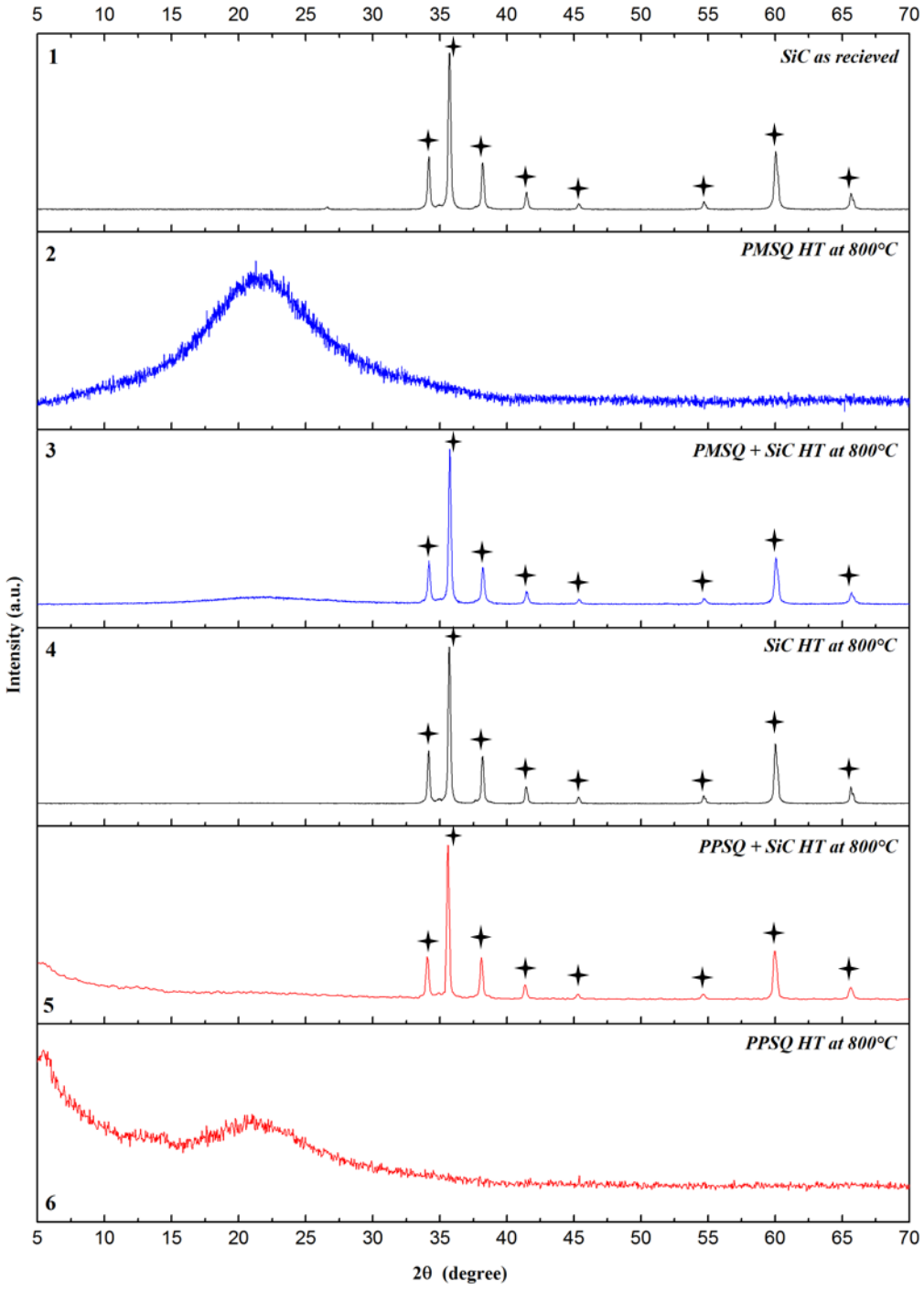

Figure 3.15. *XRD pattern comparison of PMSQ-SiC. (1) As received SiC, (2) heat treated (HT) PMSQ at 800 ºC, (3) PMSQ polymer + SiC binary mixtures heat treated at 800 ºC, (4) heat treated SiC at 800 ºC, (5) PPSQ polymer + SiC binary mixtures heat treated at 800 ºC, and (6) heat treated PPSQ at 800 ºC.*

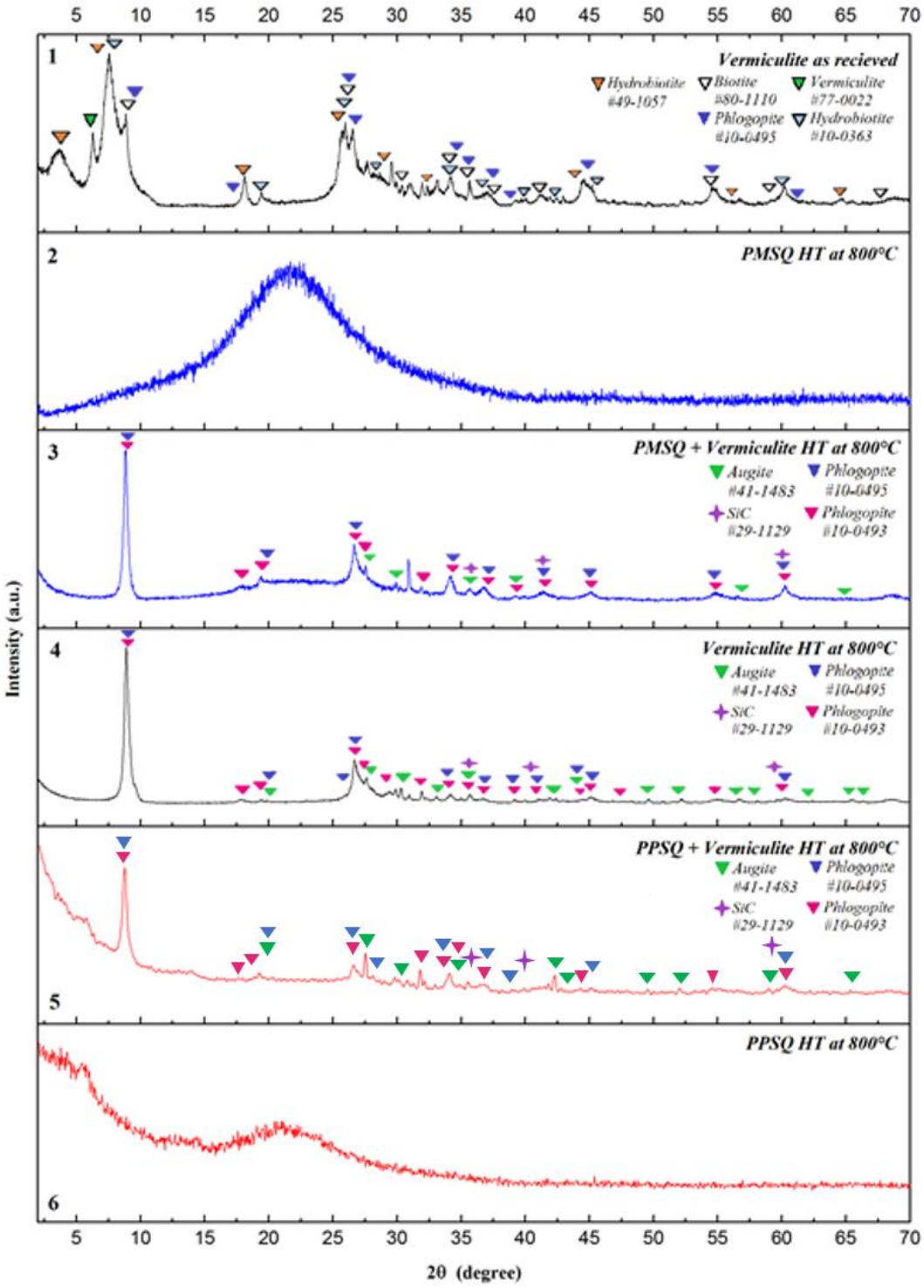

Figure 3.16. *.XRD pattern comparison of PMSQ-vermiculite. (1) As received vermiculite, (2) heat treated (HT) PMSQ at 800 ºC, (3) PMSQ polymer + vermiculite binary mixtures heat treated at 800 ºC, (4) heat treated vermiculite at 800 ºC, (5) PPSQ polymer + vermiculite binary mixtures heat treated at 800 ºC, and (6) heat treated PPSQ at 800 ºC.*

4. PMSQ AND PPSQ MATRIX COMPOSITES

4.1. Processing of PMSQ and PPSQ Matrix Composites

Polymethylsilsesquioxane (PMSQ) and polyphenylsilsesquioxane (PPSQ) matrix composite samples were produced in four step; (i) mixing of powder composite ingredients, (ii) warm pressing of prepared mixtures, (iii) crosslinking of warm pressed samples and (iv) heat treatment of crosslinked samples at five different temperatures (i.e., 400, 500, 600, 700 and 800 ^{0}C). The preparation steps and compositions of composite matrixes are presented schematically in Figure 4.1.

Two different preceramic polymers were used for the preparation of composite matrixes namely polymethylsilsesquioxane and polyphenylsilsesquioxane. These preceramic polymer are known to be converted, after the heating under air atmosphere into amorphous silicon oxycarbide (Si-O-C) ceramic. The silicon oxycarbide is based on the formation of a random network of Si−O and Si−C bonds with a free carbon phase. There are several methods have been reported to produce amorphous silicon oxycarbide ceramic from preceramic polymers. The molecular structure and type of the preceramic polymer influences the composition, the phase distribution as well as the final microstructure of the produced ceramic.

In the presented study, a facile method was used for the preparation of preceramic matrix composite material, firstly, PPSQ was dissolved in acetone (10 mg polymer/10 mL acetone) under magnetic stirring at room temperature for 3.0 min. The mixture (i.e. polymer and acetone) was left to dry under air atmosphere in an oven at 50 °C for 48 h and then ground and sieved under 63μm. The obtained fine PPSQ powder was mixed with the steel fibers, tin sulfide powder mixture (i.e., SnS_2, Sn_2S_3, and SnS), silicon carbide and vermiculite according to formulation given in Table 4.1. On the other hand, the PMSQ was used as received (the particle size < 63μm) and mixed with the steel fibers, tin sulfide powder mixture (i.e., SnS_2, Sn_2S_3, and SnS), silicon carbide and vermiculite.

The preparation of PPSQ and PMSQ preceramic matrix composite material mixtures were carried out in a mechanical blander for 15 min (Kenwood Chef). The composition of the preceramic mixtures are presented in Table 4.1. Each preceramic polymers samples (100 g) were produced by warm pressing method with the 70x80 mm dimensions in a steel mold under given following conditions. A 100 g of PMSQ

preceramic polymer mixture was transferred into preheated steel die at 60°C and warm pressed at 100 MPa for 2 min. On the other hand, the PPSQ matrix composite samples were warm pressed at 150°C, and at 100 MPa for 2 min. Then, the applied pressure on the die, containing sample, was removed, and then, left to cooling until glass transition temperature (T_g) of the used preceramic polymers about 1.0 h. The "T_g" values for PMSQ and PPSQ polymers are 45°C and 64°C, respectively. The dimension of obtained green body after warm pressing was about 70x80x6mm (Figure 4.2).

Table 4.1. *Ingredients and their weight percentage in the composite materials.*

	Preceramic Polymer Percentage	**Ingredients Percentage**			
Materials Compostion	Polymethylsilsesquioxane (PMSQ) **(10%, w/w)**	Steel fibers (40%, w/w)	Tin sulfite mixture (20%, w/w)	SiC (20%, w/w)	Vermiculite (10%, w/w)
	Polyphenylsiloxane (PPSQ) **(10%, w/w)**	Steel fibers (40%, w/w)	Tin sulfide mixture (20%, w/w)	SiC (20%, w/w)	Vermiculite (10%, w/w)

In order to obtain infusible, thermoset polymer matrix with a high ceramic yield, the produced both composite samples were crosslinked before pyrolysis process. The crosslinking process is an important step for the preparation of ceramic from preceramic polymer. This process prevents the loss of low molecular weight components of the precursors as well as fragmentation processes during the pyrolysis process, consequently, results a high ceramic yields [18]. In this work, both PMSQ and PPSQ preceramic polymers are crosslinked by silanol-silanol condensation reactions. The condensation reactions, utilizing the residual silanol groups of the resin molecules and forming Si-O-Si bonds with the elimination of water [22]. Crosslinking of the PMSQ matrix composite samples were studied at 250^0C for 4.0 h with 10^0C/min heating rate using a furnace (Carbolite, CWF 1200). On the other hand, the PPSQ samples were crosslinked in an ash furnace with the same dwelling time and heating rate except that at 300^0C. After crosslinking process, both the PMSQ and PPSQ matrix composite samples were converted in to ceramic structures by heat treatment at five different temperatures (i.e., 400, 500, 600, 700 and 800 ^{0}C) for 2.0 h with a heating rate of 2^0C/min.

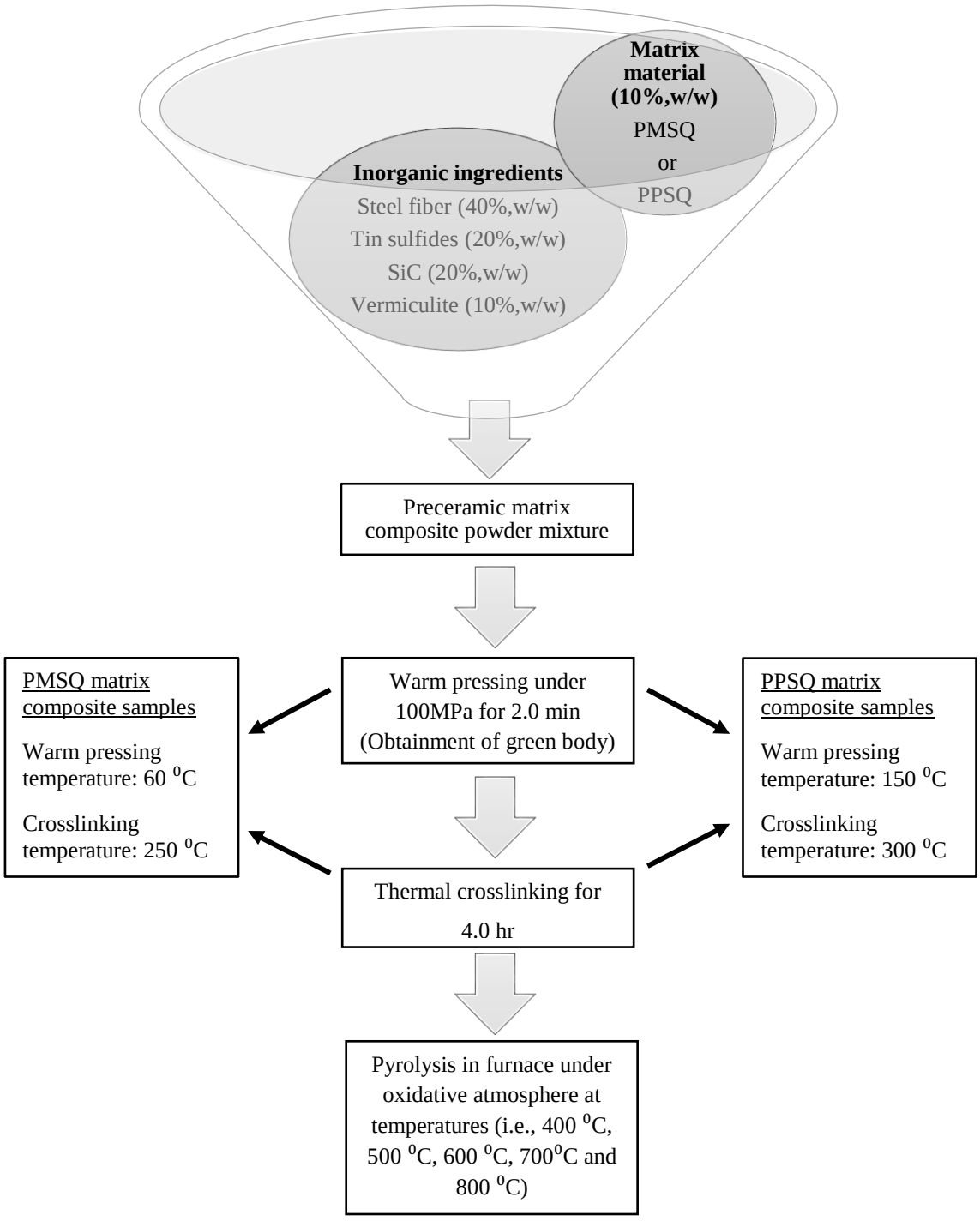

Figure 4.1. *Schematic representation of processing step of preceramic matrix composite samples.*

Heat treatment of the PMSQ matrix composite samples were realized in a furnace (NABER Industrieofenbau D-2804 Lilienthal/Bremen) while PPSQ matrix composite samples were heat treated in ash furnace. These composite materials were produced under direction of co-supervisor Professor Paolo Colombo (University of Padova, Department of Industrial Engineering, Advanced Ceramic Materials Laboratory, Padova, Italy).

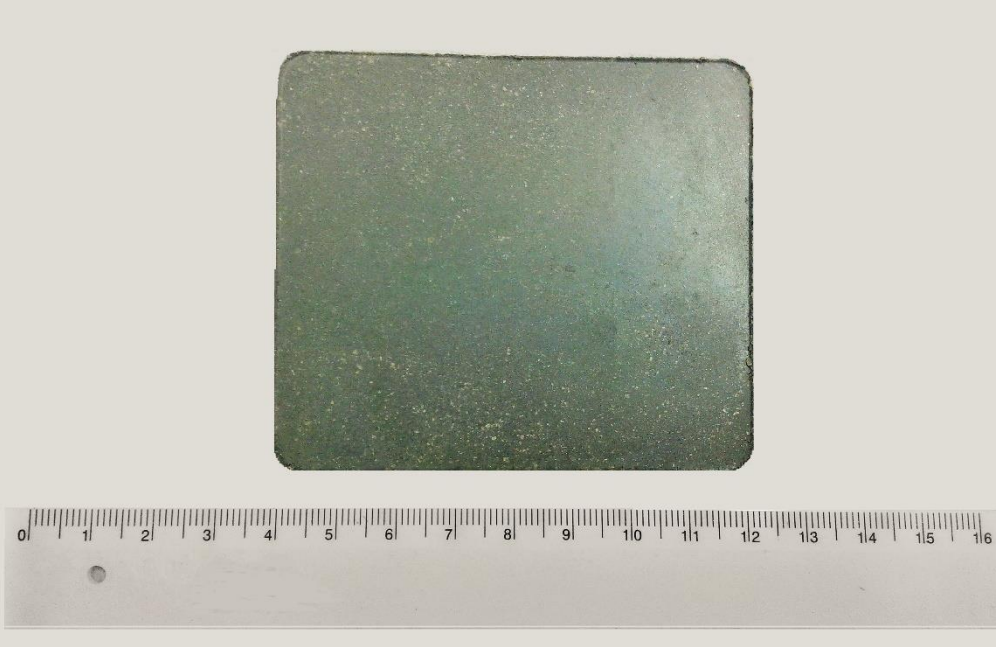

Figure 4.2. *Produced preceramic matrix composite sample by warm pressing technique.*

4.2. Characterization of PMSQ and PPSQ Matrix Composites

Pyrolytic conversion of both preceramic polymers (i.e., PMSQ and PPSQ) to silicon oxycarbide amorphous ceramic structures was monitored by different physical and analytical methods. The produced PMSQ and PPSQ matrix composite samples were characterized at three different conditions: (i) just warm pressed sample (i.e., PMSQ-WP and PPSQ-WP), (ii) just crosslinked sample after warm pressing (i.e., PMSQ-CL and PPSQ-CL), (iii) heat treated samples at different temperatures after crosslinking (i.e., PMSQ-HT400, PMSQ-HT500, PMSQ-HT600, PMSQ-HT700, PMSQ-HT800 and PPSQ-HT400, PPSQ-HT500, PPSQ-HT600, PPSQ-HT700, PPSQ-HT800).

The above given preceramic matrix composite samples were characterized by means of physical, mechanical, phase and microstructural analyses. The PMSQ and PPSQ based samples were cut into 7x7mm size dimension using two different cut-off machines

(i.e., Struers Labotom-3 and Struers Minitom, respectively). The cutting process of the sample is schematically presented in Figure 4.3.

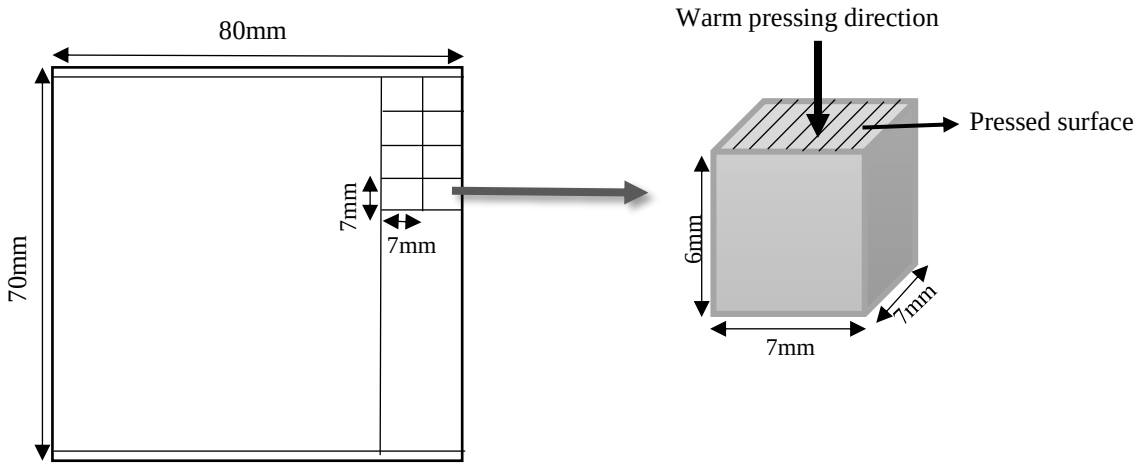

Figure 4.3. *Representative drawing of (a) warm pressed sample; and (b) the cut piece 7x7mm in size from there.*

4.2.1. Thermal analysis

To study thermal behavior of the prepared PMSQ and PPSQ matrix composite powder mixtures, simultaneous thermal analysis (STA), TGA and DTA, were carried out using a STA 449 F3 Jupiter, colorimetry (NETZSCH, Gerätebau GmbH, Selb, Germany). TG-DTA curve of the PMSQ and PPSQ matrix powder composite mixtures were obtained in air atmosphere with 10K/min heating rate in the temperature range 25–800 °C. Measurements were repeated three times for both PMSQ and PPSQ powder composite mixtures, and for all measurements the obtained results are presented in Figure 4.4 and Figure 4.5, respectively.

4.2.2. Mechanical characterization: compressive strength

For the compressive strength measurements, the surface of each cutted samples, in a size 7x7x6mm, were grinded by SiC sand-paper with 180 grit size to obtain plane-parallel surfaces. The determination of compressive strength measurements were performed by universal testing machines with a cross-head speed of 1.0 mm/min and applying load on the surface normal to the warm-pressing direction. The compressive strength measurements of the PMSQ matrix composite materials were made by (Instron 1121 UTM, Danvers, MA) while PPSQ matrix composite materials were measured by (Instron 5581 UTM, Danvers, MA). For all the prepared samples compressive strength

measurements were repeated using six samples to obtain a correlated result. The compressive strength (σc) results are given in Table 4.2.

4.2.3. Physical charactrization: density and porosity

The geometric density (ρ_g) of all the specimens was determined from their geometric dimensions and weights. The apparent (ρ_a) and true density (ρ_t) measurements of samples were carried out by using a gas (helium) pycnometer. The apparent density of the samples were measured with samples in size of 7x7x6mm. On the other hand, 7x7x6mm size samples were ground in agate mortar and then used in powder form to perform true density measurements.

Percentage of the total porosity (TP), open porosity (OP) and closed porosity (CP) values of all the samples were calculated according to following equations: 1, 2 and 3 using the density data obtained from gas pycnometer analysis. The result of the density analysis and calculated porosity of the all samples are given in Table 4.2. Additionally, experimental plot of true density, compressive strength and calculated total porosity values of samples at three different conditions were evaluated together as a function of the temperatures. These results are shown in Figure 4.6.

$$TP = \frac{\rho_t - \rho_g}{\rho_t} \times 100 \qquad (1)$$

$$OP = \frac{\rho_a - \rho_g}{\rho_a} \times 100 \qquad (2)$$

$$CP = TP - OP \qquad (3)$$

4.2.4. Phase analysis

To make a better assessment about the microstructural and mechanical behavior of the each sample, phase compositions of all the samples were studied by X-ray powder diffraction techniques. For the XRD analysis, the samples in dimension 7x7x6mm were cutted from PMSQ and PPSQ matrix composite materials, which were prepared under three different conditions, were manually grinded into fine powder into a agate mortar. The XRD patterns of just warm pressed (i.e., PMSQ-WP and PPSQ-WP), just crosslinked (i.e., PMSQ-CL and PPSQ-CL) and heat treated samples at different temperatures (i.e., PMSQ-HT400, PMSQ-HT500, PMSQ-HT600, PMSQ-HT700, PMSQ-HT800 and PPSQ-HT400, PPSQ-HT500, PPSQ-HT600, PPSQ-HT700, PPSQ-HT800) were

obtained with Cu Kα radiation between 5 and 70^0 diffraction angles (2θ) with a 1°/min scan speed by using MiniFlex 600, Rigaku instrument. The obtained XRD patterns of PMSQ and PPSQ matrix composite materials are given in Figure 4.6 and Figure 4.7, respectively.

4.2.5. Microstructural analysis

In order to examine the microstructure of produced composite samples by SEM three type of specimens were used; i) as pressed surface; ii) fracture surface; and iii) polished pressed surface as shown in Figure 4.3. For all examinations part of the samples cut into the size of 7x7mm with a cut-off machine. The specimens in 7x7mm dimension were cracked in the direction of the warm pressing, and perpendicular to the warm pressed surface for the preparation of second type of samples. Third type of specimens were cold mounted in an epoxy resin and then warm pressed surface of the samples were grinded and polished by semi-automatic grinding and polishing device (Tegramin, Struers, Ballerup, Denmark). Scanning electron microscope (SEM) studies was carried out on Zeiss, Supra 50VP (Carl Zeiss Microscopy GmbH, Jena, Germany)

SEM examinations were realized for three purpose; i) to obtain information about distribution of the used ingredients on the pressed sample surface, to observe the surface morphology of the produced samples and to obtain information about the quantity of the porosity on the surface of the samples in different conditions (i.e., WP, CL and HT at different temperatures) (Figure 4.9 and Figure 4.10); ii) secondly, fracture surface of the samples were examined to obtain information about homogenous distribution of the ingredients in the samples, and also to observe homogenous spreading of the polymer throughout the samples (Figure 4.11 and Figure 4.12); iii) finally, the polished surface of the samples were investigated to observe the oxide layer under surface and BSE images of the samples were taken at 150x and 1500x magnification (Figures 4.13, 4.14, 4.15, 4.16, 4.17, 4.18, 4.19, 4.23, 4.24, 4.25, 4.26, 4.27, 4.28 and 4.29)

Additionally, EDX point analysis were realized. EDX point analysis were acquired for just reticulated sample at 250^0C (Figure 4.20), heat treated sample at 400^0C (Figure 4.21), and 700^0C (Figure 4.22).

4.3. Result and Discussion

4.3.1. Thermal analysis

There are three main weight loss steps were observed for the PMSQ matrix composite at between 60 and 120^{0}C, 120 and 320^{0}C, and 460 and 600^{0}C. As seen in Figure 4.4, at between 360 and 460^{0}C, there was slight weight gain, on the other hand, a significant weight gain was observed at between 600 and 800^{0}C, and the mass change was found to be 5.36%. The first weight loss about -0.20% can be related with the loss of the bound water molecules. Additionally, the crosslinking reaction of the PMSQ polymer and the phase transformation of tin sulfides mixture likely causes the second weight loss at between 120 and 320 ^{0}C, and the observed mass change was about -1.73%. At the temperature range 50-275^{0}C, the dehydration reactions of vermiculite was also caused a weight loss at this temperature range. Whereas the weight loss in the temperature 460 - 600^{0}C (mass change -1.07%) should be caused by oxidation of tin sulfides and organic to inorganic transformation of the preceramic polymer. As can be seen from Figure 3.10, the exothermic DTA curve at between 300 and 521 ^{0}C was compatible with the TG-DTA graph of tin sulfide powder mixture. On the other hand, the observed peak at 651 ^{0}C (as seen in Figure 4.4) was not detected within studied TG-DTA analysis of all the raw materials. As reported earlier, it is known that preceramic polymers are used to create oxidation protective coatings on steels [4]. It should be noted that the spreading of the preceramic polymers around the steel fibers can yield formation a protective layer during oxidation of preceramic polymer to Si-O-C form, and the formed ceramic layer may retard the oxidation of the steel fibers in the composite materials. It should be also stated that tin sulfides can likely act as a reducing agent, and retard the oxidation of the steel fiber until 600 ^{0}C, which actually begin to occur above 300 ^{0}C as seen in Figure 3.9. The result of the thermal analysis show that PMSQ composite materials gained weight about 2.36% when the thermal analysis was studied from room temperature to 800^{0}C under air atmosphere.

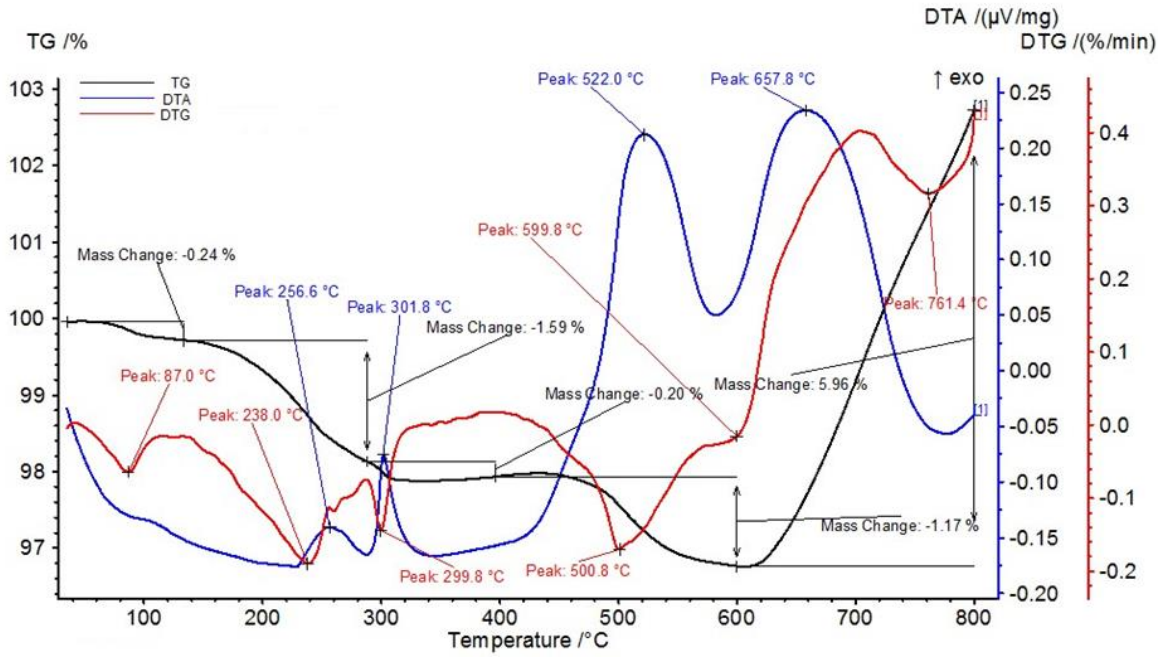

Figure 4.4. *TG-DTA curve of PMSQ matrix composite powder mixtures.*

As can be seen from Figure 4.5, mainly three weight loss steps and one weight gain step are observed. The observed weight loss steps were between; at 40 and 150^{0}C, 150 and 360^{0}C, and 420 and 680^{0}C. Whereas the weight gain step was seen in the temperature range at 680 - 800^{0}C (about 2.0%). In the first step, the observed mass change was found to be -0.49%, could be due to the loss of bound water molecules. In the second step, at between 150 and 360^{0}C, the crosslinking reactions of PPSQ, phase transformation of tin sulfides and dehydration reactions of vermiculite caused about -1.65% mass loss. At the third weight loss step, initiation of organic to inorganic transformation of PPSQ preceramic polymer (at around 420^{0}C) and oxidation of tin sulfide caused a mass reduction about -5.18%. In Figure 4.5, the DTA curve at 254 and 519^{0}C show an exothermic behavior arising from oxidation of tin sulfide powder mixture. As observed like in DTA graph of PMSQ composite matrix (Figure 4.4), the exothermic DTA peak at 609^{0}C was not compatible with any of the TG-DTA curves of the studied raw materials (Figure 3.9- Figure 3.12). As noted above, the observed exothermic DTA peak at 609^{0}C can belong to the oxidation peak of the steel fibers, which is retarded the oxidation of steel fiber due to the formation of protective Si-O-C layer around the steel fibers, and reducing agent effect of tin sulfide powder mixture. As can be seen in DTA curve (Figure 4.5) the increase in mass gain at 680^{0}C can be originated from the oxidation of both steel

fiber and tin sulfide mixture. As a result the PPSQ matrix composite powder mixture had a mass reduction -5.32% at the end of the thermal analysis which was carried out from room temperature to 800^0C.

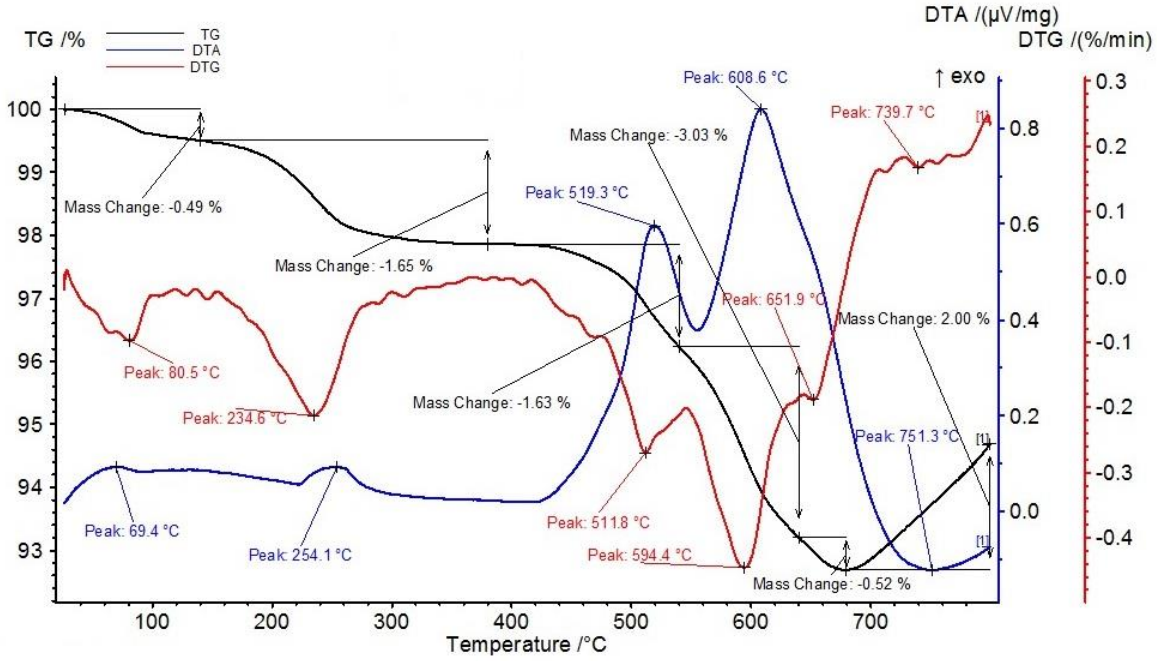

Figure 4.5. *TG-DTA curve of PPSQ matrix composite powder mixtures.*

4.3.2. Mechanical and physical characterization

Results of density measurements, calculated amount of porosity and compressive strength measurements are given in Table 4.2 and Figure 4.6. Continuous increase in the true density is caused by organic to inorganic transformation of the polymer. In general, density increases with the pyrolysis temperature due the increased network connectivity occurred by realizing the hydrogen present in residual C–H bonds [5]. Density increases by a factor of 2 to 3 from the precursor (1 g/cm^3) to the ceramic residue (SiO_2, 2.2-2.6 g/cm^3 and SiC, 3.0-3.2 g/cm^3) [1].

Table 4.2. *Results of compressive strength, density measurements and total porosity calculations.*

	Mechanical and physical analysis results	Warm pressing temperature	Crosslinking temperature	Heat treatment temperatures				
PMSQ matrix composite samples		**60°C**	**250°C**	**400°C**	**500°C**	**600°C**	**700°C**	**800°C**
	бc (MPa)	99 ± 9	98 ± 6	68 ± 15	113 ± 16	159 ± 19	87 ± 21	77 ± 14
	ρ_g (g/cm$_3$)	3.250 ± 0.151	3.286 ± 0.222	2.935 ± 0.122	3.145 ± 0.087	3.364 ± 0.087	3.076 ± 0.105	3.144 ± 0.110
	ρ_a (g/cm$_3$)	3.662 ± 0.002	3.738 ± 0.008	3.827 ± 0.003	3.925 ± 0.003	4.264 ± 0.001	4.196 ± 0.002	4.195 ± 0.004
	ρ_t (g/cm$_3$)	3.720 ± 0.002	3.747 ± 0.001	3.805 ± 0.001	3.889 ± 0.002	4.181 ± 0.001	4.158 ± 0.002	4.216 ± 0.003
	OP (%)	11.3	12.1	23.3	19.9	21.1	26.7	25.1
	TP (%)	12.6	12.3	22.9	19.1	19.5	26.0	25.4
	CP (%)	1.4	0.2	-0.4	-0.7	-1.6	-0.7	0.4
PPSQ matrix composite samples		**150°C**	**300°C**	**400°C**	**500°C**	**600°C**	**700°C**	**800°C**
	бc (MPa)	120 ± 4	115 ± 9	133 ± 3	125 ± 2	125 ± 4	69 ± 3	74 ± 3
	ρ_g (g/cm$_3$)	3.419 ± 0.020	3.116 ± 0.046	3.147 ± 0.032	3.122 ± 0.021	3.210 ± 0.018	3.072 ± 0.034	2.894 ± 0.067
	ρ_a (g/cm$_3$)	3.515 ± 0.015	3.55 ± 0.014	3.622 ± 0.018	4.064 ± 0.028	4.353 ± 0.042	4.129 ± 0.023	3.949 ± 0.014
	ρ_t (g/cm$_3$)	3.593 ± 0.012	3.643 ± 0.011	3.75 ± 0.022	4.241 ± 0.025	4.314 ± 0.033	4.113 ± 0.014	4.035 ± 0.023
	OP (%)	2.7	12.2	13.1	23.2	26.3	25.6	26.7
	TP (%)	4.8	14.5	16.1	26.4	25.6	25.3	28.3
	CP (%)	2.1	2.2	3.0	3.2	-0.7	-0.3	1.6

As observed from the Figure 4.6, a sharp increase in the calculated total porosity is observed at between 250 and 400 ^{0}C for PMSQ matrix composite. In the TG-DTA graph of PMSQ (Fig. 3.7), a weight loss was observed about 7.35% at above given temperature range due to released water during the crosslinking reaction. The observed slight decrease

in total porosity at between 500 and 600^{0}C could be associated with the oxidation of the materials (i.e., steel fibers and tin sulfite mixture). Figure 4.7 shows the XRD patterns of the PMSQ matrix composite samples which were heat treated at different temperatures. The first oxide formations (SnO_2 and Fe_3O_4) were observed at 500^{0}C. The formation of metal oxides may fill the pores which remain after decomposition of tin sulfides and pore space which remain after pyrolysis of the preceramic polymer. Additionally, melting of SnS_2 at 600^{0}C may contribute a decrease in the total porosity by increasing oxide formation. On the other hand, an enhancement in the total porosity was observed again at between 700 and 800 ^{0}C which can be substantially related with pyrolysis reactions of the preceramic polymer as seen from Figure 3.7. On the other hand, a sharp increase in amount of the total porosity of the PPSQ matrix composite samples was observed at between 150 and 500^{0}C, can be due to the crosslinking and pyrolysis reactions of the preceramic polymers. The amounts of the total porosity values are nearly same at three different temperatures namely 500, 600 and 700^{0}C, whereas an increase in total porosity was observed at 800^{0}C. It could be due to the dehydrogenation reaction of PPSQ polymer, this reaction take placed at around 650^{0}C [91]. Organic to inorganic transformation reactions of the studied preceramic polymers lead to increase in the total porosity at all the tested heat treatment temperatures.

As can be seen in Figure 4.6, as expected, compressive strength values of the PMSQ matrix samples were inversely proportional with the total amount of porosity. Additionally, it can be seen from BSE the images of the PMSQ surfaces from pressed site Figure 4.9, as observed from this figure, the microstructural feature of the pressed samples verified the compressive strength results. The release of gaseous product, and shrinkage of polymer during pyrolysis can cause high porosity. Thus, the formed porous structures lead the formation of macro-cracks at the heat treated sample at 400 ^{0}C which can yield a low compressive strength. On the other hand, at between 500 and 600 ^{0}C, a reduction in the amount of formed porosity and cracks formation were observed, thus, increasing in the integrity of the samples provide higher compressive strength values compared with sample treated at 400 ^{0}C. Macro-cracks formation were again observed at 700 and 800 ^{0}C, the steel fibers in the composite ingredients were subjected a high rate oxidation compared with sample heat treated at 600 ^{0}C, thus, the high rate oxidation at the elevated temperature caused a sharp decrease in the compressive strength of the materials heated

at these high temperatures. In the case of PPSQ matrix composite sample, compressive strength values were slightly inversely proportional with the amount of the formed total porosity. Compressive strength values in the temperature range 300 - 600^{0}C were close to each other, and a maximum compressive strength value was obtained at 400^{0}C.

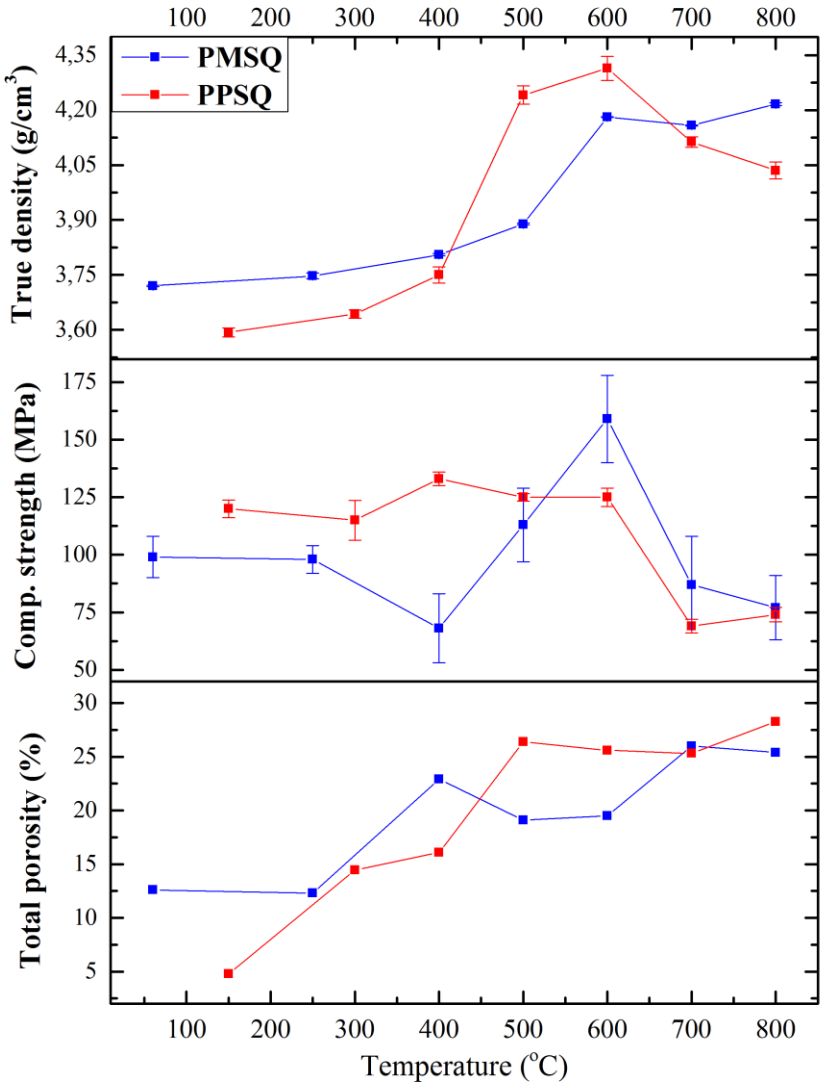

Figure 4.6. *Plots of true density, compressive strength and calculated total porosity values of PMSQ and PPSQ matrix samples processed at three different temperatures.*

At this temperature, the crosslinking reaction is completed, and organic to inorganic transformation of the preceramic polymer was began which cause the high weight loss in

material. Slight decrease in compressive strength value at 500^0C is probably caused by the micro- and macro-crack formation at that temperature which is seen in Figure 4.10. Increase in macro-crack formation and oxidation of steel fibers were more pronounced at 700^0C compared with other tested temperatures (Figure 4.10), which resulted a decrease in the compressive strength value at this temperature. It should be noted that the obtained low compressive strength value at 800^0C, could be originated from the degradation of the composite body with increasing oxidation rate.

For both preceramic polymer composites, a sharp decrease in compressive strength at 600^0C was observed due to the oxidation of the steel fibers at that temperature. It should be noted that when compressive strength values of the PPSQ and PMSQ matrix composites samples are compared with each other, it can be seen that PMSQ samples have maximum compressive strength values but it does not show stable values at the studied different temperatures, however, the compressive strength values of the PPSQ matrix composite samples at between 150 and 600^0C yield more stable results.

4.3.3. Phase analysis

The studied XRD pattern of the PMSQ and PPSQ matrix composite samples and their observed phases in three different conditions are given in Figure 4.7 and Table 4.3, and Figure 4.8 and Table 4.4., respectively. The XRD patterns of just warm pressed samples of both the composite compositions give peaks related with the ingredients materials. Identified phases are vermiculite (#77-0022), hydrobiotite (#10-0363), biotite (#80-1110), moissanite (SiC, #74-1302), iron (Fe, #87-0722), tin sulfide (Sn_2S_3, #72-0031), berndtite (SnS_2, #23-0677) and herzenbergite (SnS, #39-0354) with their ICDD numbers. The XRD analysis show that the used tin sulfide powder mixture include Sn_2S, Sn_2S_3, and SnS compounds. As can be observed from Figure 4.7, the patterns of the just crosslinked sample (at 250°C and 300°C) and the heat treated samples at 400 ^{0}C have very similar patterns with the just warm pressed samples. As reported previously, the vermiculite contains water and hydroxyl groups, the bound water remains its structure above 100^0C. The vermiculite can be rehydrated around 700 ^{0}C [89]. It also reported that the type of the cations and the layers charge can affect the dihydroxylation behavior of the vermiculite [92, 93]. The intensity of the SnS_2 peak at 400^0C was decreased which is caused most likely the structural transformation of SnS_2 to Sn_2S_3 [94]. As can be seen from Table 4.3, the first oxides cassiterite, (SnO_2, #41-1445), magnetite (Fe_3O_4, #75-

1610) and additionally hematite (Fe_2O_3, #33-0664) phases for just PPSQ matrix composite sample were formed at 500^0C. The low intensity iron peak was not identified at 65^0. Additionally, the significant decrease in the intensity of SnS_2 and Sn_2S_3 peaks were observed in the XRD patterns of the PMSQ matrix composite samples due to the SnO_2 formation. This observation is compatible with the thermal analysis result of tin sulfide as shown in Figure 3.10. On the other hand, in the XRD patterns of the PPSQ matrix composite, SnS_2 and Sn_2S_3 peaks were disappeared at 500^0C. The indicated fayalite phase at 400^0C by EDX analysis is presented in (Figure 4.21). The same fayalite phase was also identified in the XRD pattern of the heat treated sample at 600 ^{0}C, the realization of the fayalite phase most probably could be due to the increased amount of oxidation. In the XRD patterns of the heat treated samples at 600 ^{0}C, phologopite (#10-0495), fayalite, (Fe_2SiO_4, #71-1669), iron silicon oxide ($Fe5.36Si_{0.64}O_8$, #81-0532), and iron tin ($FeSn_2$, #25-0415) phases were identified, and these phase were different from the heat treated samples at 500 ^{0}C. And also observable hematite (Fe_2O_3, #33-0664) phase formation was seen for PMSQ matrix composite sample at 600^0C. The observable change in the 6-10^0 range showed that dehydration of the vermiculite was completed, and dihydroxylation process was realized at 600 ^{0}C. This observation is also confirmed by the TG-DTA analysis, and the observed curve of the vermiculite is presented in Figure 3.12 [87]. In the XRD graph of PMSQ matrix composite samples, the observed peaks for SnS_2 and Sn_2S_3 were disappeared, and the intensity of the SnO_2 is increased, and this was also confirmed in Figure 3.10. As shown in Figure 4.7, the heat treated sample has an iron sulfide (FeS, #76-0962) phase at 700 ^{0}C, and is not observed for the sample treated at 600 ^{0}C. As shown in Figure 4.7 and Figure 4.8, an increased in the intensity of hematite (Fe_2O_3) peak and a decreased intensity of the herzenbergite (SnS) peak were observed, and could be due to the onset of degradation of the both composite compositions samples at 700^0C, which can be seen in Figure 4.9 and Figure 4.10. In the XRD patterns of heat treated samples at 800^0C, iron tin (Fe_3Sn, #73-2029) phase was observed for both composite compositions (Figure 4.9 and Figure 4.10). Apart from that, iron sulfide (FeS, #76-0962) and iron carbide ($CFe_{2.5}$, #36-1248) phases are identified in the PMSQ and PPSQ matrix composite sample, respectively. As can be seen from Figure 4.19 and Figure 4.29, the steel fibers are almost entirely oxidized which is confirmed by the disappeared peak of Fe at 44.75^0 at 800 ^{0}C. In literature, a significant linear dependence has been reported between the amount of the free carbon and the amount of phenyl groups [51, 95].

It may be said that, disappearance of SnS_2 and Sn_2S_3 peaks at 500^0C and formation of iron carbide phase at 800^0C in the PPSQ matrix composite can be caused from the high free carbon content of the PPSQ based composition. The excess amount of carbon may be increase the decomposition of the tin sulfides by forming carbon disulfide (CS_2), and the formation of iron carbide ($CFe_{2.5}$) phase at high temperature.

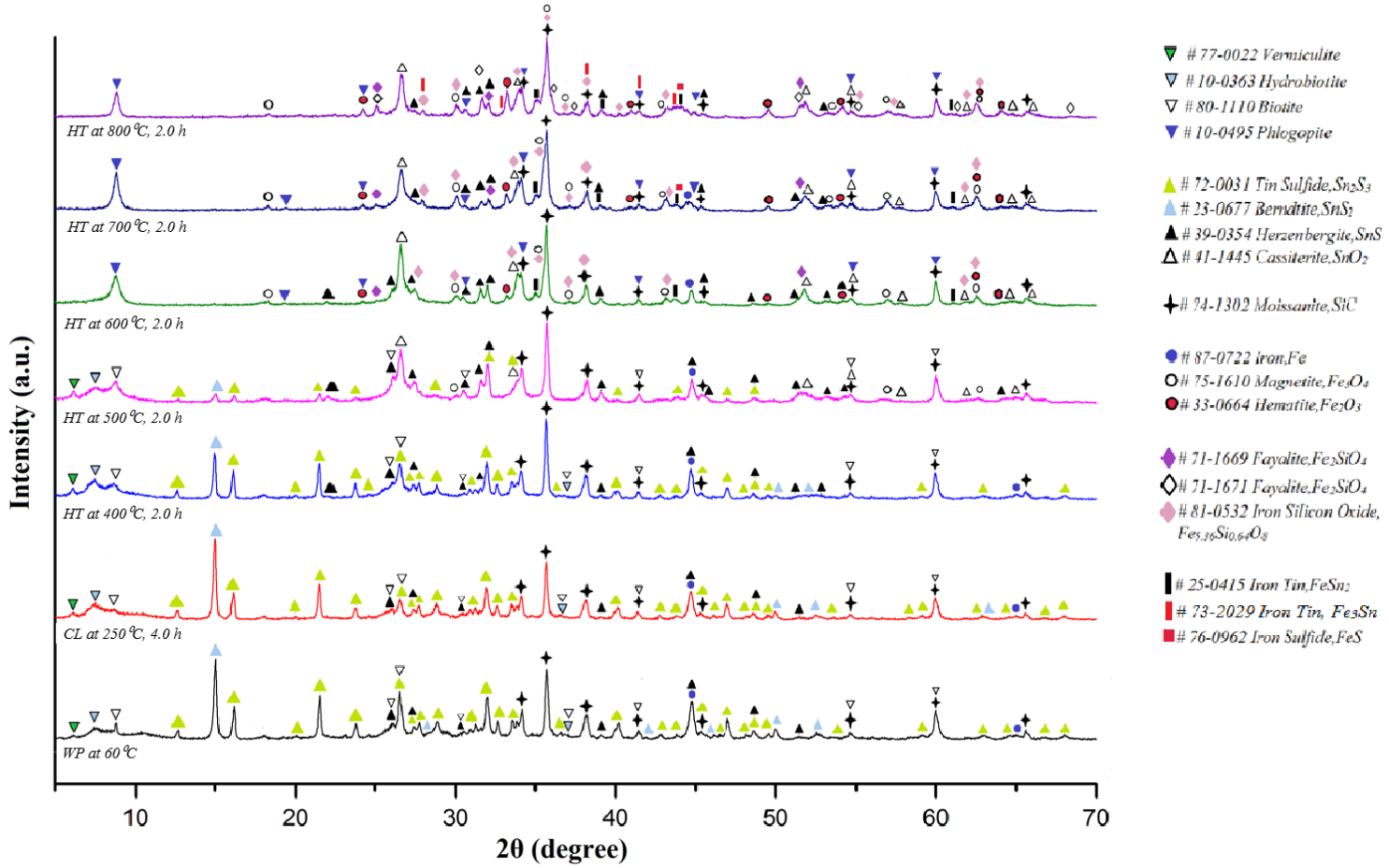

Figure 4.7. *XRD patterns of just warm pressed sample (PMSQ-WP), just crosslinked sample after warm pressing (PMSQ-CL), heat treated samples at different temperatures after crosslinking (PMSQ-HT400, PMSQ -HT500, PMSQ -HT600, PMSQ -HT700, and PMSQ -HT800).*

Table 4.3. *Obtained phases from the XRD analysis of PMSQ matrix composite samples.*

Obtained Phases from the Different Conditions of PMSQ Matrix Composite Samples							
Warm pressed	Crosslinked (CL)	Heat treated at different temperatures (HT)					
60^0C	250^0C	400^0C	500^0C	600^0C	700^0C	800^0C	**PMSQ Matrix Composite Samples**
Vermiculite (#77-0022)	Vermiculite (#77-0022)	Vermiculite (#77-0022)	Vermiculite (#77-0022)	Phologopite (#10-0495)	Phologopite (#10-0495)	Phologopite (#10-0495)	
Hydrobiotite (#10-0363)	Hydrobiotite (#10-0363)	Hydrobiotite (#10-0363)	Hydrobiotite (#10-0363)	Moissanite, SiC (#74-1302)	Moissanite, SiC (#74-1302)	Moissanite, SiC (#74-1302)	
Biotite (#80-1110)	Biotite (#80-1110)	Biotite (#80-1110)	Biotite (#80-1110)	Iron, Fe (#87-0722)	Iron, Fe (#87-0722)	Herzenbergite, SnS (#39-0354)	
Moissanite, SiC (#74-1302)	Moissanite, SiC (#74-1302)	Moissanite, SiC (#74-1302)	Moissanite, SiC (#74-1302)	Herzenbergite, SnS (#39-0354)	Herzenbergite, SnS (#39-0354)	Cassiterite, SnO_2 (#41-1445)	
Iron, Fe (#87-0722)	Iron, Fe (#87-0722)	Iron, Fe (#87-0722)	Iron, Fe (#87-0722)	Cassiterite, SnO_2 (#41-1445)	Cassiterite, SnO_2 (#41-1445)	Magnetite, Fe_3O_4 (#75-1610)	
Tin Sulfide, Sn_2S_3 (#72-0031)	Tin Sulfide, Sn_2S_3 (#72-0031)	Tin Sulfide, Sn_2S_3 (#72-0031)	Tin Sulfide, Sn_2S_3 (#72-0031)	Magnetite, Fe_3O_4 (#75-1610)	Magnetite, Fe_3O_4 (#75-1610)	Hematite, Fe_2O_3 (#33-0664)	
Berndtite, SnS_2 (#23-0677)	Berndtite, SnS_2 (#23-0677)	Berndtite, SnS_2 (#23-0677)	Berndtite, SnS_2 (#23-0677)	Hematite, Fe_2O_3 (#33-0664)	Hematite, Fe_2O_3 (#33-0664)	Fayalite, Fe_2SiO_4 (#71-1669)	
Herzenbergite, SnS (#39-0354)	Herzenbergite, SnS (#39-0354)	Herzenbergite, SnS (#39-0354)	Herzenbergite, SnS (#39-0354)	Fayalite, Fe_2SiO_4 (#71-1669)	Fayalite, Fe_2SiO_4 (#71-1669)	Fayalite, Fe_2SiO_4 (#71-1671)	
			Cassiterite, SnO_2 (#41-1445)	Iron silicon oxide, $Fe_{5.36}Si_{0.64}O_8$	Iron silicon oxide, $Fe_{5.36}Si_{0.64}O_8$	Iron silicon oxide, $Fe_{5.36}Si_{0.64}O_8$	
			Magnetite, Fe_3O_4 (#75-1610)	Iron Tin, $FeSn_2$ (#25-0415)	Iron Tin, $FeSn_2$ (#25-0415)	Iron Tin, $FeSn_2$ (#25-0415)	
					Iron Sulfide, FeS (#76-0962)	Iron Sulfide, FeS (#76-0962)	
						Iron Tin, Fe_3Sn (#73-2029)	

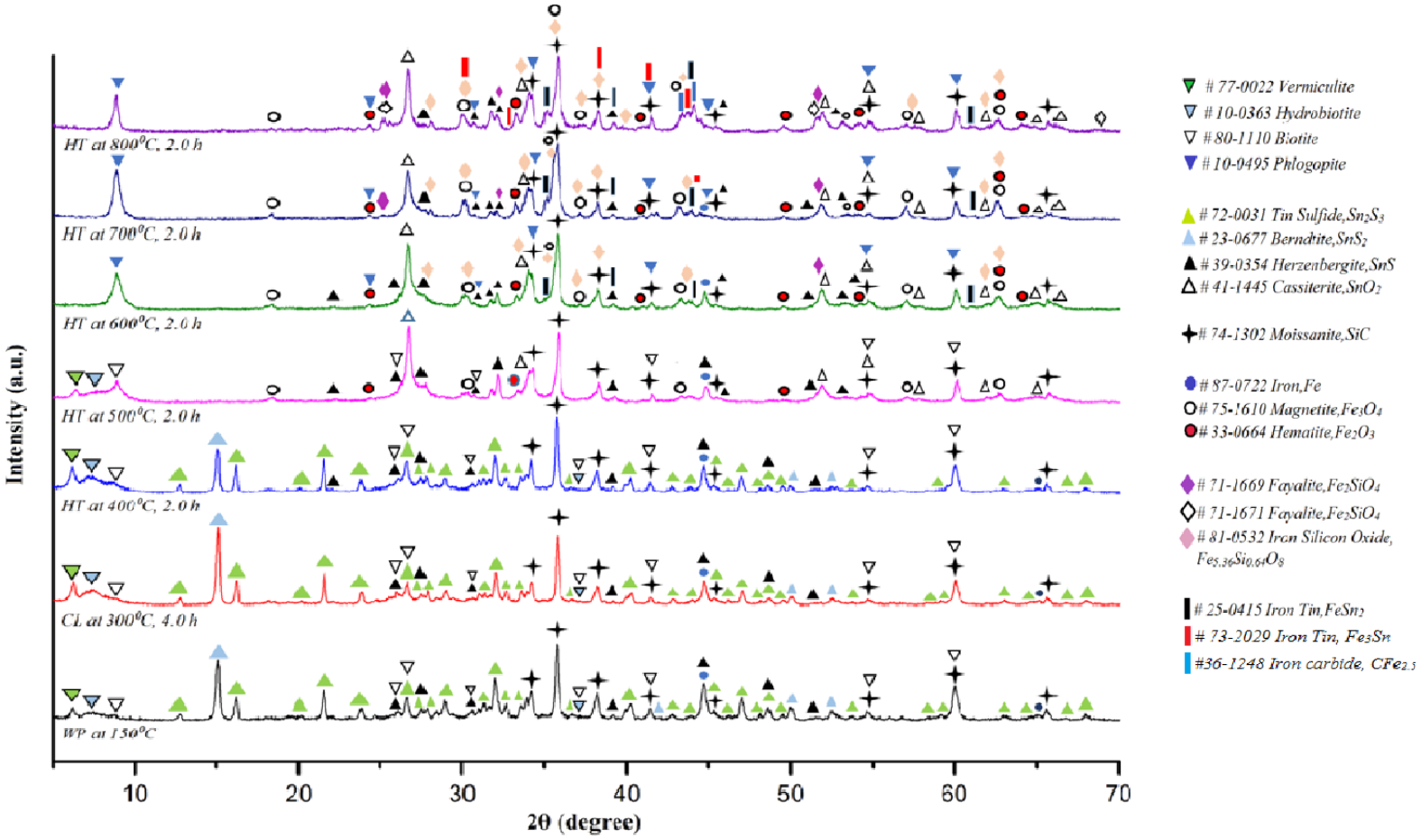

Figure 4.8. *XRD patterns of just warm pressed sample (PPSQ-WP), just crosslinked sample after warm pressing (PPSQ-CL), heat treated samples at different temperatures after crosslinking (PPSQ-HT400, PPSQ -HT500, PPSQ -HT600, PPSQ -HT700, and PPSQ -HT800).*

Table 4.4. *Obtained phases from the XRD analysis of PPSQ matrix composite samples.*

Obtained Phases from the Different Conditions of PPSQ Matrix Composite Samples							
Warm pressed	Crosslinked (CL)	Heat treated at different temperatures (HT)					
60^0C	250^0C	400^0C	500^0C	600^0C	700^0C	800^0C	**PPSQ Matrix Composite Samples**
Vermiculite (#77-0022)	Vermiculite (#77-0022)	Vermiculite (#77-0022)	Vermiculite (#77-0022)	Phologopite (#10-0495)	Phologopite (#10-0495)	Phologopite (#10-0495)	
Hydrobiotite (#10-0363)	Hydrobiotite (#10-0363)	Hydrobiotite (#10-0363)	Hydrobiotite (#10-0363)	Moissanite, SiC (#74-1302)	Moissanite, SiC (#74-1302)	Moissanite, SiC (#74-1302)	
Biotite (#80-1110)	Biotite (#80-1110)	Biotite (#80-1110)	Biotite (#80-1110)	Iron, Fe (#87-0722)	Iron, Fe (#87-0722)	Herzenbergite, SnS (#39-0354)	
Moissanite, SiC (#74-1302)	Moissanite, SiC (#74-1302)	Moissanite, SiC (#74-1302)	Moissanite, SiC (#74-1302)	Herzenbergite, SnS (#39-0354)	Herzenbergite, SnS (#39-0354)	Cassiterite, SnO_2 (#41-1445)	
Iron, Fe (#87-0722)	Iron, Fe (#87-0722)	Iron, Fe (#87-0722)	Iron, Fe (#87-0722)	Cassiterite, SnO_2 (#41-1445)	Cassiterite, SnO_2 (#41-1445)	Magnetite, Fe_3O_4 (#75-1610)	
Tin Sulfide, Sn_2S_3 (#72-0031)	Tin Sulfide, Sn_2S_3 (#72-0031)	Tin Sulfide, Sn_2S_3 (#72-0031)	Tin Sulfide, Sn_2S_3 (#72-0031)	Magnetite, Fe_3O_4 (#75-1610)	Magnetite, Fe_3O_4 (#75-1610)	Hematite, Fe_2O_3 (#33-0664)	
Berndtite, SnS_2 (#23-0677)	Berndtite, SnS_2 (#23-0677)	Berndtite, SnS_2 (#23-0677)	Berndtite, SnS_2 (#23-0677)	Hematite, Fe_2O_3 (#33-0664)	Hematite, Fe_2O_3 (#33-0664)	Fayalite, Fe_2SiO_4 (#71-1669)	
Herzenbergite, SnS (#39-0354)	Herzenbergite, SnS (#39-0354)	Herzenbergite, SnS (#39-0354)	Herzenbergite, SnS (#39-0354)	Fayalite, Fe_2SiO_4 (#71-1669)	Fayalite, Fe_2SiO_4 (#71-1669)	Fayalite, Fe_2SiO_4 (#71-1671)	
			Cassiterite, SnO_2 (#41-1445)	Iron silicon oxide, $Fe_{5.36}Si_{0.64}O_8$ (#81-0532)	Iron silicon oxide, $Fe_{5.36}Si_{0.64}O_8$ (#81-0532)	Iron silicon oxide, $Fe_{5.36}Si_{0.64}O_8$ (#81-0532)	
			Magnetite, Fe_3O_4 (#75-1610)	Iron Tin, $FeSn_2$ (#25-0415)	Iron Tin, $FeSn_2$ (#25-0415)	Iron Tin, $FeSn_2$ (#25-0415)	
			Hematite, Fe_2O_3 (#33-0664)		Iron Sulfide, FeS (#76-0962)	Iron carbide, $CFe_{2.5}$ (#36-1248)	
						Iron Tin, Fe_3Sn (#73-2029)	

Some of the following phases are identified such as hyrobiotite (PDF# 10-0363), biotite (PDF#80-1110), phologopite (PDF#10-0495), iron sulfide (FeS, PDF#76-0962), fayalite (Fe_2SiO_4, PDF#71-1669, PDF#71-1671), iron silicon oxide (Fe5.36Si0.64O8, PDF#81-0532), iron tin (FeSn2, PDF#25-0415), iron carbide (CFe2.5, PDF#36-1248), according to the semi-automatic phase identification software program Match!.

4.3.4. Microstructural analysis

The SEM images of the warm pressed samples surface were obtained at different heat treatment temperatures. To observe the effect of the heat treatment on the pore size, pore distributions and the amount of the formed pores, the surface morphology of the samples and the crack formations of the tested materials were obtained by BSE imaging mode at low magnification (150x).

As can be observed from Figure 4.9 and Figure 4.10, the ingredients of the composite material were not homogenously distributed through the sample, and was more pronounced for the steel fibers. Therefore, the steel fiber groups are particularly observed within all the sample structures. This might be caused by the difference in the densities of the used ingredients. For PMSQ matrix composite samples, it should be noted that there were no significant change, in terms of morphology, between the just warm pressed sample at 60 ^{0}C and just reticulated sample at 250 ^{0}C. After heat treatment at 400 ^{0}C, the first significant weight reduction was observed, which also resulted the formation of many pores and cracks. These observations can be due to the release of organic part of the polymer in the gaseous form and also the shrinkage of polymer. The observable macro-cracks in PMSQ-HT400 sample were disappeared after heat treatment at 500^{0}C, and also the amount of the formed pores was decreased. At this low magnification (i.e., 150x), the PMSQ-HT600 sample had lower porosity than those of the heat treated ones at 500 ^{0}C (Figure 4.9d and 4.9e). Additionally, the integrities of the PMSQ-HT500 and PMSQ-HT600 samples were higher than that of the sample treated at 400 ^{0}C. The samples treated at between 700 and 800^{0}C, showed a decrease in the pore fraction while the formation of micro and macro-cracks increased.

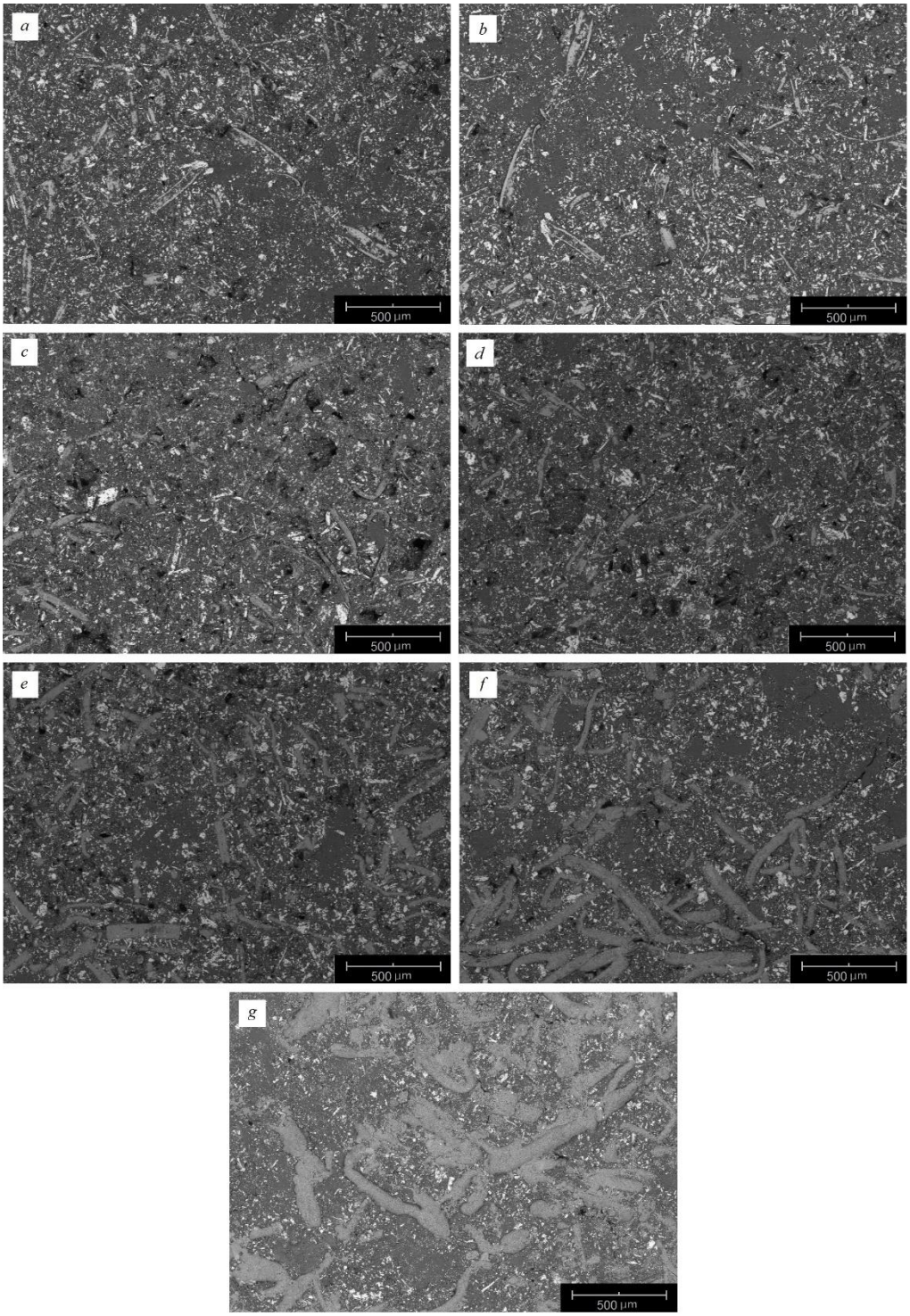

Figure 4.9. *BSE images of as pressed surface of PMSQ matrix composite samples in three different conditions at 150x magnification; (a) just warm pressed sample at 60 ^{0}C (PMSQ-WP), (b) just crosslinked sample after warm pressing at 250 ^{0}C (PMSQ-CL), and heat treated samples at different temperatures after crosslinking (c) PMSQ-HT400, (d) PMSQ -HT500, (e) PMSQ -HT600, (f) PMSQ -HT700, and (g) PMSQ -HT800.*

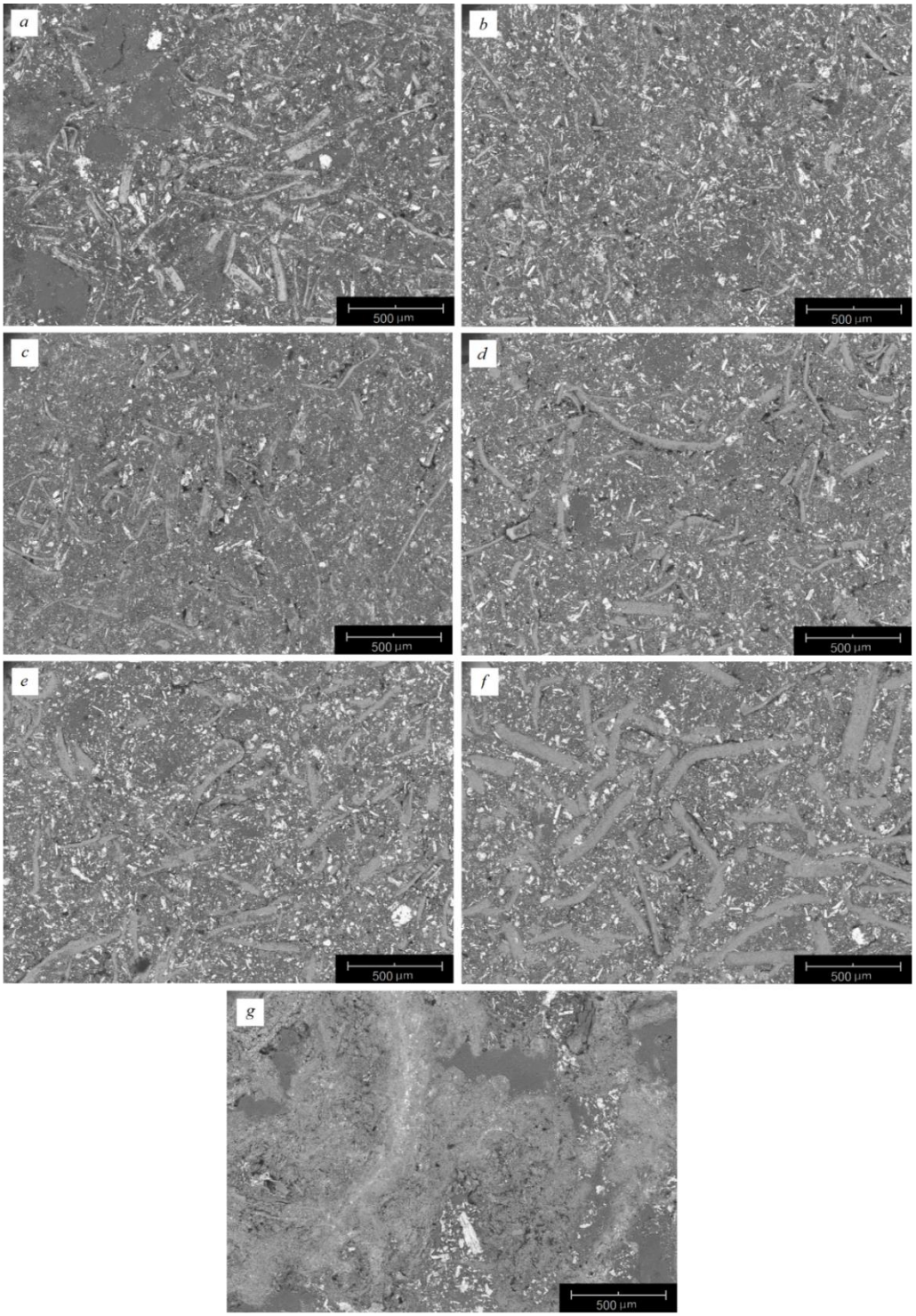

Figure 4.10. *BSE images of as pressed surface of PPSQ matrix composite samples in three different conditions at 150x magnification; (a) just warm pressed sample at 150 ºC (PPSQ-WP), (b) just crosslinked sample after warm pressing at 300 ºC (PPSQ-CL), and heat treated samples at different temperatures after crosslinking (c) PPSQ-HT400, (d) PPSQ -HT500, (e) PPSQ -HT600, (f) PPSQ -HT700, and (g) PPSQ -HT800.*

As seen from the BSE image of the PPSQ matrix composite samples, the observation was obtained from pressed surface side (Figure 4.10), the amount of porosity was increased in the PPSQ-CL sample compared with the PPSQ-WP sample. The observed integrity of the sample seems to provide during the crosslinking step (i.e., at 300 ^{0}C). Further increase in the amount of the porosity was also observed in heat treated samples at between 400 and 500^{0}C. Although the observed pore quantity is similar for both samples (i.e., PPSQ-HT400 and PPSQ-HT500) at this low magnification, the formations of the micro- and macro-cracks are observed within the samples after heat treatment at 500^{0}C. The heat treated sample at 600 and 700^{0}C show decrease in pore quantity in comparison with PPSQ-HT500 sample, nonetheless, an increase in micro-crack formation in the PPSQ-HT600 sample, and an increase in macro-crack formation in the PPSQ-HT700 sample are observed. At 800^{0}C heat treatment, the ingredient steel fibers are highly oxidized and an oxide networks are formed on the surface of sample, and this sample yielded an increase in the micro pore quantity.

Observed change in the amount of the porosity from all the BSE investigated samples “obtained from pressed surface side” are consistent with the calculated amount of the total porosity results given in Figure 4.6. It should be also stated that non-homogenous distribution of the steel fibers can enhance oxide clusters in the sample of composite structure, and on the surface. It is thought that more homogenous distribution of the steel fibers may change the oxidation kinetics.

The obtained BSE images of the cracked samples surface are shown in Figure 4.11 and Figure 4.12. As it can be seen from these figures, both the PMSQ and PPSQ preceramic polymers are homogenously dispersed through the samples at all the heat treatment temperatures. The observed dense dark area in the crack surface of the PPSQ-HT800 sample represents the vermiculite particles.

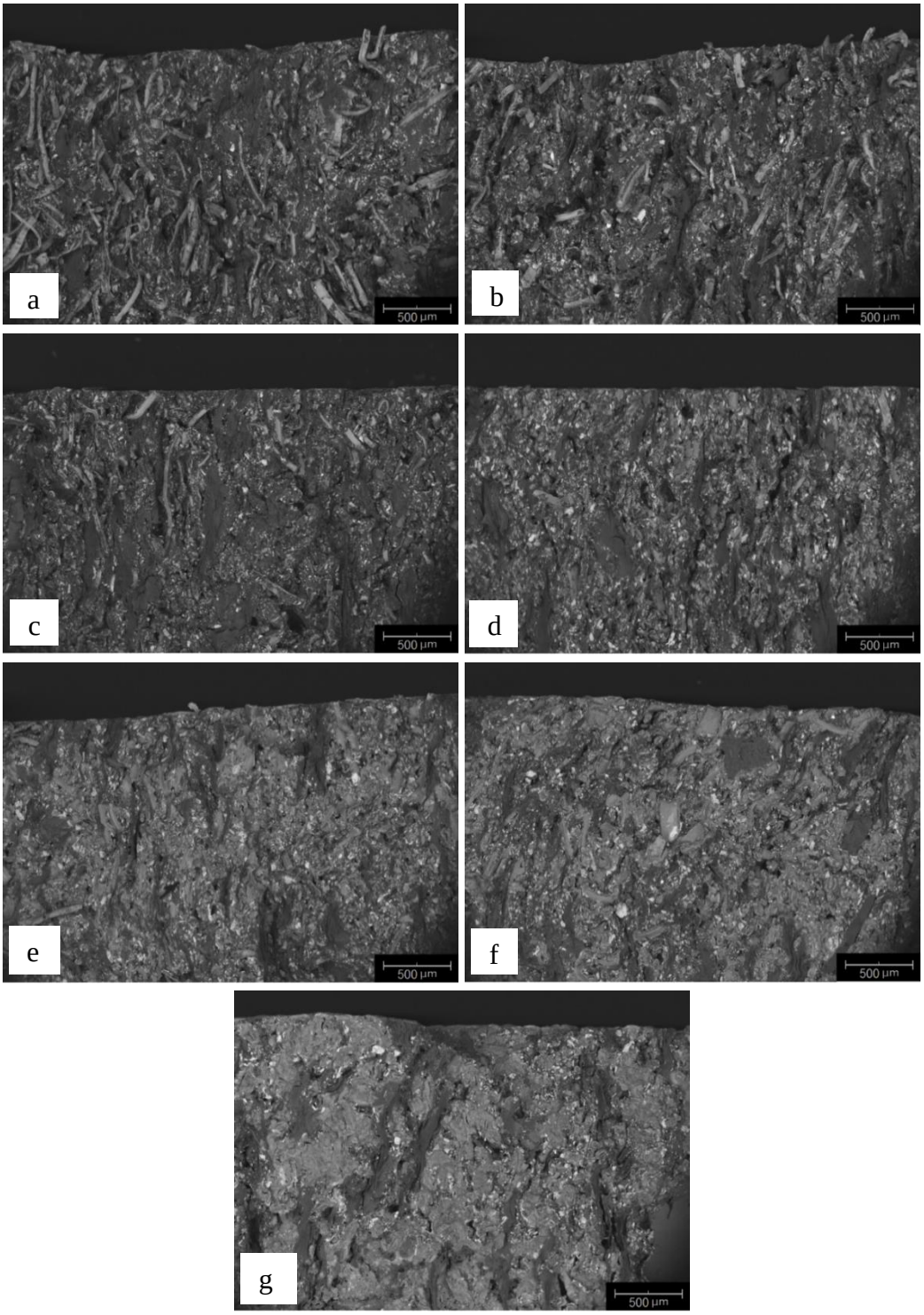

Figure 4.11. *BSE images of fracture surface of PMSQ matrix composite samples in the direction of warm pressing at 100x magnification; (a) just warm pressed sample at 60 ^{o}C (PMSQ-WP), (b) just crosslinked sample after warm pressing at 250 ^{o}C (PMSQ-CL), and heat treated samples at different temperatures after crosslinking (c) PMSQ-HT400, (d) PMSQ -HT500, (e) PMSQ -HT600, (f) PMSQ -HT700, and (g) PMSQ -HT800.*

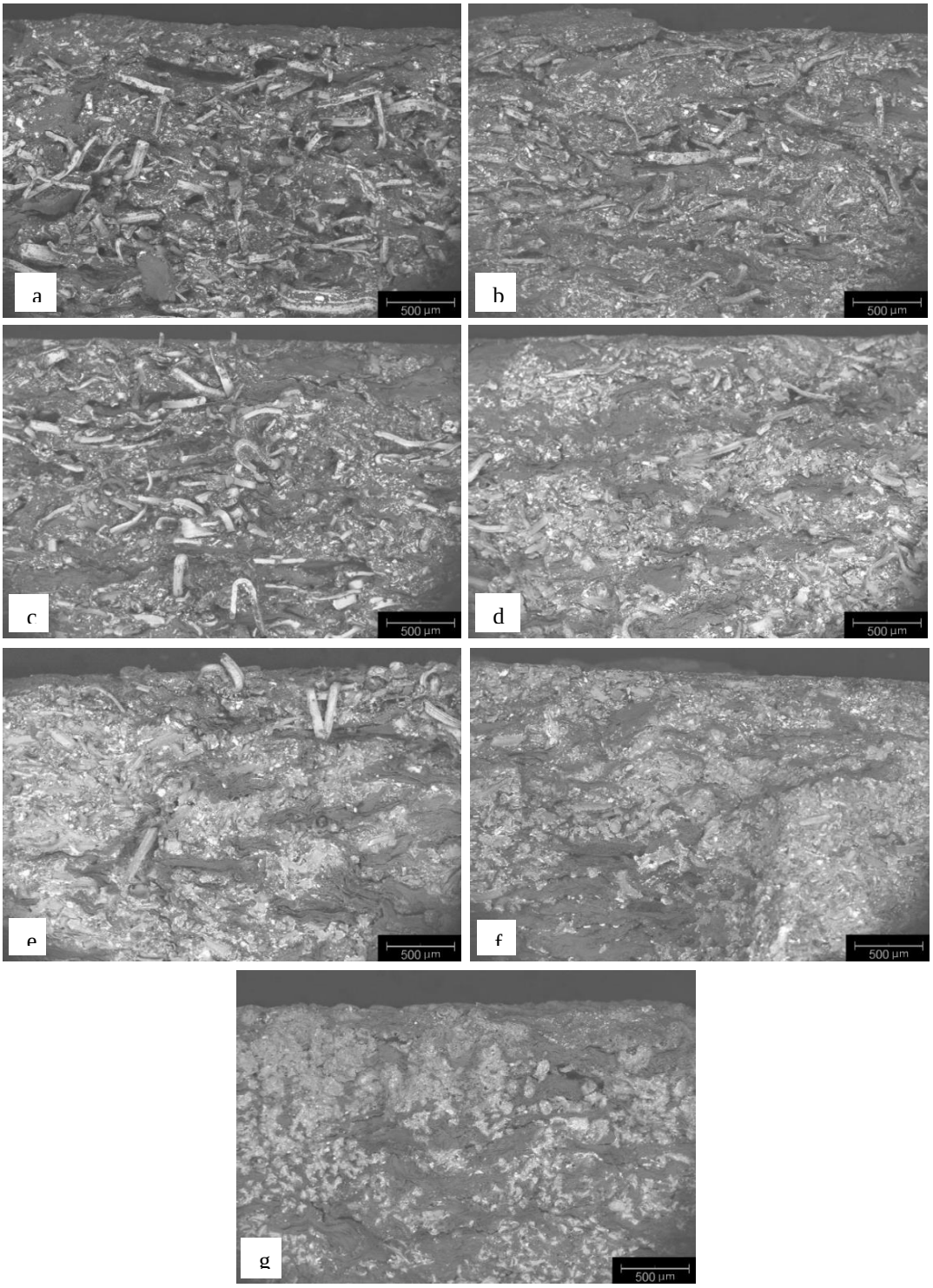

Figure 4.12. *BSE images of fracture surface of PMSQ matrix composite samples in the direction of warm pressing at 100x magnification; (a) just warm pressed sample at 150 ºC (PPSQ-WP), (b) just crosslinked sample after warm pressing at 300 ºC (PPSQ-CL), and heat treated samples at different temperatures after crosslinking (c) PPSQ-HT400, (d) PPSQ -HT500, (e) PPSQ -HT600, (f) PPSQ -HT700, and (g) PPSQ -HT800.*

The BSE investigations images of polished surface of the PMSQ and PPSQ matrix composite samples are obtained at 150x and 1500x magnification, and represented in Figures 4.13, 4.14, 4.15, 4.16, 4.17, 4.18, and 4.19, and Figure 4.23, 4.24, 4.25, 4.26, 4.27, 4.28 and 4.29, respectively. As can be seen from Figure 4.13, the ingredients of the composite material were not well aggregated with each other, and provided an information about the integrity of the sample at low temperature. In comparison with just warm pressed sample at 60 ^{0}C, the integrity of the PMSQ-CL sample was provided by crosslinking of the PMSQ polymer at 250 ^{0}C (Figure 4.14). The observed dark black areas in Figure 4.14 can be caused from crosslinking of the preceramic polymers which is indicated by spectrum 4 in the EDX analysis (Figure 4.20). On the other hand, integrity of the PPSQ matrix composite samples were provided in the just warm pressed step at 150^{0}C (Figure 4.23). In Figure 4.15 and 4.25, the formation of thin oxide layer around the steel fibers was observed for the first time at 400^{0}C. The EDX point analysis was carried out on the polished surface of the PMSQ-HT400 sample, an oxide layer was also observed around the steel fiber (Figure 4.21). Existence of Fe, Si, O elements (Spectrum 3) on oxide layer was obtained, and mainly signals of Si, O, C elements (Spectrum 4) were taken from the darkest region of the BSE images. This formed thin oxide layer was not observable in the XRD pattern of the both composite compositions, could be due to presence of its low amount (Figure 4.7 and Figure 4.8). It is known that organic to inorganic transformation start above 400^{0}C by the thermal decomposition of preceramic polymer. After the completion of the polymer-to-ceramic conversion, the obtained ceramics showed an amorphous structure. The amorphous network was constituted by a mixture of covalent bonds, such as Si–C, Si–O, and C–C [16]. This observation indicated that Si, O, and C elements were the origin of this amorphous structure. As can be observed from Figure 4.16 and 4.26, the oxide network formation begins to form around the steel fibers after heat treatment at 500 ^{0}C. The formed oxide layer around the steel fibers grows by encircling the silicon carbide and tin sulfide grains. At higher magnification (1500x), the stuck of SiC grains inside the steel fiber was also observed. It is thought that the heat treatment at higher temperature caused softening of the plastically deformed steel fibers, which was deformed by the SiC grains during warm pressing. Thus, stuck of SiC grains were observed in the composite structures. As can be seen from Figure 4.17 and 4.27, after heat treatment at 500 ^{0}C, the thickness of oxide layer around the steel fibers was significantly increased in comparison with BSE image obtained at 1500x magnification.

Nascent oxide network was beginning the formation at 500 ^{0}C and was completed at 600 ^{0}C. This network provides an interconnection between the ingredients. Figure 4.18 and 4.28 show the high degree oxidation of steel fibers at 700^{0}C which is constituent about 40% (w/w) of the composite, and resulted formation of a regional oxide areas. These formed oxide area disturb the integrity and the homogeneity of the samples which have great influence on the mechanical properties of the materials. Figure 4.22 shows the EDX point analysis on pyrolyzed preceramic polymer region which mainly C, Si, O elements signals are received. Intensity of carbon element is increased and region seems darker in comparison with the heat treated sample at 400 ^{0}C in Figure 4.22. As observed in Figure 4.19 and 4.29, the deterioration of the material is taken place at 800 ^{0}C. This can be due to the almost entirely oxidized structure and crack formations which are likely responsible lowest compressive strength among all the heat treated samples at this high temperature.

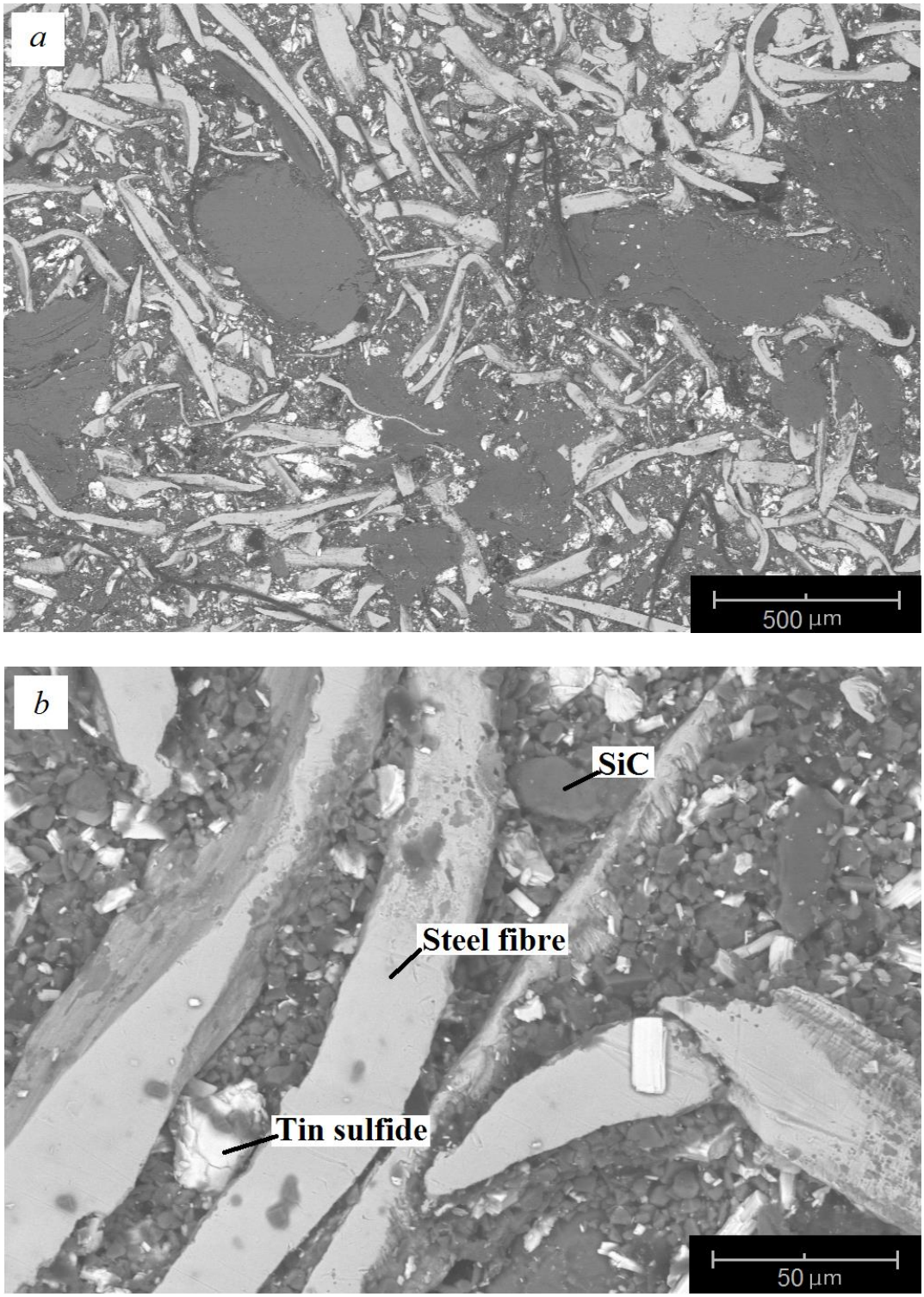

Figure 4.13. *BSE images of polished surface PMSQ-WP sample at 60 °C at 150x (a) and 1500x (b) magnification.*

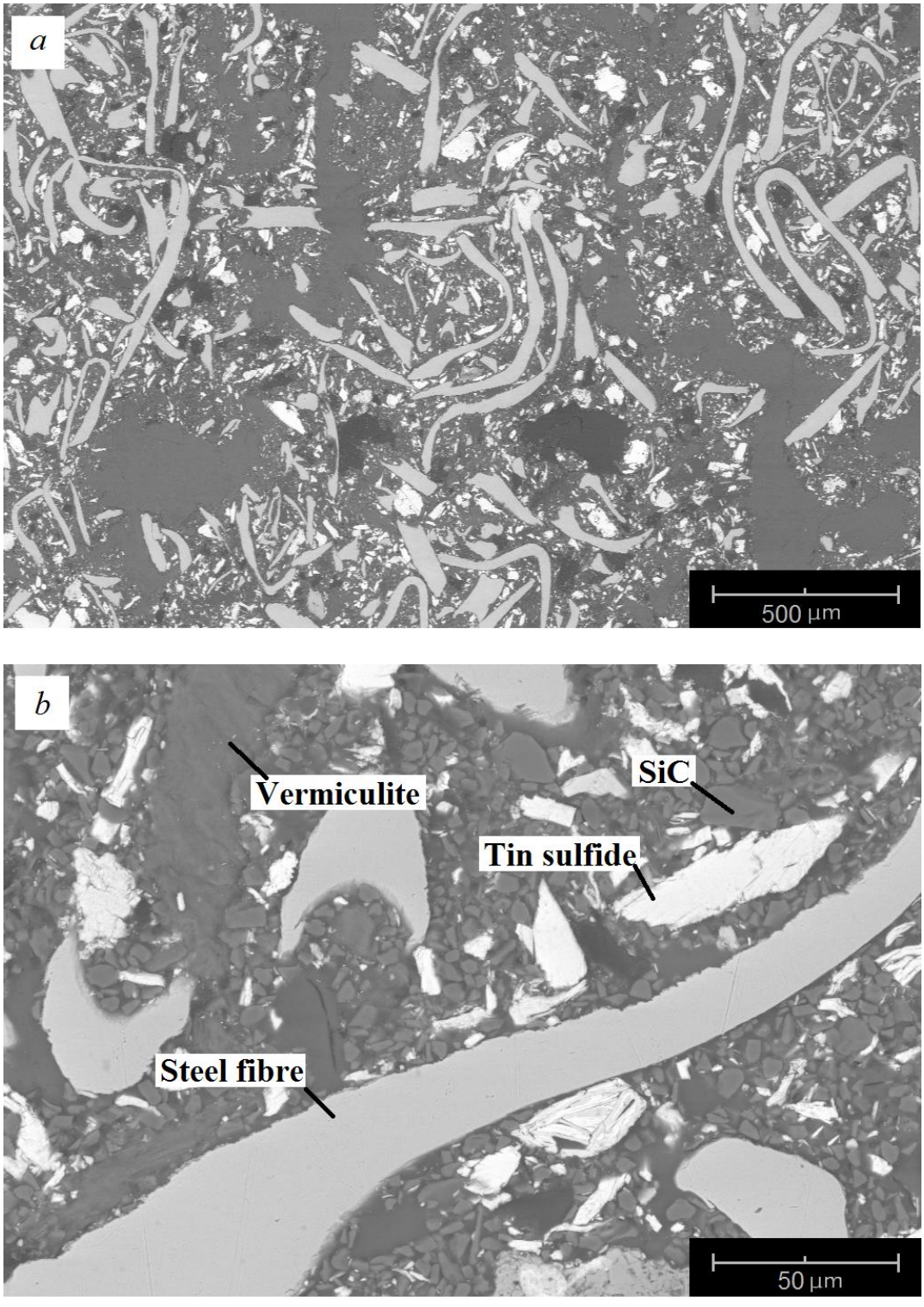

Figure 4.14. *BSE images of polished surface PMSQ-CL sample at 250 ^{0}C at 150x (a) and 1500x (b) magnification.*

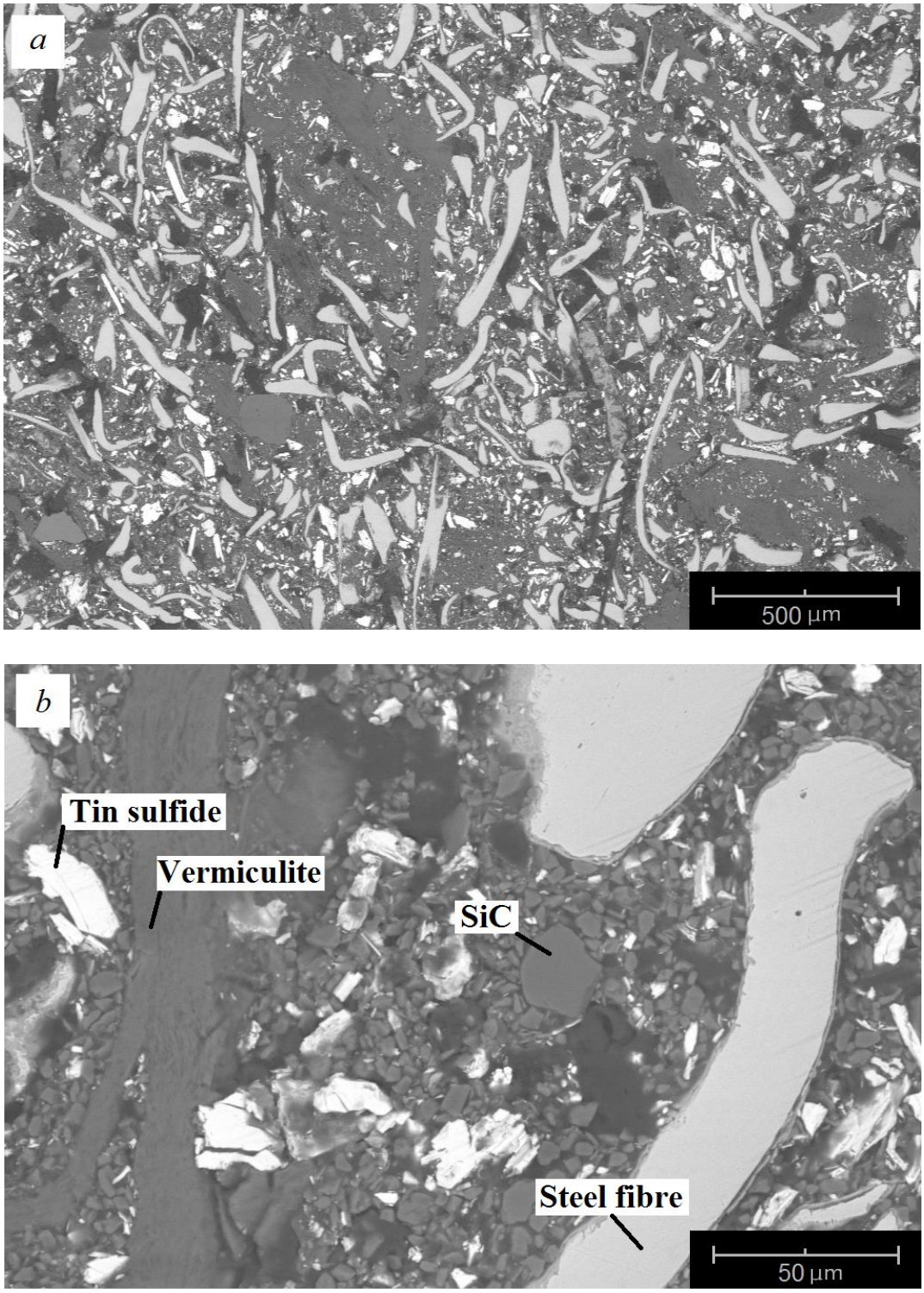

Figure 4.15. *BSE images of polished surface PMSQ-HT400 sample at 150x (a) and 1500x (b) magnification.*

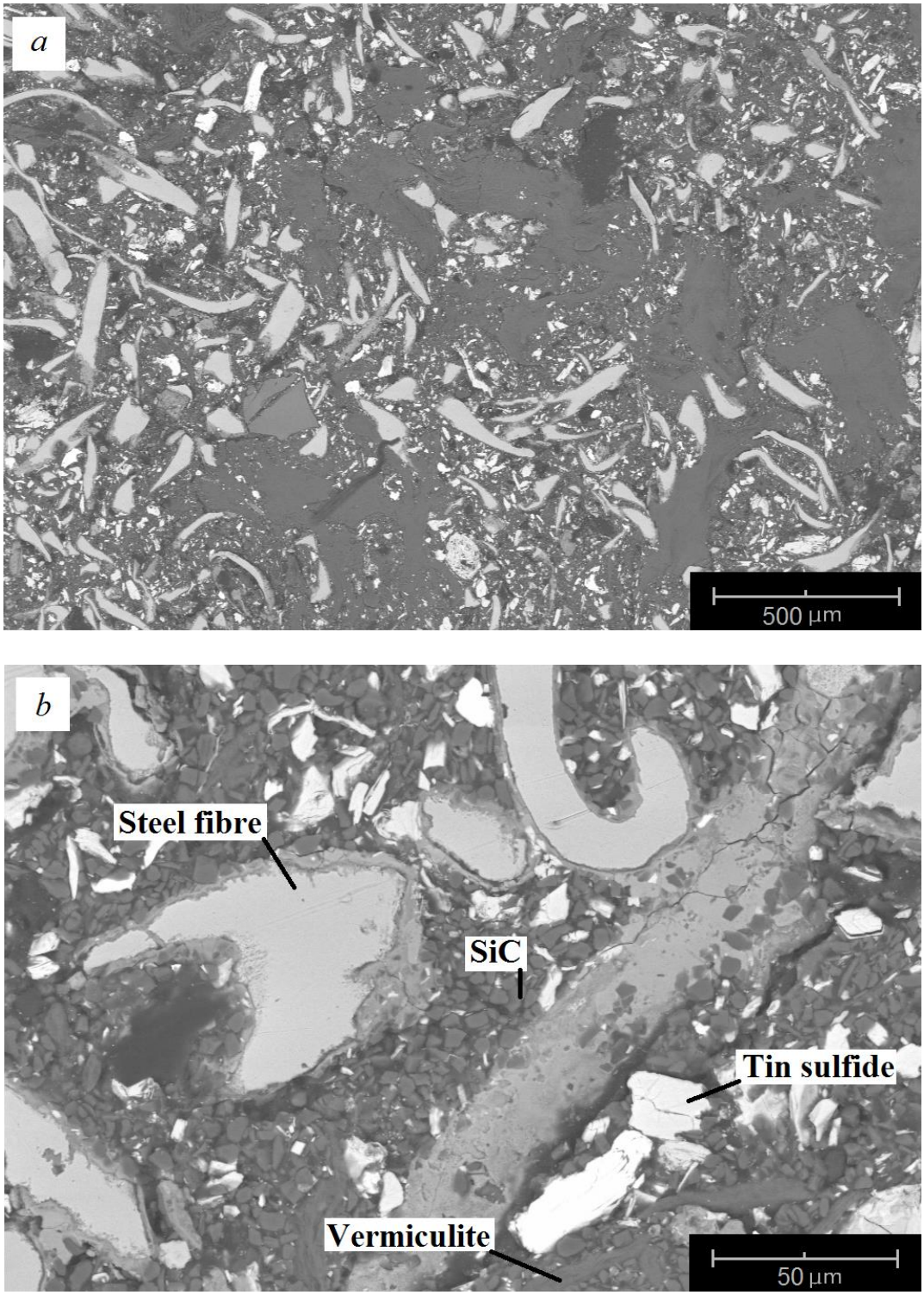

Figure 4.16. *BSE images of polished surface PMSQ-HT500 sample at 150x (a) and 1500x (b) magnification.*

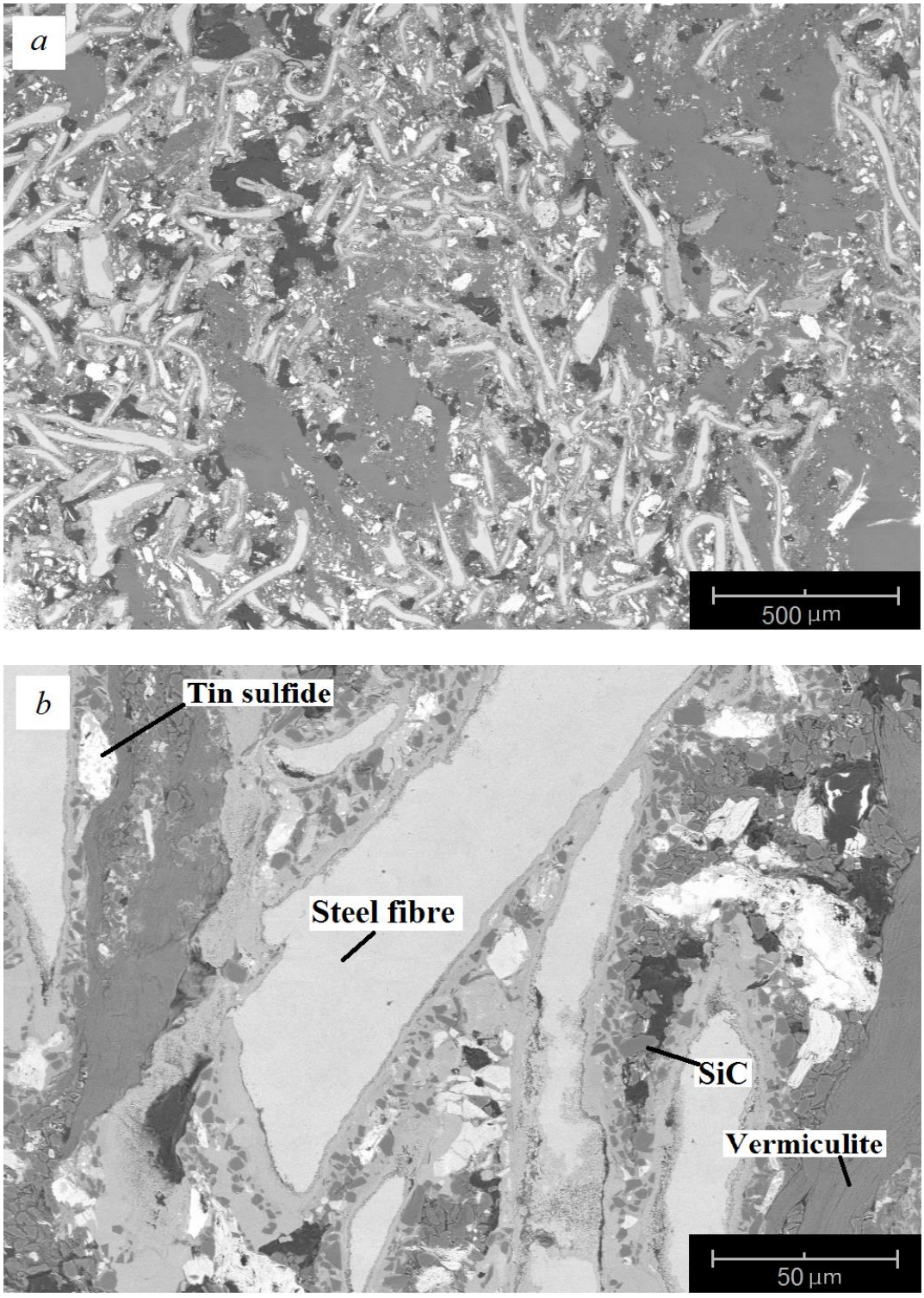

Figure 4.17. *BSE images of polished surface PMSQ-HT600 sample at 150x (a) and 1500x (b) magnification.*

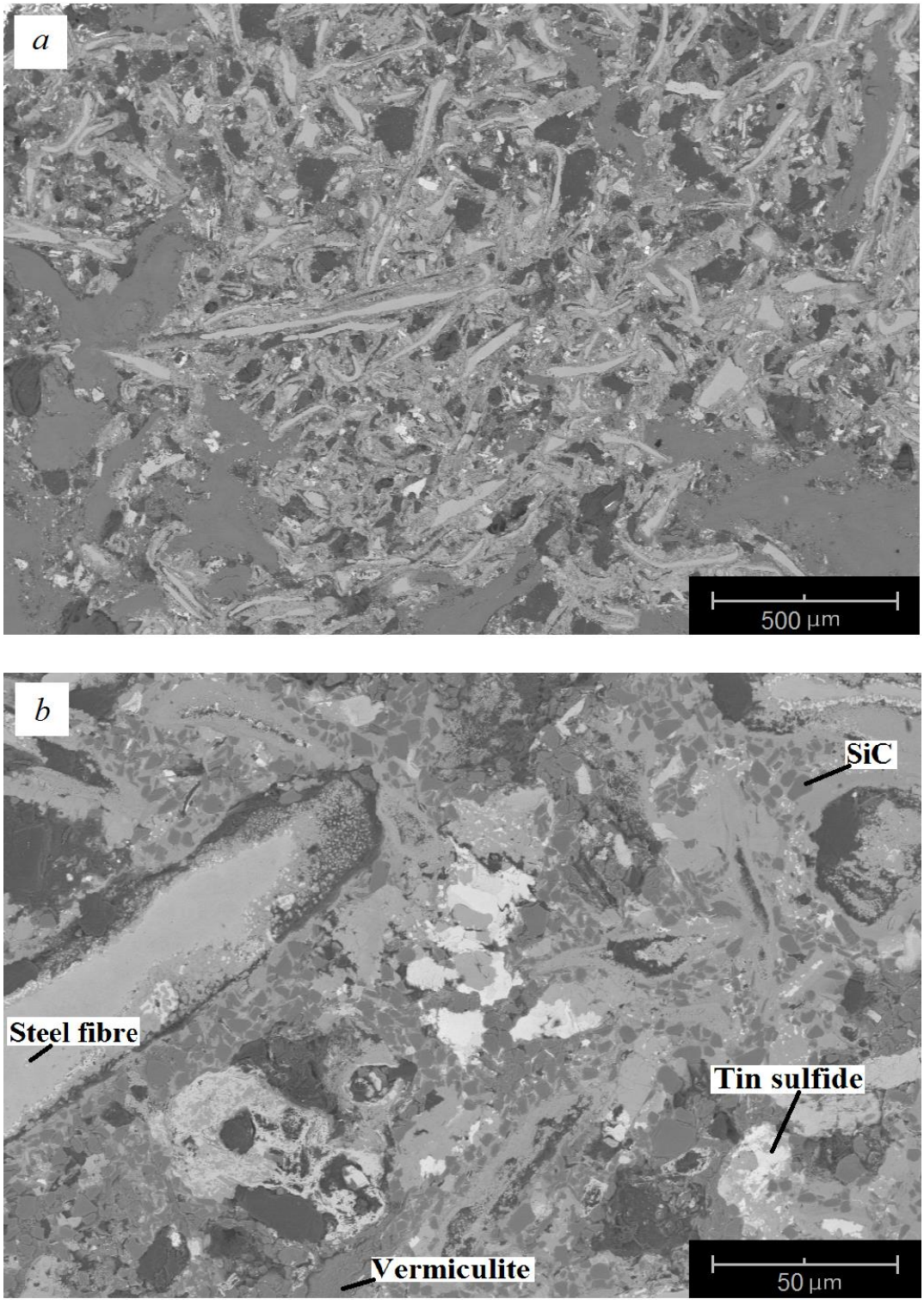

Figure 4.18. *BSE images of polished surface PMSQ-HT700 sample at 150x (a) and 1500x (b) magnification.*

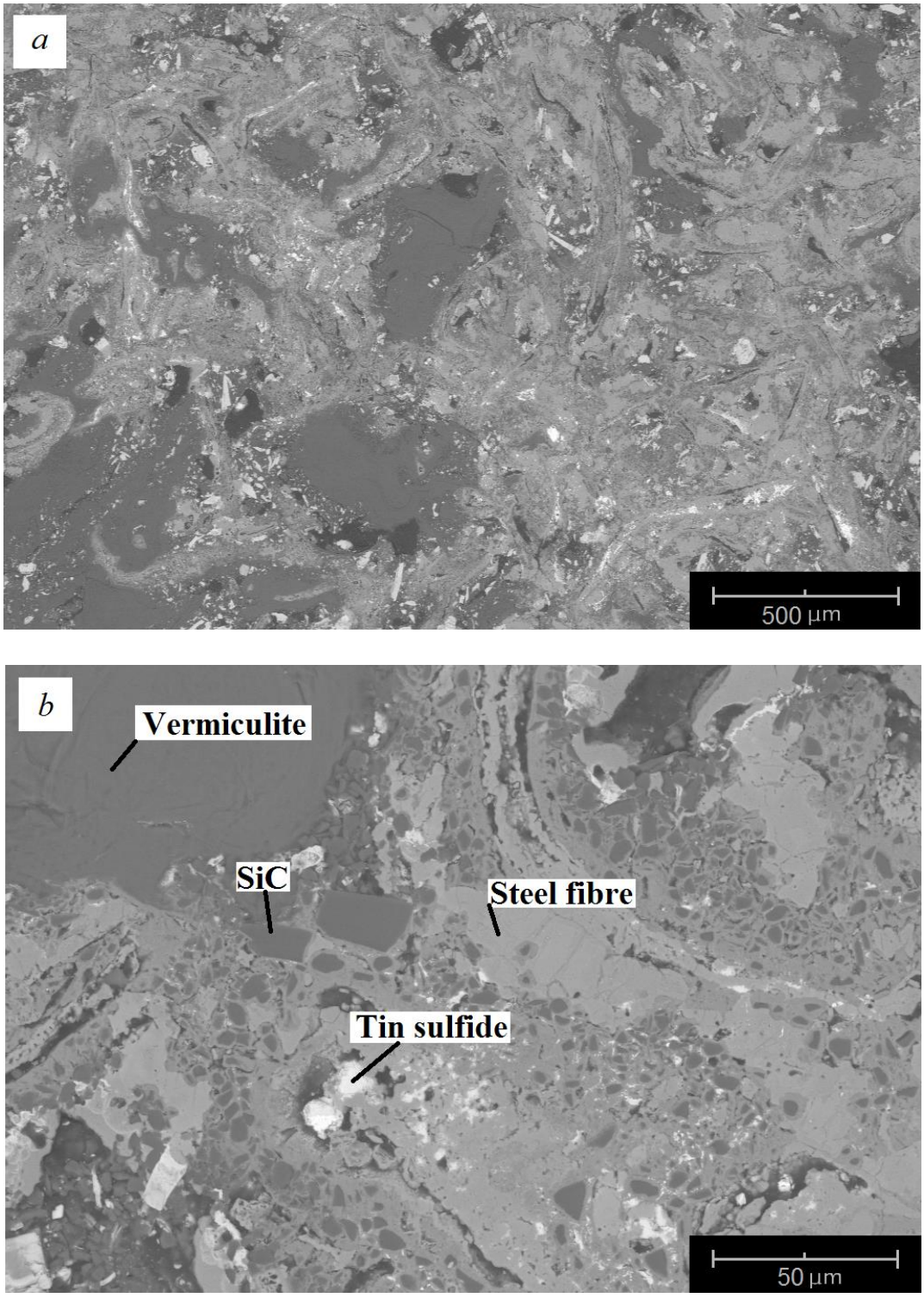

Figure 4.19. *BSE images of polished surface PMSQ-HT800 sample at 150x (a) and 1500x (b) magnification.*

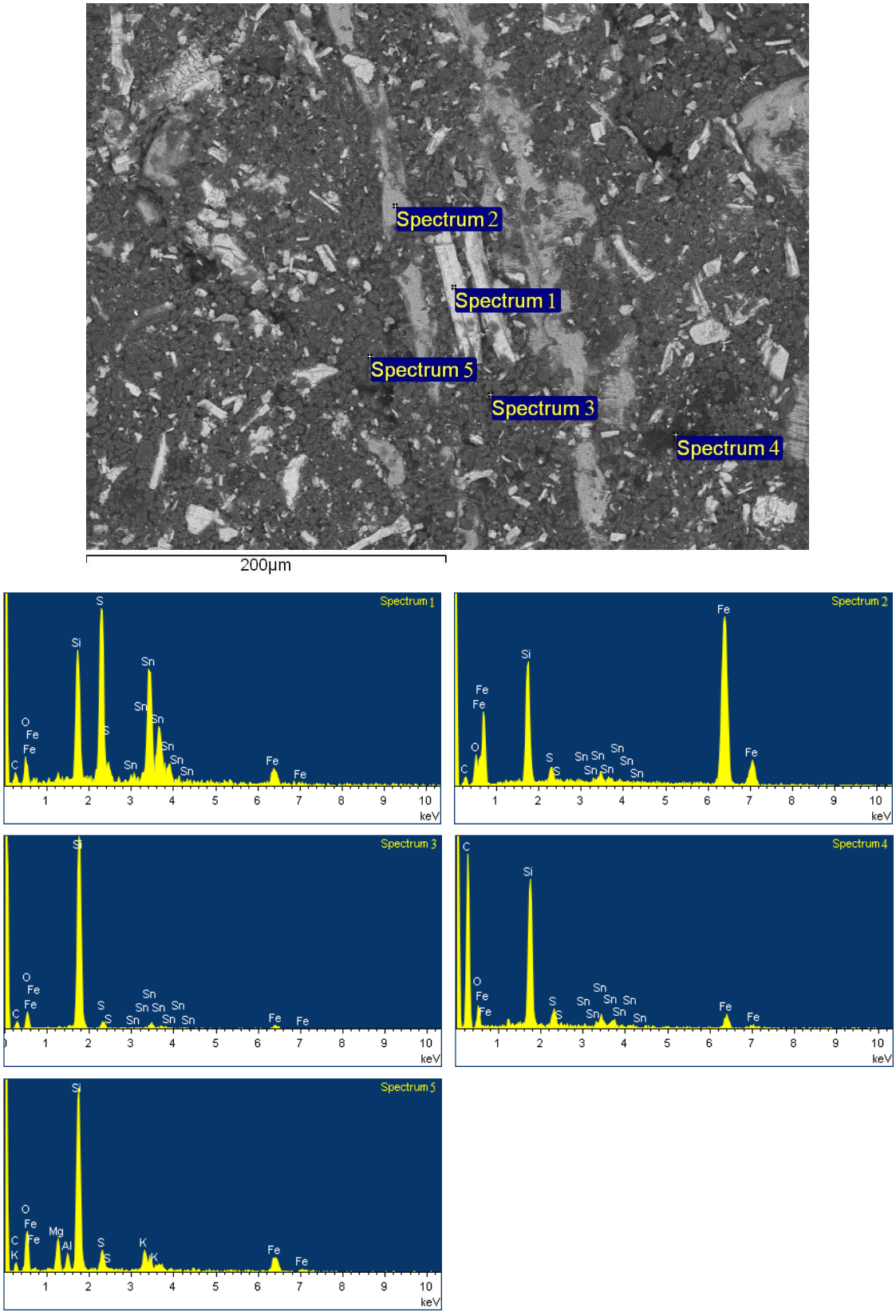

Figure 4.20. *EDX point analysis of PMSQ-CL sample at 250 °C. Spectrums show each ingredient in the composite structure; tin sulfide particle, steel fiber, SiC particles, crosslinked polymer and vermiculite particle respectively.*

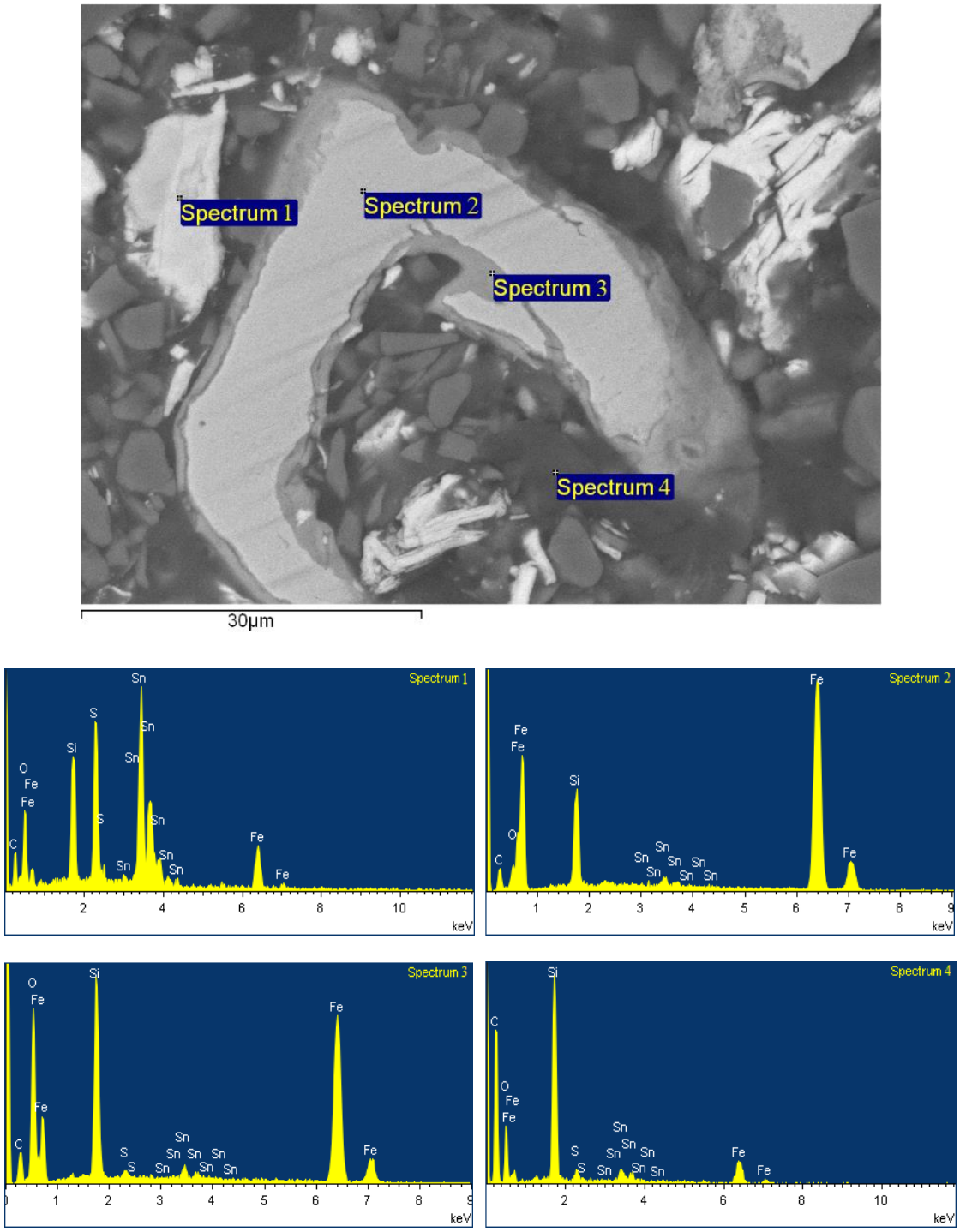

Figure 4.21. *EDX point analysis of PMSQ-HT400 sample.*

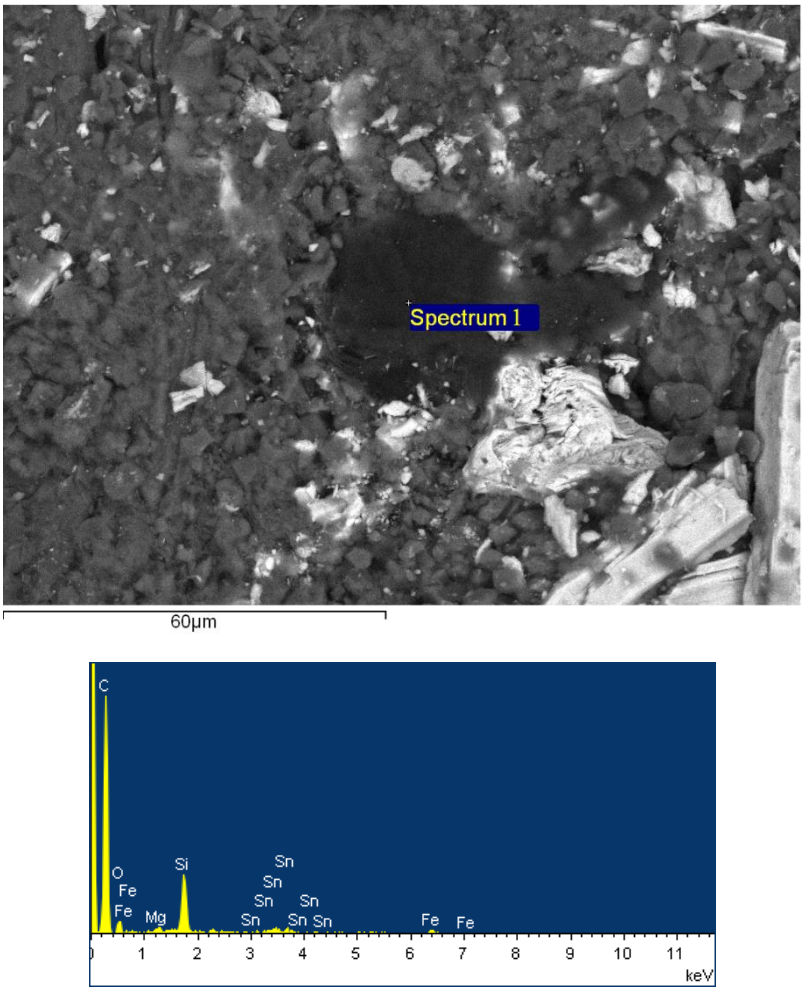

Figure 4.22. *EDX point analysis on pyrolyzed preceramic polymer region of PMSQ-HT700 sample.*

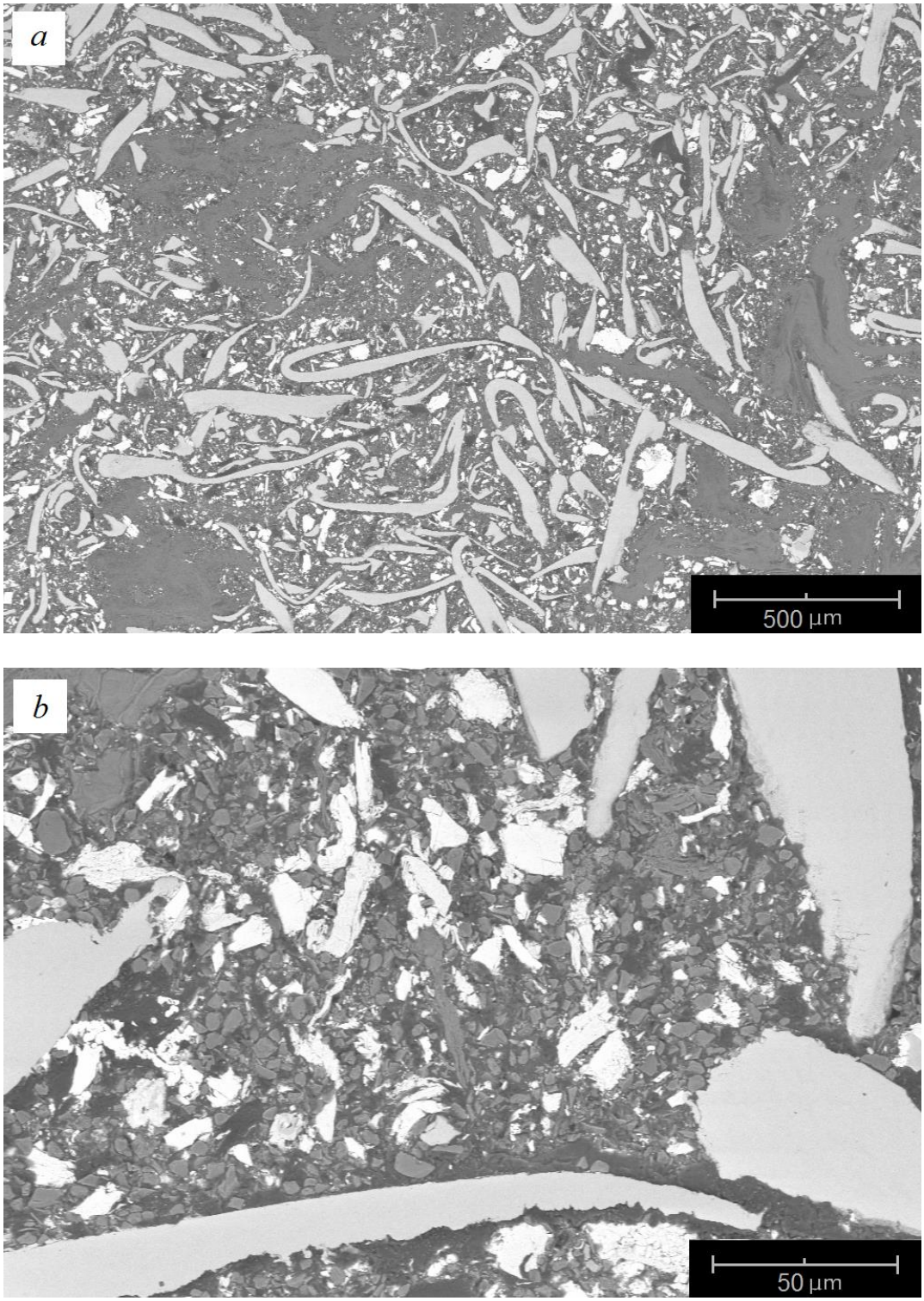

Figure 4.23. *BSE images of polished surface PPSQ-WP sample at 150°C at 150x (a) and 1500x (b) magnification.*

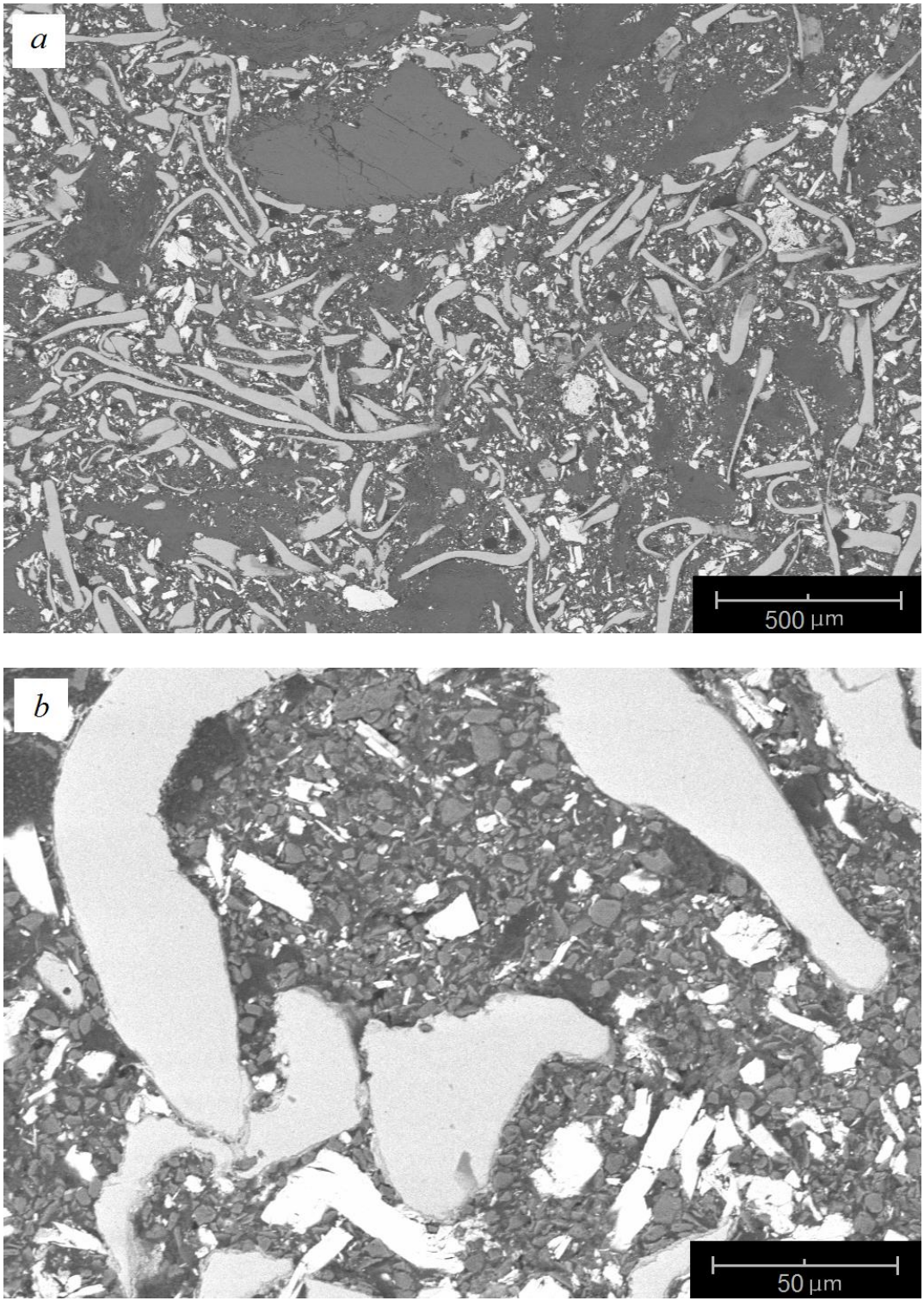

Figure 4.24. *BSE images of polished surface PPSQ-CL sample at 300°C at 150x (a) and 1500x (b) magnification.*

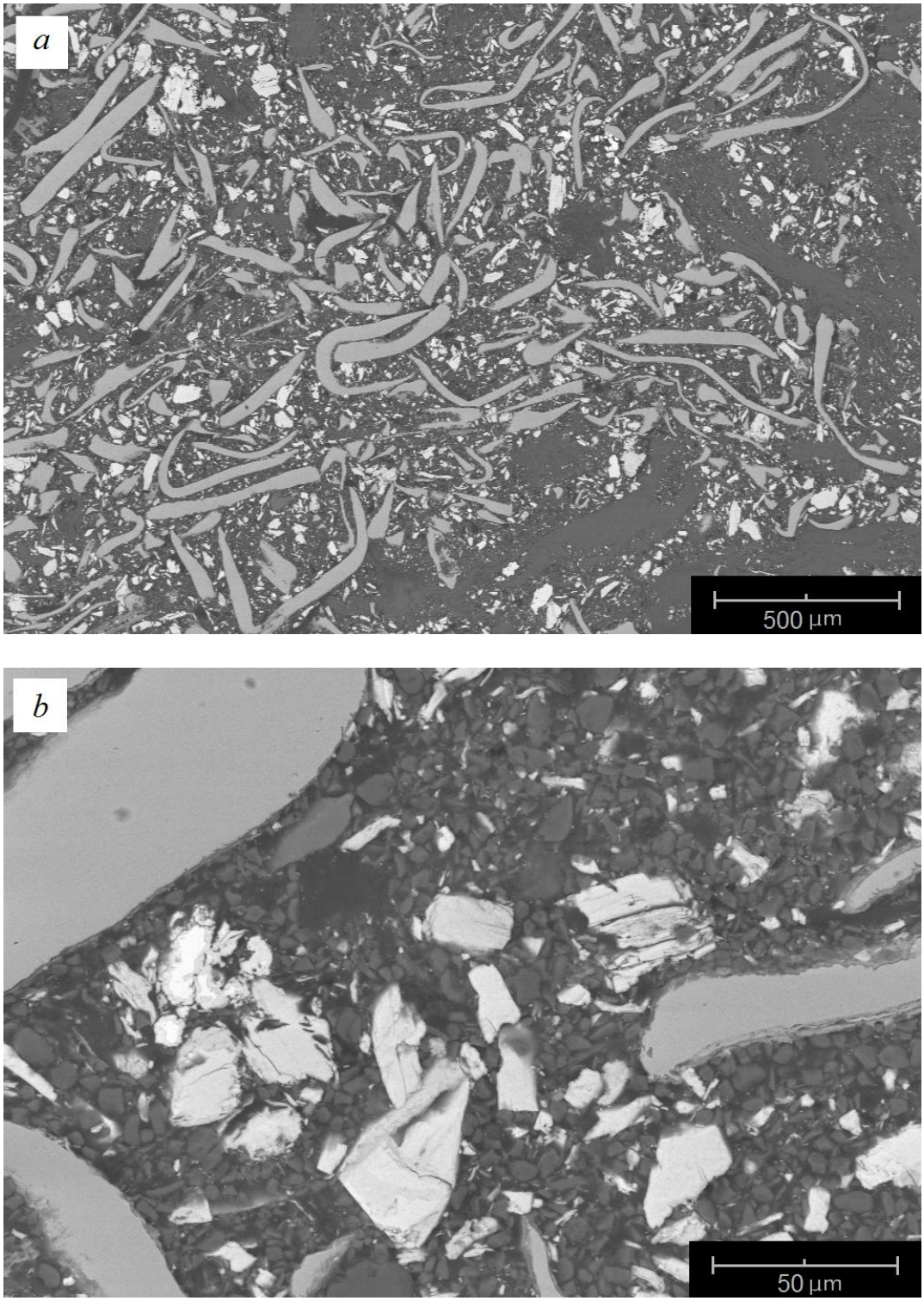

Figure 4.25. *BSE images of polished surface PPSQ-HT400 sample at 150x (a) and 1500x (b) magnification.*

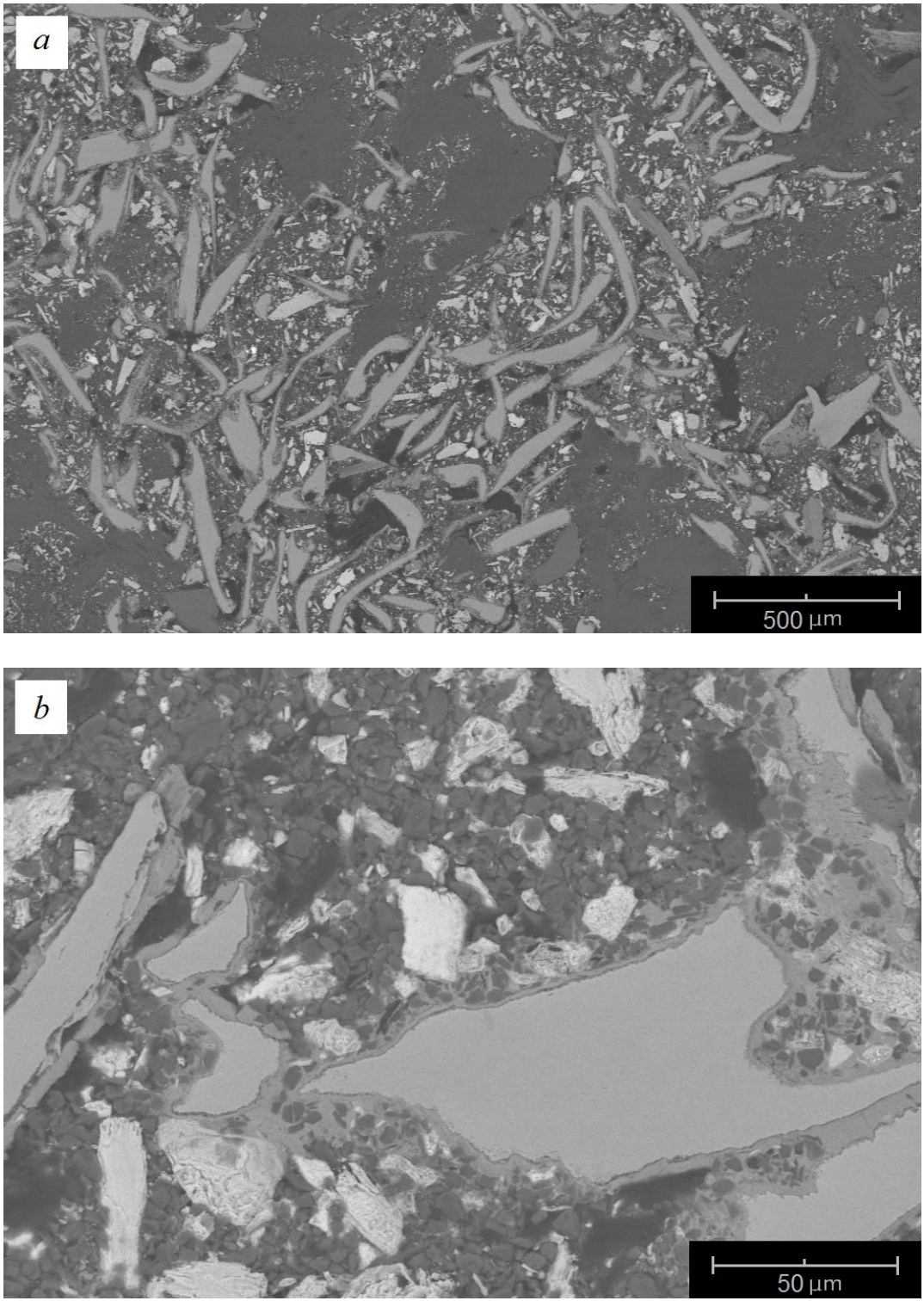

Figure 4.26. *BSE images of polished surface PPSQ-HT500 sample at 150x (a) and 1500x (b) magnification.*

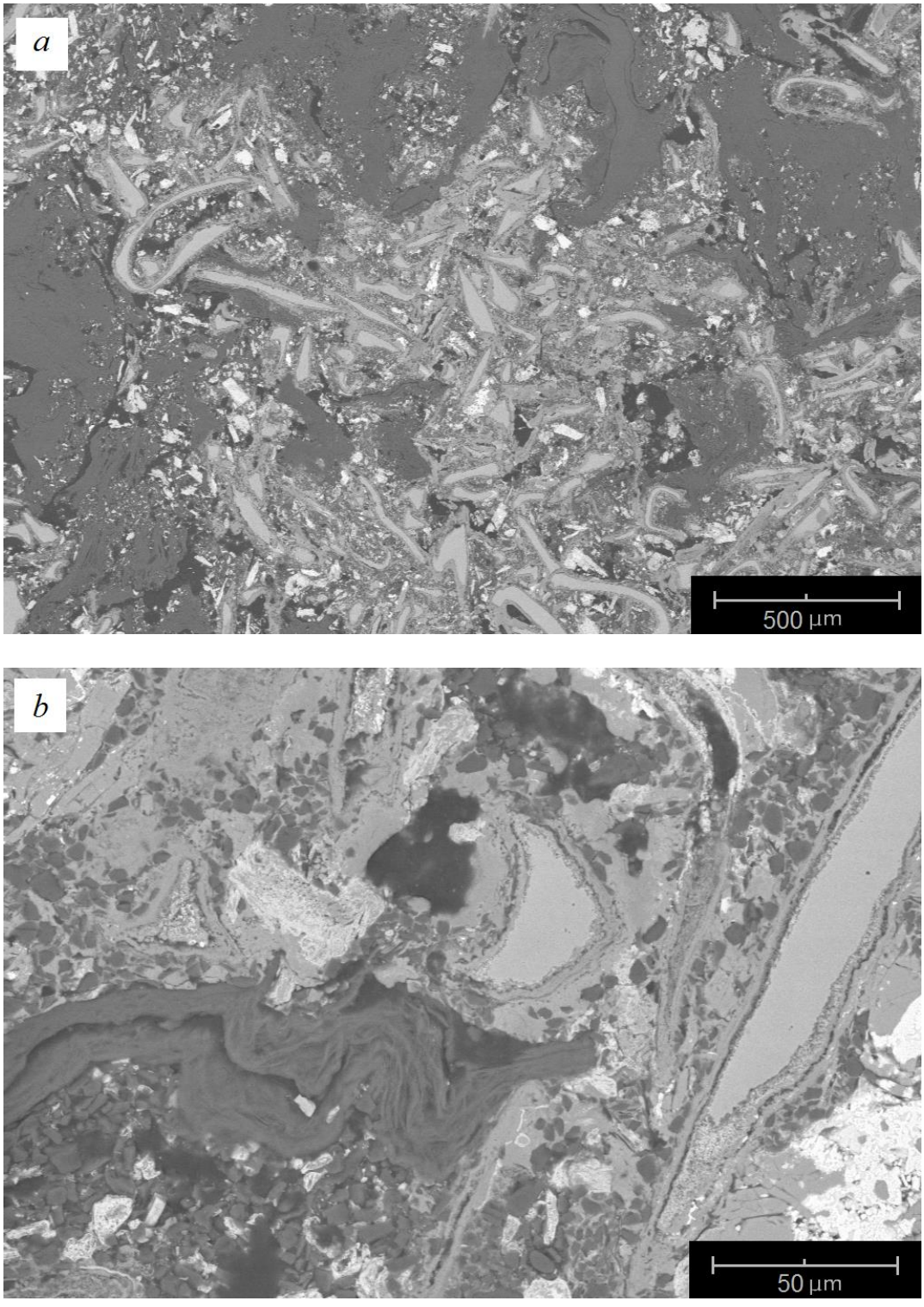

Figure 4.27. *BSE images of polished surface PPSQ-HT600 sample at 150x (a) and 1500x (b) magnification.*

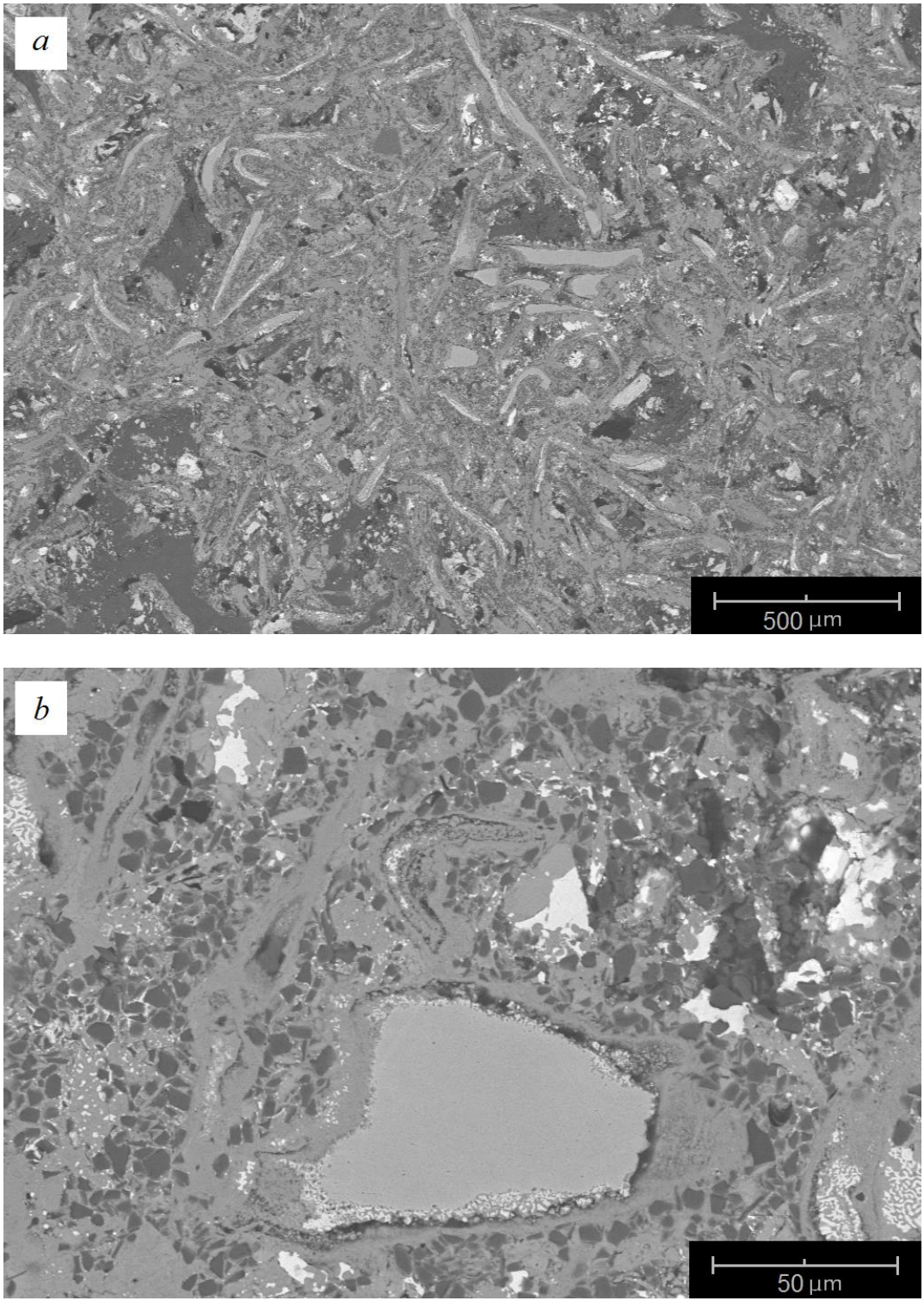

Figure 4.28. *BSE images of polished surface PPSQ-HT700 sample at 150x (a) and 1500x (b) magnification.*

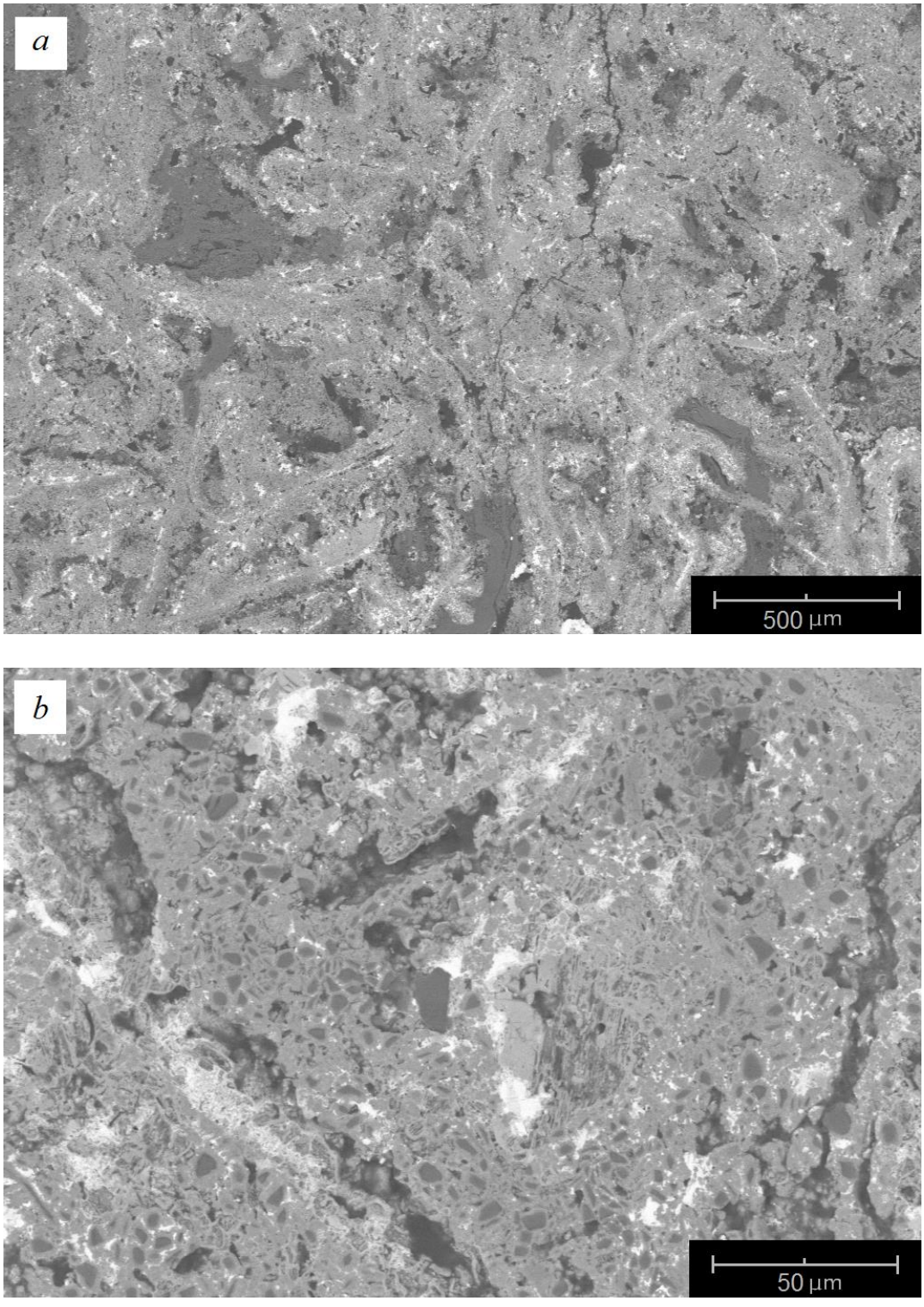

Figure 4.29. *BSE images of polished surface PPSQ-HT800 sample at 150x (a) and 1500x (b) magnification.*

5. CONCLUSION

Preceramic polymers are suitable materials to process with plastic forming techniques. They could be prepared in low viscous precursor at low temperature (~45-150^{0}C) or in solution form. The ceramic materials can also be produced from preceramic polymers by addition of desired ingredient at low temperature. The following plastic forming techniques (i.e., warm pressing, PIP, RTM, fiber drawing and injection molding) can be used to obtain desired shaped product because the starting preceramic polymer material can be melted at low temperatures (~ 400-1400^{0}C). Therefore, preparation of polymer derived ceramic materials have several advantages over conventional powder processing methods in that control of shape and purity of material is possible and it requires lower cost. These preceramic polymers are used in various applications due to its physical-chemical, mechanical, thermal and electrical properties with the possibility of obtainment of desired property product with various shaping technology. Therefore, they have found application in several fields such as information technology, transport, defense, energy as well as environmental systems, biomedical components and micro- or nanoelectromechanical systems. Mainly applications of preceramic polymers can be sorted as ceramic fibers, ceramic coatings and porous ceramics, micro components, and ceramic matrix composites.

In the presented study, two different preceramic polymer were used for preparation of composite materials namely, polymethylsilsesquioxane (PMSQ) and polyphenylsilsesquioxane (PPSQ). In the preparation of two different preceramic matrix composites four different ingredients were added into the composite preparation mixtures (i.e., steel fiber, tin sulfide, silicon carbide and vermiculite). From these mixtures preceramic matrix composites were produced in four step; (i) mixing of powder composite ingredients, (ii) warm pressing of prepared mixtures, (iii) crosslinking of warm pressed samples and (iv) heat treatment of crosslinked samples at five different temperatures (i.e., 400, 500, 600, 700 and 800 ^{0}C).

These produced composite materials were characterized by thermogravimetric analysis (TGA) and differential thermal analysis (DTA), helium pycnometer, compressive strength, X-ray diffraction (XRD) and scanning electron microscope (SEM) techniques. From these used characterization methods the following information were obtained (i) the effect of different side groups (i.e., methyl and phenyl) in

polysilsesquioxane polymer and pyrolysis temperature on the thermal properties, densification and amount of porosity, (ii) compressive strength, phase development and microstructure of the final product of the composite materials. The thermogravimetric analysis were realized from room temperature to 800^0C for the PMSQ and PPSQ matrix composite powder mixtures.

From the TG-DTA analysis of the used preceramic polymer, the information about the thermal degradation properties was obtained. The presence of bulky phenol groups on the PPSQ retarded the thermal degradation and increase mass loss compared with the PMSQ preceramic polymer. Additionally, the spreading of the preceramic polymers on the steel fibers resulted formation of a protective coating layer during the organic to inorganic transformation of preceramic polymers (i.e., Si-O-C form). It should be also noted that the formed ceramic layer also retarded the oxidation of the steel fibers in the composite materials.

For the compressive strength analysis, when compressive strength values of the PPSQ and PMSQ matrix composites samples were compared with each other, it was observed that the PMSQ samples had a maximum compressive strength values at 600^0C, among all the tested samples but the observed compressive strength values were not stable at the other studied temperature ranges. On the other hand, the compressive strength values of the PPSQ matrix composite samples at between 150 and 600^0C yielded a more stable results with each other.

At 500^0C, the first oxides cassiterite, (SnO_2, #41-1445), and magnetite (Fe_3O_4, #75-1610) are observed in both PMSQ and PPSQ matrix composite samples, however hematite (Fe_2O_3, #33-0664) phase was observed for only in PPSQ matrix composite. In the XRD patterns of heat treated samples at 800^0C, iron tin (Fe_3Sn, #73-2029) phase is observed for both composite compositions. Apart from that, iron sulfide (FeS, #76-0962) and iron carbide ($CFe_{2.5}$, #36-1248) phases are identified in the PMSQ and PPSQ matrix composite samples, respectively. In literature, a significant linear dependence has been reported between the amount of the free carbon and the amount of phenyl groups. It was also reported that increase in free carbon content can be decreased the oxidation resistance of the material. The early formation of the hematite phase in PPSQ matrix composite can be originated from this phenomena. And also, the disappearance of SnS_2 and Sn_2S_3 peaks at 500^0C and formation of iron carbide phase at 800^0C in the PPSQ matrix composite can

be caused from the high free carbon content of the PPSQ based composition. The excess amount of carbon may be increase the decomposition of the tin sulfides by forming carbon disulfide (CS_2), and the formation of iron carbide ($CFe_{2.5}$) phase at high temperature.

The formation of the pore and pore size distribution was depended on the used polymer type and its side groups and the applied heat treatment temperature. The matrix preceramic polymers were well distributed within the composite mixture and hold together all the used ingredient in the aggregated network. As a result the selection of preceramic polymer affected the physical, chemical, and morphological properties of the resultant materials. Thus, selection of a proper preceramic polymer type could permit to synthesis of a material with desired properties.

REFERENCES

[1] Greil, P. (2000). Polymer Derived Engineering Ceramics. *Advanced Engineering Materials, 2(6),* 339-348.

[2] Akkaş, H. D., Öveçoğlu, M. L., & Tanoğlu, M. (2004). Development of Si-O-C Based Ceramic Matrix Composites Produced via Pyrolysis of a Polysiloxane. *Key Engineering Materials, 264–268,* 961-964.

[3] Greil, P. (1999). Near net shape manufacturing of ceramics. *Materials Chemistry and Physics, 61,* 64-68.

[4] Torrey, J. D., Bordia, R. K., Henager, C. H., Blum, Y., Shin, Y., & Samuels, W. D. (2006). Composite polymer derived ceramic system for oxidizing environments. *Journal of Materials Science, 41*(14), 4617–4622.

[5] Colombo, P., Mera, G., Riedel, R., & Sorarù, G. D. (2010). Polymer-derived ceramics: 40 Years of research and innovation in advanced ceramics. *Journal of the American Ceramic Society, 93*(7), 1805–1837.

[6] Wang, K. (2010). *Polymer derived and ceramics matrix composite coatings: processing, characterization and performance.* Doctor of Philosophy, Department of Materials Science and Engineering, University of Washington.

[7] Kipping, F. S. & Sands, J. E. (1921). XCIII. Organic derivatives of silicon. Part XXV. Saturated and unsaturated silicohydrocarbons, Si_4Ph_8. *Journal of the Chemical Society, Transactions, 119,* 830-847.

[8] Burkhard, C. A. (1949). Polydimethylsilanes. *Journal of the American Chemical Society, 71(3),* 963-964.

[9] Ainger, F. W. & Herbert, J. M. (1960). The Preparation of Phosphorus-Nitrogen Compounds as Non-Porous Solids. Edited by Popper, P. in *Special Ceramics* (pp. 168–182). New York: Academic press.

[10] Chantrell, P. G. & Popper, P. (1965). Inorganic Polymers and Ceramics. Edited by P. Popper in *Special Ceramics* (pp. 87–103). New York: Academic press.

[11] Verbeek, W. (1974). Production of shaped articles of homogeneous mixtures of silicon carbide and nitride. US Patent 3853567, 1974.

[12] Winter, G., Werbeek, W., & Mansmann, M. (1976). Production of Shaped Articles of Silicon Carbide and Silicon Nitride.

[13] Yajima, S., Hayashi, J., & Omori, M. (1975). Continuous Silicon Carbide Fiber of High Tensile Strength. *Chemistry Letters*, (9), 931–934.

[14] Yajima, S., Hasegawa, Y., Hayashi, J., & Iimura, M. (1978). Synthesis of continuous silicon carbide fibre with high tensile strength and high Young's modulus: Part 1 Synthesis of polycarbosilane as precursor. *Journal of Materials Science*, *13*(12), 2569–2576.

[15] Riedel, R., & Dressler, W. (1996). Chemical formation of ceramics. *Ceramics International*, *22*(3), 233–239.

[16] Parcianello, G. (2012). *Advanced ceramics from preceramic polymers and fillers*. Doctoral Thesis. Padova. University of Padova.

[17] Riedel, R., Mera, G., Hauser, R., & Klonczynski, A. (2006). Silicon-Based Polymer-Derived Ceramics: Synthesis Properties and Applications-A Review. *Journal of the Ceramic Society of Japan*, *114*(1330), 425–444.

[18] Mera, G., Gallei, M., Bernard, S., & Ionescu, E. (2015). Ceramic Nanocomposites from Tailor-Made Preceramic Polymers. *Nanomaterials*, *5*(2), 468–540.

[19] Bujalski, D. R., Grigoras, S., Lee, W. N., Wieber, M., & Zank, G. A. (1998). Stoichiometry control of SiOC ceramics by siloxane polymer functionality, *8*(6), 1427–1433.

[20] Colas, A. (2005). Silicones : Preparation , Properties and Performance. *Dow Corning, Life Sciences.*

[21] Zhou, W., Yang, H., Guo, X., & Lu, J. (2005). Thermal degradation behaviors of some branched and linear polysiloxanes. *Polymer degradation and stability, 91,* 1471-1475.

[22] Baney, R. H., Itoh, M., Sakakibara, A. & Suzukit, T. (1995). Silsesquoixane. *Chem. Rev. 95*, 1409-1430.

[23] Kroke, E., Li, Y., Konetschny, C., Lecomte, E., Fasel, C., & Riedel, R. (2000). Silazane derived ceramics and related materials. *Materials Science and Engineering: R: Reports*, *26*(4–6), 97–199.

[24] Iwamoto, Y., Kikuta, K.-I., & Hirano, S.-I. (2000). Synthesis of Poly-Titanosilazanes and Conversion into Ceramics. *Journal of the Ceramic Society of Japan*, *108*(4), 350–356.

[25] Bechelany, M. C., Proust, V., Gervais, C., Ghisleni, R., Bernard, S., & Miele, P. (2014). In situ controlled growth of titanium nitride in amorphous silicon nitride: A general route toward bulk nitride nanocomposites with very high hardness. *Advanced Materials*, *26*(38), 6548–6553.

[26] Yuan, J., Luan, X., Riedel, R., & Ionescu, E. (2015). Preparation and hydrothermal corrosion behavior of Cf/SiCN and Cf/SiHfBCN ceramic matrix composites. *Journal of the European Ceramic Society*, *35*(12), 3329-3337.

[27] Yuan, J., Hapis, S., Breitzke, H., Xu, Y., Fasel, C., Kleebe, H. J., … Ionescu, E. (2014). Single-source-precursor synthesis of hafnium-containing ultrahigh-temperature ceramic nanocomposites (UHTC-NCs). *Inorganic Chemistry*, *53*(19), 10443–10455.

[28] Jones, R. G., Ando, W., & Chojnowski, J. (2001). *Silicon-Containing Polymers: The Science and Technology of Their Synthesis and Applications*, *30*, 768.

[29] Haug, R., Weinmann, M., Bill, J., & Aldinger, F. (1999). Plastic forming of preceramic polymers. *Journal of the European Ceramic Society*, *19*(1), 1–6.

[30] Shah, S. R., & Raj, R. (2002). Mechanical properties of a fully dense polymer derived ceramic made by a novel pressure casting process. *Acta Materialia*, *50*(16), 4093–4103.

[31] Galusek, D., Sedláček, J., & Riedel, R. (2007). Al2O3-SiC composites prepared by warm pressing and sintering of an organosilicon polymer-coated alumina powder. *Journal of the European Ceramic Society*, *27*(6), 2385–2392.

[32] Colombo, P., Bernardo, E., & Parcianello, G. (2013). Multifunctional advanced ceramics from preceramic polymers and nano-sized active fillers. *Journal of the European Ceramic Society*, *33*(3), 453–469.

[33] Bunsell, A. R., & Piant, A. (2006). A review of the development of three generations of small diameter silicon carbide fibres. *Journal of Materials Science*, *41*(3), 823–839.

[34] Okamura, K., Shimoo, T., Suzuya, K., & Suzuki, K. (2006). SiC-based ceramic fibers prepared via organic-to-inorganic conversion process-a review. *Journal of the Ceramic Society of Japan*, *114*(6), 445.

[35] Wang, C., Wang, J., Park, C. B., & Kim, Y. W. (2009). Processing of porous silicon oxycarbide ceramics from extruded blends of polysiloxane and low-density polyethylene. *Journal of Ceramic Processing Research*, *10*(2), 238–242.

[36] Walter, S., Suttor, D., Erny, T., Hahn, B., & Greil, P. (1996). Injection Moulding of Polysiloxane / Filler Mixtures for Oxycarbide Ceramic Composites. *Journal of the European Ceramic Society*, *2219*(95), 387–393.

[37] Colombo, P., Paulson, T. E., & Pantano, C. G. (2005). Synthesis of Silicon Carbide Thin Films with Polycarbosilane (PCS). *Journal of the American Ceramic Society*, *40*(9), 2333–2340.

[38] Smirnova, T. P., Badalian, A. M., Yakovkina, L. V., Kaichev, V. V., Bukhtiyarov, V. I., Shmakov, A. N., Asanov, I. P., Rachlin, V. I., Fomina, A. N. (2003). SiCN alloys obtained by remote plasma chemical vapour deposition from novel precursors. *Thin Solid Films*, *429*(1–2), 144–151.

[39] Goerke, O., Feike, E., Heine, T., Trampert, A., & Schubert, H. (2004). Ceramic coatings processed by spraying of siloxane precursors (polymer-spraying). *Journal of the European Ceramic Society*, *24*(7), 2141–2147.

[40] Yang, B. H., Deschatelets, P., & Brittain, S. T. (2006). Fabrication of High Performance Ceramic, *(1)*, 54–58.

[41] Lee, H. J., Yoon, T. H., & Kim, D. P. (2007). Fabrication of microfluidic channels derived from a UV/thermally cured preceramic polymer via a soft lithographic technique. *Microelectronic Engineering*, *84*(12), 2892–2895.

[42] http://www.starfiresystems.com/pip-process.html

[43] Ichikawa, H., Teranishi, H., & Ishikawa, T. (1987). Effect of curing conditions on mechanical properties of SiC fibre (Nicalon). *Journal of Materials Science Letters*, *6*(4), 420–422.

[44] Sorarù, G. D., Pederiva, L., Latournerie, J., & Raj, R. (2002). Pyrolysis Kinetics for the Conversion of a Polymer into an Amorphous Silicon Oxycarbide Ceramic. *Journal of the American Ceramic Society*, *85*(9), 2181–2187.

[45] Yoon, T.-H., Hong, L.-Y & Kim, D.-P. (2011). Preparation and Applications of Ceramic Composite Phases from Inorganic Polymers. Edited by Woo H.-G & Li, H., in *Advanced Functional Materials* (pp. 103- 152). Hangzhou: Zhejiang University Press.

[46] Deshpande, G., Rezac, M. E., & Irisawa, T. (2001). The effect of phenyl content on the degradation of poly(dimethyl diphenyl) siloxane copolymers. *Polymer Degradation and Stability*, *74*(2), 363–370.

[47] Narisawa, M. (2010). Silicone resin applications for ceramic precursors and composites. *Materials*, *3*(6), 3518–3536.

[48] Mu, J., Perlmutter, D. D., & Cited, L. (1981). Thermal decomposition of inorganic sulfates and their hydrates. *Industrial & Engineering Chemistry Process Design and Development*, *20*(4), 640–646.

[49] Zeschky, J., Höfner, T., Arnold, C., Weiβmann, R., Bahloul-Hourlier, D., Scheffler, M., & Greil, P. (2005). Polysilsesquioxane derived ceramic foams with gradient porosity. *Acta Materialia*, *53*(4), 927–937.

[50] Jun, M., Shi, L., Shi, Y., Luo, S., & Xu, J. (2002). Pyrolysis of polymethylsilsesquioxane. *Journal of Applied Polymer Science*, *85*(5), 1077–1086.

[51] Hurwitz, F. I., Heimann, P., Farmer, S. C., & Hembree, D. M. (1993). Characterization of the pyrolytic conversion of polysilsesquioxanes to silicon oxycarbides. *Journal of Materials Science*, *28*(24), 6622–6630.

[52] Corriu, R. J. P. (2000). Ceramics and nanostructures from molecular precursors. *Angewandte Chemie - International Edition*, *39*(8), 1376–1398.

[53] Baldus, P., Jansen, M., & Spom, D. (1999). Ceramic fibers for matrix composites in high-temperature engine applications. *Science, 285*, 699-703.

[54] Bernard, S., Weinmann, M., Cornu, D., Miele, P., & Aldinger, F. (2005). Preparation of high-temperature stable Si-B-C-N fibers from tailored single source polyborosilazanes. *Journal of the European Ceramic Society*, *25*(2–3 SPEC. ISS.), 251–256.

[55] Cornu, D., Bernard, S., Duperrier, S., Toury, B., & Miele, P. (2005). Alkylaminoborazine- Based Precursors for the Preparation of Boron Nitride Fibers by the Polymer-Derived Ceramics (PDCs) Route. *J. Eur. Ceram. Soc.*, *25*, 111–21.

[56] Kokott, S., Heymann, L., & Motz, G. (2008). Rheology and Processability of Multi-Walled Carbon Nanotubes-ABSE Polycarbosilazane Composites. *J. Eur. Ceram. Soc*., 28, 1015–21.

[57] Pivin, J. C., Sendova-Vassileva, M., Colombo, P., & Martucci, A. (2000). Photoluminescence of Composite Ceramics Derived from Polysiloxanes and Polycarbosilanes by Ion Irradiation. *Mater. Sci. Eng., B69–70*, 574–7 (2000).

[58] Gadow, R. & Kern, F. (2002). Liquid-Phase Coating of Carbion Fibers with Pre-Ceramic Polymer Precursors: Process and Applications. *Adv. Eng. Mater. , 4*, 883-6.

[59] Bill, J., & Heimann, D. (1996). Polymer-Derived Composites Ceramic Coatings on C / C-Sic. *Journal of European Ceramic Society*, *2219*(96), 1115–1120.

[60] Kim, Y. W., Kim, S. H., Wang, C., & Park, C. B. (2003). Fabrication of microcellular ceramics using gaseous carbon dioxide. *J. Amer. Ceram. Soc., 86(12*), 2231-2233.

[61] Scheffler, F., Zampieri, A., Schwieger, W., Zeschky, J., Scheffler, M., & Greil, P. (2005). Zeolite covered polymer derived ceramic foams: Novel hierarchical pore systems for sorption and catalysis. *Advances in Applied Ceramics, 104 (1),* 43-48.

[62] Colombo, P. & Bernardo, E. (2003). Macro- and micro-cellular porous ceramics from preceramic polymers. *Compos. Sci. Tech., 63*, 2353-2359.

[63] Colombo, P. & Hellmann, J. R. (2002). Ceramic foams from preceramic polymers. *Materials Research Innovations, 6,* 260-272.

[64] Vakifahmetoglu, C., Zeydanli, D., & Colombo, P. (2016). Porous polymer derived ceramics. *Materials Science and Engineering R: Reports*, *106*, 1–30.

[65] Binhussain, M. A., Colombo, P., Bernardo, E., Binmajed, M. A., Marangoni, M., Atalasi, H. H., Alajmi, A. M., Altamimi, A. (2015). Porous glass ceramic composition and method for manufacturing the same. US 20150158760 A1

[66] Schulz, M. (2009). Microfabrication and MEMS/NEMS. Edited by Colombo, P., Riedel, R., G. D. Sorarù, and Kleebe, H. J. in Polymer Derived Ceramics: From Nano-Structure to Applications (pp. 340-54). Lancaster, PA: DEStech Publications.

[67] Zocca, A., Gomes, C. M., Staude, A., Bernardo, E., Günster, J., & Colombo, P. (2013). SiOC ceramics with ordered porosity by 3D-printing of a preceramic polymer. *Journal of Materials Research*, *28*(17), 2243–2252.

[68] Pierin, G., Grotta, C., Colombo, P., & Mattevi, C. (2015). Direct Ink Writing of micrometric SiOC ceramic structures using a preceramic polymer. *Journal of the European Ceramic Society*, *36*(7), 1589–1594.

[69] Scheffler, M., Bordia, R., Travitzky, N., & Greil, P. (2005). Development of a rapid crosslinking preceramic polymer system. *Journal of the European Ceramic Society*, *25*(2–3 SPEC. ISS.), 175–180.

[70] Zhu, Y., Huang, Z., Dong, S., Yuan, M., & Jiang, D. (2008). Manufacturing 2D Carbon-Fiber-Reinforced SiC Matrix Composites by Slurry Infiltration and PIP Process. *Ceram. Inter.*, *34*, 1201–5.

[71] Qi, G J., Zhang, C.R., Hu, H.F., & Cao, F. (2006). Preparation of amorphous composites with polymer-derived silicon nitride matrix reinforced by three-dimensional silica fiber. *J. Non- Cryst. Solids, 352(2),* 189-192.

[72] Ueno, K., Kose, S., & Kinoshita, M. (1993). Toughness enhancement by polycarbosilane coating on SiC whiskers incorporated in Si_3N_3 matrix composite. *J. Mater. Sci., 28(21),* 5770-5774.

[73] Seitz, J., & Bill, J. (1996). Production of compact polysilazane-derived Si/C/N-ceramics by plastic forming. *Journal of Materials Science Letters*, *15*, 391–393.

[74] Konetschny, C., Galusek, D., Reschke, S., Fasel, C., & Riedel, R. (1999). Dense silicon carbonitride ceramics by pyrolysis of cross-linked and warm pressed polysilazane powders. *Journal of the European Ceramic Society*, *19*, 2789–2796.

[75] Herzog, A., Thünemann, M., Vogt, U., & Beffort, O. (2005). Novel application of ceramic precursors for the fabrication of composites. *Journal of the European Ceramic Society*, *25*(2–3 SPEC. ISS.), 187–192.

[76] Valle, M., Ferrari, S., Orlandi, M., Turani, S., & Pagani, M. (2009). Use of polysiloxane resins in friction materials. *Advances in Applied Ceramics*, *108*(8), 461–467.

[77] Li, J., Bernard, S., Salles, V., Gervais, C., & Miele, P. (2010). Preparation of polyborazylene-derived bulk boron nitride with tunable properties by warm-pressing and pressureless pyrolysis. *Chemistry of Materials*, *22*(6), 2010–2019.

[78] Konegger, T., Liersch, A., Gierl, C., & Scheffler, M. (2013). Bulk ceramic composites derived from a preceramic polysilazane with alumina and zirconia fillers. *Advanced Engineering Materials*, *15*(5), 394–406.

[79] Greil, P. (1998). Near Net Shape Manufacturing of Ceramic Components. *CFI Ceramic Forum International*, *75*(8), 15–21.

[80] Steinau, M., Travitzky, N., Gegner, J., Hofmann, J., & Greil, P. (2008). Polymer-derived ceramics for advanced bearing applications. *Advanced Engineering Materials*, *10*(12), 1141–1146.

[81] Chollon, G. (2010). Oxidation Behaviour of Polymer-Derived Ceramics. Edited by Colombo, P., Riedel, R., Soraru, G. D. and Kleebe, H.-J in *Polymer Derived Ceramics: From Nano-structure to Applications* (pp.292-308). Lancaster, PA: DEStech Publications.

[82] Koteeswara Reddy, N., Devika, M., & Gopal, E. S. R. (2015). Review on Tin (II) Sulfide (SnS) Material: Synthesis, Properties, and Applications. *Critical Reviews in Solid State and Materials Sciences*, *40*(6), 359–398.

[83] Roy, J., Chandra, S., Das, S., & Maitra, S. (2014). Oxidation behaviour of silicon carbide - A review. *Reviews on Advanced Materials Science*, *38*(1), 29–39.

[84] Diamant, R. M. E. (1986). Wall, floor and roof insulation in *Thermal and Acoustic Insulation*. (pp. 136-141)

[85] Torriani, I. L. (2000). Poly (phenylsilsesquioxane) s : Structural and morphological Characterization, 1580–1589.

[86] Kamkui, H. M., Laminsi, S., Njopwouo, D., Djowe, A. T., & Yaoundé, B. (2014). Deep Insight in Thermal Synthesis of Tin Disulphide (SnS_2) Microplates, Starting From Tin Sulphate And Sulfur : Growth Mechanism Based On Lux Flood's Theory Of Acid And Base. *Chalcogenide Letters, 11*(5), 219–226.

[87] Balek, V., Pérez-Rodríguez, J. L., Pérez-Maqueda, L. A., Šubrt, J., & Poyato, J. (2007). Thermal Behaviour of Ground Vermiculite. *Journal of Thermal Analysis and Calorimetry, 88 (3),* 819–823.

[88] Ionescu, E., Linck, C., Fasel, C., Müller, M., Kleebe, H. J., & Riedel, R. (2010). Polymer-derived SiOC/ZrO2 ceramic nanocomposites with excellent high-temperature stability. *Journal of the American Ceramic Society*, *93*(1), 241–250.

[89] Křístková, M., Weiss, Z., Filip, P. (2004). Hydration Properties of Vermiculite in Phenolic Resin Friction Composites. *Applied Clay Science, 25*, 229– 236.

[90] Kornmann, X., Lindberg, H., Berglund, L.A. (2001). Synthesis of Epoxy-Clay Nanocomposites. Influence of the Nature of the Curing Agent on Structure. *Polymer, 42*, 4493-4499.

[91] Zhang, G., Shi, M., Huang, C., & Huang, Z. (2016). Synthesis and Properties of Polyphenylsilsesquioxane Modified Phenolic Resin by *in-situ* Polymerization from Phenyltriethoxysilane Precursor. *Journal of Macromolecular Science, Part B, 55*(8), 810–821.

[92] Jiménez de Haro, M. C., Pérez Maqueda, L. A., Stepkowska, E. T., Martínez, J. M., Pérez-Rodríguez J. L. (2003). The Influence of Exchangeable Cation on Thermal Behaviour of Ground Vermiculite. *Journal of Thermal Analysis and Calorimetry, 71*, 761–771.

[93] Graf, H., Reichenbach, V. and Beyer, J. (1994). Dehydration and Rehydration of Vermiculites: I. Phlogopitic Mg-Vermiculite. *Clay Minerals, 29,* 327-340.

[94] Mei, L., Xu, C., Yang, T., Ma, J., Chen, L., Li, Q., & Wang, T. (2013). Superior electrochemical performance of ultrasmall SnS2 nanocrystals decorated on flexible RGO in lithium-ion batteries. *Journal of Materials Chemistry A, 1*(30), 8658.

[95] Burns, G. T., Taylor, R. B., Xu, Y., Zangvil, A., & Zank, G. a. (1992). High-temperature chemistry of the conversion of siloxanes to silicon carbide. *Chemistry of Materials*, *4*(6), 1313–1323.

RESUME

Personal Information

Name-Surname : Tuğçe Aybüke ARICA

Mother Language : Turkish

Foreign Language : English

Birth : January 5, 1992

Mail : taarica@anadolu.edu.tr

Education

2014 – 2017	Master of Engineering (M. Eng.), *Department of Material Science and Engineering,* *Anadolu University*
2009 – 2014	Bachelor of Engineering (B.Eng.), *Department of Material Science and Engineering,* *Anadolu University*

Work Experience

Jun. 2015 – Sept. 2015	**University of Padova** *Erasmus Summer Intern*
Aug. 2013 – Sept. 2013	**Turkish Aerospace Industries, Inc. (TAI)** *Composite Manufacturing Engineering Intern*
Jul. 2013 – Aug.t 2013	**ASELSAN** *Research and Development Intern*

Scientific Activities

- 2016, *Scientific Research Projects of Anadolu University, Silicon Based Preceramic Polymers as a Matrix Material in Composite Technology, Anadolu. University.*